# MECHANICAL PROPERTIES OF CARBON-BASED EPOXY GROUT AS INFILL MATERIAL FOR STEEL PIPELINE REPAIR

LIM KAR SING
DOH SHU ING
CHIN SIEW CHOO
CHENG HOCK TIAN
NORDIN YAHYA
NORHAZILAN BIN MD NOOR
LIBRIATI BINTI ZARDASTI

RESEARCH VOTE NO.:
RDU1703239

Faculty of Civil Engineering & Earth Resources
Universiti Malaysia Pahang

2019

## DEDICATION

First and foremost, I would like to express my gratitude to Research and Inovation Department (PNI), Universiti Malaysia Pahang (UMP) for the financial support provided throughout this research. My also would like to express my appreciation to my internal research team members from UMP, Dr. Doh Shu Ing, Dr. Ir. Chin Siew Choo and Dr. Cheng Hock Tian and external research team members from Universiti Teknologi Malaysia (UTM), Prof. Dr. Nordin Bin Yahya, Assoc. Prof. Dr. Norhazilan Bin Md Noor and Dr. Libriati Binti Zardasti for their technical support.

My special thanks is also extended to my industry collaborator, Orbiting Scientific & Technology Sdn. Bhd. for their great technical support in sharing their knowledge and equipments which contributes a lot to the success of this study.

Last but not least, I would like to thanks all my students whom have directly or in directly involved themselve in this research. They are Mr. Kam Seng Hai, Ms. Ain Shahira Binti Kasmaon, Ms. Thoo Hui Sxin, Mr. Tay Hong Wei, Ms. Leong Kah En, Ms. Chia Shin Chian and Ms. Lim Kah Qi.

## ABSTRACT

The industry nowadays is incorporating the composite repair system for repairing pipelines rather than the conventional steel repair. The mechanism of this repair method usually consists of three components which are the composite wrap, infill material and the adhesive. However, there have been very little researches on the function of the infill in the repair mechanism. This work is concerning the enhancement of the performance or the strength properties of the infill material in pipeline repair by reinforcing the putty with carbon-based nano fillers which are graphene nanoplatelets (Gnp) and carbon nanotubes (CNT). The enhancement of the performance of the infill has been carried out by dispersing the carbon-based nano fillers into epoxy resin with a three roll mill. In the mechanical properties testing, it is found that the both carbon-based nano fillers are effective material to improve the tensile strength of the epoxy grout. However, the modified samples in the compressive properties test show a contrast to the tensile test. All the modified samples exhibit a lower compressive strength than the control sample and the milled down sample. In conclusion, graphene nanoplatlets and CNT can be a very good material to enhance the mechanical properties of epoxy grout, however, with this specific brand of epoxy grout that contains steel filler in the resin, the CNT only improve the tensile properties but the compressive properties of the epoxy grout decrease as compared to the control sample.

## ABSTRAK

Industri pada masa kini lebih gemar menggunakan sistem pembaikan komposit untuk membaiki saluran paip berbanding dengan pembaikian keluli konvensional. Mekanisme kaedah pembaikian ini biasanya terdiri daripada tiga komponen iaitu pembalut komposit, dempul dan pelekat. Walau bagaimanapun, standard reka bentuk pembaikan saluran paip pada masa kini hanya mengambil kira kekuatan baki paip yang rosak dan kekuatan pembalut komposit. Penyelidikan tentang fungsi dempul dalam mekanisme pembaikian paip adalah sangat terhad sehingga kini. Kajian ini berfokus untuk meningkatkan prestasi atau sifat mekanikal dempul dalam pembaikian saluran paip dengan mengukuhkan dempul melalui penambahan pengisi nano berasaskan karbon, iaitu graphene nanoplatelets (Gnp) dan nanotube karbon (CNT). Peningkatan prestasi dempul telah dijalankan melalui perpisahan pengisi nano berasaskan karbon di resin dempul dengan mesin *three roll mill*. Dalam ujian sifat ketegangan, kedua-dua pengisi nano berasaskan karbon didapati merupakan bahan yang berkesan untuk meningkatkan kekuatan tegang dempul. Walau bagaimanapun, sampel yang diubahsuai menunjukkan penurunan kekuatan dalam ujian mampatan. Semua sampel yang diubahsuai mempamerkan kekuatan mampatan yang lebih rendah berbanding sampel kawalan dan sampel yang dikalender. Kesimpulannya, graphene nanoplatelets (Gnp) dan CNT menunjukkan potensi untuk menjadi bahan yang sangat baik untuk meningkatkan sifat-sifat mekanikal bahan dempul. Walau bagaimanapun, dengan dempul yang mengandungi pengisi keluli yang bersaiz besar, penambahan CNT hanya dapat meningkatkan sifat tegangan manakala sifat mampatan bahan dempul telah terjejas berbanding sampel kawalan.

## TABLE OF CONTENT


**TITLE PAGE**

**DEDICATION** **i**

**ABSTRACT** **ii**

**ABSTRAK** **iii**

**TABLE OF CONTENT** **iv**

**CHAPTER 1** **1**

1.0 General Problem Statement 1

1..1 Research Objective 2

1.2 Research Scope 2

**CHAPTER 2** **3**

2.0 Effective dispersion of graphene nanoplatelets in epoxy grout for pipeline rehabilitation

**CHAPTER 3** **11**

3.0 Effective Dispersion of Carbon Nanotube in Epoxy Grout for Structural Rehabilitation

**CHAPTER 4** **18**

4.0 Mechanical Properties Characterization and Finite Element Analysis of Epoxy Grouts in Repairing Damaged Pipeline

**CHAPTER 5** **29**

5.0 Behaviour of Steel Pipelines with Composite Repairs Analysed Using Experimental and Numerical Approaches

**CHAPTER 6** **42**

6.0 Mechanical Properties of Graphene Nanoplatelets-Reinforced Epoxy Grout in Repairing Damaged Pipelines

**CHAPTER 7** **49**

7.0 Conclusion 49

7.1 Recommendations 49

**REFERENCES** **50**

# CHAPTER 1

## 1.0 General Problem Statement

Steel pipelines are the most effective and safe ways for oil and gas transportation over a long distance. However, steel pipes that are laid underground can go through adverse deterioration in the form of corrosion, crack, dents, wearing, buckling, gouging, leaks and rupture. According to the United States Department of Transport (2007), the average annual corrosion-related cost is estimated at $7 billion to monitor, replace and maintain gas and liquid transmission pipelines. About 80% of the cost is related to maintenance and operation of corrosion related problems. A corroded pipeline will reduce its strength and eventually reduce service life. Hence, corrosion and metal loss cause failures in pipelines and their repair techniques is one of the prime interests of the researchers all over the world (Shamsuddoha *et al.*, 2013; Saeed, 2015). For years, the most traditional repair solution for a damaged steel pipe is to remove the pipe entirely or just a localised damaged section and then replaces it by a new one or cover with a steel patch through welding, respectively. These conventional repair techniques incorporate external steel clamps that are either welded or bolted to the outside surface of the pipes. The shortcomings of these techniques are the welding or clamping of pipelines itself is bulky, costly and time consuming especially for underground pipelines (Kou and Yang, 2011). Thus, researchers continuously look for other repair techniques that are relatively lightweight, easily applicable and can be an effective repair solution.

Several literatures have shown that fibre-reinforced polymer (FRP) composites can be effectively used for the construction and retrofit of marine and underground structures (Gibson, 2003; Cercone and Lockwood, 2005; Alexander and Francini, 2006; Alexander, 2007; Seica and Packer, 2007; Duell *et al.*, 2008; Leong *et al.*, 2011; Chan *et al;*, 2015). FRP composites have been chosen to repair steel pipelines due to their lightweight, high strength and stiffness, excellent fatigue properties and good corrosion resistance. Despite the many advantages offered by composite repair systems shown in past literature, several issues regarding the behaviour and overall performance of the composite repair systems are not yet fully understood at present. These issues including complexity of surface preparation, hollowness, delamination and debonding between steel and composite, performance and contribution of infill, load transfer mechanism, effect of defect geometries, and conservativeness in existing closed-form solution (Ma *et al.*, 2011; Shamsuddoha *et al.*, 2012; United State Department of Transport, 2013; Saeed, 2015; Lim et al., 2016). These are the gaps in current body of knowledge and demands further investigation in order to have better understanding on the behaviour of composite repaired steel pipeline, hence improve the efficiency of composite repair systems.

The design of composite repair system can be found in ASME PCC-2- Part 4, Nonmetallic and Bonded Repairs (2011) and ISO/TS 24817, Composite Repairs for Pipework (2006). Current practice in choosing the infill material is “by experience” or follows the recommendation of composite wrap supplier. There are no specific guidelines on the required properties of infill

material to be used in a specific repair case. The possible reason being limited information of the behaviour of infill material as part of repair system. This can leads to less effective repair and eventually increase the risk of failure for repaired pipeline. Hence, this research focused on contribution of infill material and potential properties improvement of existing infill material using graphene nanoplatlets and carbon nanotube (CNT). Hypothetically, detail investigation using numerical analysis can provide useful information on the role of infill material as part of composite repair system, hence better understanding. A good infill has the potential to increase the efficiency and performance of overall repair system and reduce the total cost by minimizing the used of composite sleeve. Moreover, enhancement of engineering properties of infill material is expected to serve as load carrying component under critical circumstances such as failure of composite sleeve.

## 2.0 Research Objective

The objectives of this study are:

1. To characterize the mechanical properties of selected epoxy grouts to be used as infill material in composite repair.
2. To study the performance of selected epoxy grout by addition of carbon-based nano filler.
3. To analyse the efficiency of modified infill material as part of composite repair system through finite element analysis.

## 3.0 Research Scope

In order to achieve the research objectives, three research stages have been conducted. Firstly, the properties of selected infill materials have been determined through laboratory test. It was then followed by the experimental work on enhancement of the properties using carbon-based nano filler which are graphene nanoplatlets and carbon nanotube (CNT) to determine its behaviour. Lastly, a finite element (FE) model was developed and validated based on the pressure test data for repaired pipe using existing experimental data followed by modification on infill properties in the validated FE model to evaluate the performance of overall repair system.

# Effective dispersion of graphene nanoplatelets in epoxy grout for pipeline rehabilitation

K. S. Lim, A. S. Kasmaon, S. C. Chin, and S. I. Doh

Citation: AIP Conference Proceedings **2020**, 020036 (2018); doi: 10.1063/1.5062662
View online: https://doi.org/10.1063/1.5062662
View Table of Contents: http://aip.scitation.org/toc/apc/2020/1
Published by the American Institute of Physics

# Effective Dispersion of Graphene Nanoplatelets in Epoxy Grout for Pipeline Rehabilitation

K. S. Lim [1, a)], A. S. Kasmaon[1, b)], S. C. Chin[1, c)] and S. I. Doh[1, d)]

[1]*Faculty of Civil Engineering and Earth Resources, Universiti Malaysia Pahang, 26300 Gambang, Kuantan, Pahang, MALAYSIA.*

[a)] Corresponding author: limks@ump.edu.my
[b)] ainshahirakasmaon@gmail.com
[c)] scchin@ump.edu.my
[d)] dohsi@ump.edu.my

**Abstract.** After years of operation, oil and gas pipelines are subjected to various damage mechanisms such as third party damage, material defect, and corrosion. These damaged pipelines need to be repaired/rehabilitated to ensure safe operation in the future. Nowadays, numerous rehabilitation techniques and repair methods are available for onshore and offshore pipelines including the usage of Fibre-Reinforced Polymer composite. A composite repair system consists of three parts which are composite wrapper, adhesive and infill materials and it is the most preferable techniques in repairing damaged pipeline in oil and gas industry. High strength infill materials has the potential in improving overall repair performance of composite repair system. The purpose of this research is to investigate the effectiveness of graphene nanoplatelets as reinforcement to enhance the mechanical properties of epoxy grout used as infill materials by adding 0.01%, 0.05% and 0.1% of graphene nanoplatelets. The dispersion was done by calendaring technique using a three-roll mill machine where the graphene particles were de-agglomerated to achieve homogenous dispersion. The results of tensile and compression tests show increment of strength for all graphene-modified samples. The strength increment was recoded range from 23% to 50% and 9% to 22% under tensile and compression test, respectively. The highest tensile strength was recorded at 20.89 MPa for sample with 0.1% graphene while sample with 0.05% graphene shows 82.67 MPa in compressive strength. This signifies the effectiveness dispersion of graphene nanoplatelets as reinforcement in the epoxy grout. As a conclusion, graphene nanoplatelets has great potential to improve the mechanical properties of epoxy grout with the aid of proper dispersion process.

## INTRODUCTION

Structure rehabilitation techniques involving repairing or upgrading pipelines systems in civil engineering applications are techniques that commonly used in oil and gas industry. Pipelines in oil and gas industry are being used to transport products such as oil and gas across various soil environments and from offshore to onshore plant. Most of the pipelines that have been used for transporting products are subjected to various types of damage after long service year [1-4]. The factors that contribute to the pipelines damage include corrosion, natural forces, construction defect and third party damage [5-7]. Obviously, pipeline surface that is exposed to water and soil environment will have higher corrosion risk due to active chemical reaction by its surrounding environment [8]. Most of the pipelines that have been operated for long duration and suffer from damages need repair and maintenance to ensure that it can operate smoothly and safely [9]. This is very important for the safety and economy purpose of public and pipeline operators.

Generally, repairing methods have been developed in order to extend the safety and durability of damaged pipeline. There are two ways to repair pipeline which are conventional steel sleeve and composite repair system [3]. Conventionally, pipelines are repaired by removing the entire damaged section or using steel sleeve/clamp to reinforce the damaged pipe. The conventional repair method has several disadvantages including safety issues due to hot work, bulky, have limited applications for joints or bends and subjected to corrosion risk in the future. The

*Advances in Civil Engineering and Science Technology*
AIP Conf. Proc. 2020, 020036-1–020036-7; https://doi.org/10.1063/1.5062662
Published by AIP Publishing. 978-0-7354-1738-0/$30.00

Clock Spring Company show that the composite pipe repairs are stronger than the original pipe, allowing the repaired pipe to perform at original Maximum Allowable Operating Pressure (MAOP) and it has been endorsed by peer review and third party testing in oil and gas industry [10]. A composite repair system generally consists of 3 components; composite wrap, infill material, and adhesive. The advantages of composite repair system include lightweight, high strength and stiffness, and good corrosion resistance. Even though composite repair systems offer numerous advantages, several issues regarding the performance of the composite repair systems are not fully understood. These issues include conservativeness in existing design codes, effect of defect geometry, and performance and contribution of infill materials [11,12]. In addition, the composite wrap which deemed as main strength contributor in the repair system could exhibit degradation over time when exposed to UV rays, moisture and high temperatures which may potentially leads to sudden failure before the FRP composite reach its full performance. Repair efficiency may be increase with the high performance infill material if it can be serve as second protection layer if failure of composite occurs. However, some of the researchers ignoring the function of the infill materials and mostly focused on the improvement and the performance of the composite wrapping component. These researchers assume that the epoxy grout used is only to fill the void/defect of the damaged pipeline without reinforcement on the pipeline. However, this assumption is not supported by any strong evidence.

Previous studies have pointed out that the infill has the potential to serve as load bearing component [12,13]. A higher performance infill may improve the overall repair performance. Since the discovery of graphene nanoplatelets, it have been widely used and proven effective in improving the mechanical properties of epoxy grout with typical amount of graphene nanoplatelets added ranging from 0% to 2.5% [14-17]. Therefore, graphene nanoplatelets is considered suitable to be used as reinforcement in this research due to its extraordinary properties. Singhi stated that dispersion of nanofillers inside the epoxy resin can be very challenging for researchers. One of the reasons is the low viscosity of resin will cause poorer dispersion of nanofiller [17]. This is one of the reasons why this research needs to be conducted to achieve better result of dispersion. Therefore, this study aims to investigate the dispersion of the graphene nanoplatelets inside the epoxy composite and it is hypothesized that good dispersion will enhance the performance of the infill materials towards pipelines repair. With the enhancement of infill's mechanical properties, it can potentially increase the overall load bearing capacity by the repair system.

## RESEARCH METHODS

The infill used in this study is commercially available steel-filled epoxy grout. The modification of neat epoxy starts with mixing epoxy resin and graphene nanoplatelets using planetary centrifugal mixer, the Kakuhunter SK-350TII. The graphene was added at different percentage into the epoxy resin and transfer into Kakuhunter SK-350TII machine for 120 seconds for mixing and degassing purposes. The mixer is capable to accommodate mixing and degassing for various materials regardless of any viscosity to achieve a homogeneous mixing. The mixing process is shown in Fig. 1.

The dispersion process took place right after the mixing process is completed using three-roll mill. The modified epoxy resin was then poured into the roller of three-roll mill EXACKT 80E machine. The calendaring process of the three roll mill utilized the shear force created between the rollers to separate the agglomeration of graphene nanoplatelets and dispersing it as evenly as possible. The dispersion occurred for three times started with speed 200 m/s for the first and second rounds and increases to 350 m/s for the final round. Figure 2 shows the calendaring process of three-roll mill.

The percentage of the graphene nanoplatelets used in this study was 0.01%, 0.05% and 0.1%. After the dispersion process is completed, the epoxy grout was moulded into prism shape with dimension of 12.7 mm x 12.7 mm x 50.8 mm for compression test in accordance to ASTM D695. The materials were also moulded into dog-bone shape for tensile test. According to ASTM D638 standards, the specimen is of Type 1 with dimensions 13 mm x 3.2 mm at the narrow section and thickness of 3.2 mm. Finally, the specimens undergo curing process for 24 hours at room temperature. Table 1 summarize the details for mechanical properties tests.

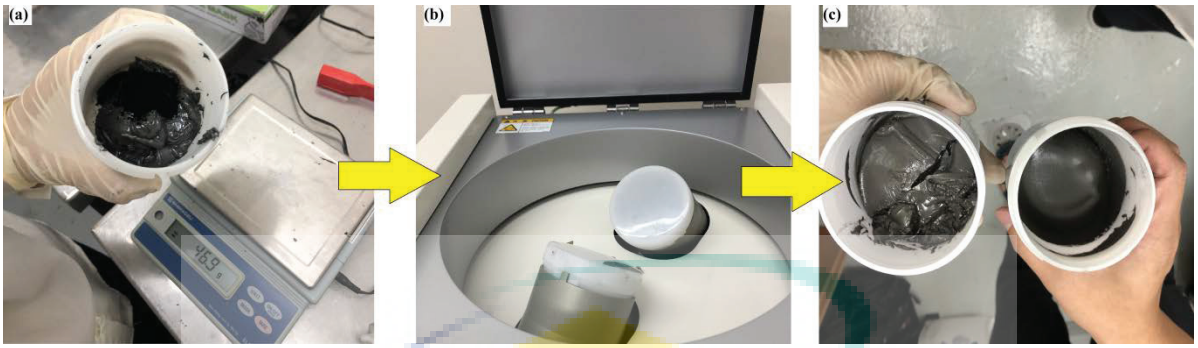


**FIGURE 1.** (a) neat epoxy resin with graphene nanoplatelets; (b) mixing process with planetary centrifugal mixer; (c) neat epoxy resin (left) and mixed resin-graphene nanoplatelets

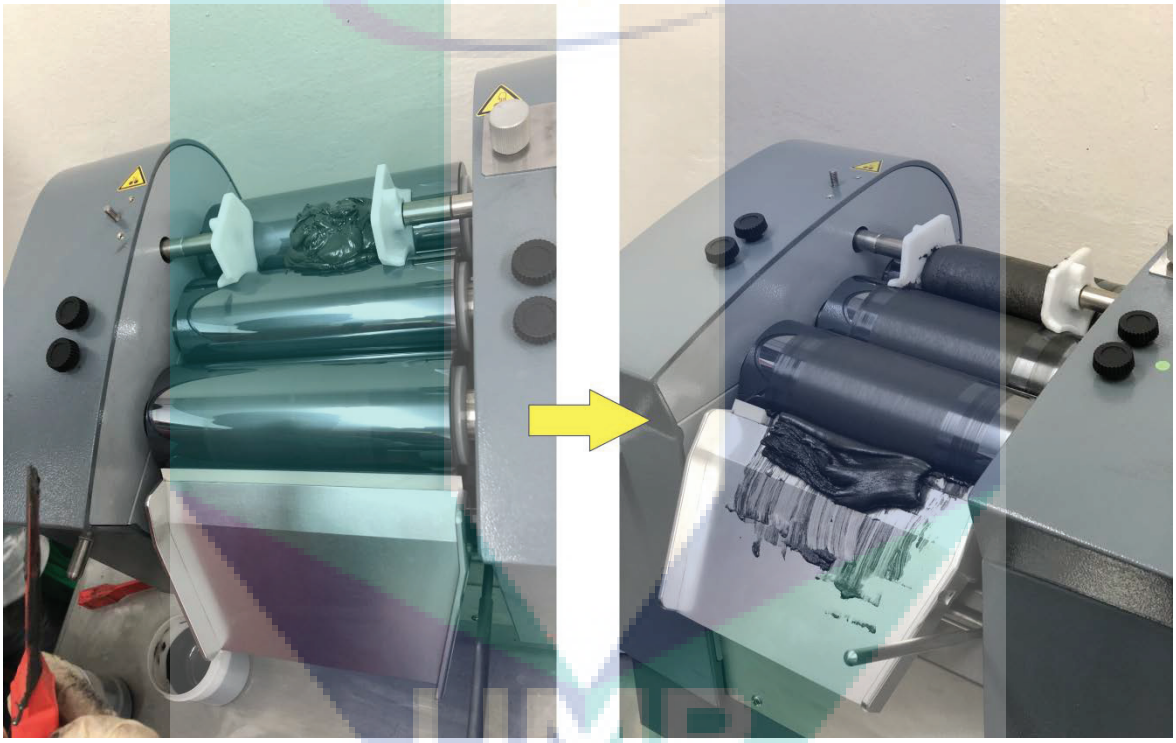

**FIGURE 2.** Dispersion of modified epoxy resin by using three-roll mill EXACKT 80E machine.

**TABLE 1.** Summary of test detail.

| Test | Compression | Tensile |
|---|---|---|
| Standards | ASTM D695 | ASTM D638 |
| Number of samples | 5 | 5 |
| Dimensions (mm) | 12.7x12.7x 50.8 | 13 x 3.2 |
| Loading rate (mm/min) | 1.3 | 3.75 |
| Geometry | Prismatic | Dumbbell |

## RESULTS AND DISCUSSION

### Mechanical Properties of Modified Epoxy Grout

The results of tensile and compressive strength for all tested grouts are summarized in Table 2. The plus and minus sign (±) after the average value represents standard deviation of the sample. Five specimens of modified graphene were studied under tensile test and compression test. The strength values presented in the table are the average of the maximum stress of 5 specimens when the failure of specimen occurred. Infill with high tensile strength may potentially increase the overall load bearing capacity while high compressive strength is important to aid for load transfer from defective pipe to composite wrap.

The tensile strength was observed to be ranged between 13 MPa to 20 MPa for tensile test and 67 MPa to 82 MPa for compressive test, respectively. As shown in Table 2, the tensile strength increase as the percentage of graphene nanoplatelets added into the epoxy resin increases. When comparing with the control specimen, the tensile strength of modified epoxy grouts shows increment of 23%, 38% and 50% for 0.01%, 0.05% and .01% of graphene added, respectively. On the other hand, under compressive test, the modified epoxy grout has ability to increase the compressive strength in all samples. The highest compressive strength is recorded at 82.67 MPa which is sample with 0.05% graphene added to the epoxy grout. There is a 22% of strength increment as compared to control samples. The compressive strength of 0.1% and 0.01% graphene also shows 9% and 20% increment when comparing with control sample, respectively. This shows that the optimum percentage for the compressive strength improvement is 0.05% for the tested graphene percentage.

**TABLE 2.** Tensile and compressive strength.

| Epoxy Grout | Tensile Strength (MPa) | Compressive Strength (MPa) |
|---|---|---|
| Control sample | 13.12 ± 4.95 | 67.08 ± 10.24 |
| 0.01% of graphene | 16.22 ± 8.18 | 80.80 ± 5.10 |
| 0.05% of graphene | 18.18 ± 1.38 | 82.67 ± 6.83 |
| 0.1% of graphene | 20.89 ± 8.09 | 73.02 ± 11.61 |

Figures 3 and 4 show the stress and strain relationship for tensile and compression tests, respectively. As can be observed in both figures, only linear behaviour is exhibited which represents elastic behaviour up to failure. There is no noticeable plastic deformation can be detected in the figures. This signifies the brittle nature of the all samples. This finding also supported when close observation is done to examine the failure pattern of the samples. Figure 5 shows the failure pattern for tensile (top) and compressive sample (bottom). The tensile sample split into two parts while a vertical crack was noticed for compressive sample at maximum stress.

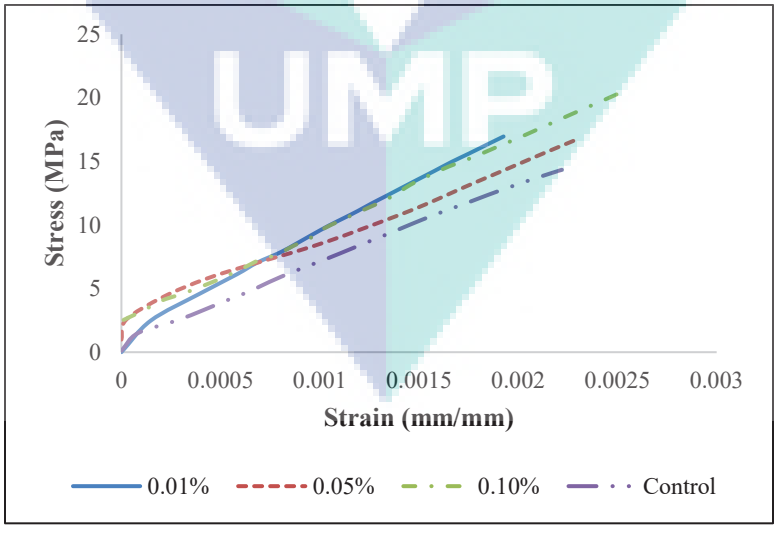


**FIGURE 3.** Relationship of stress-strain for tensile strength.

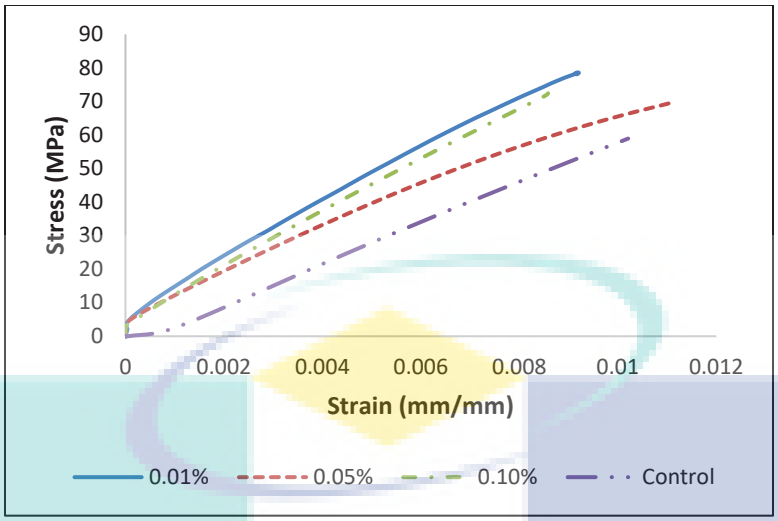


**FIGURE 4.** Relationship of stress-strain for compressive strength.


**FIGURE 5.** Failure pattern of tensile (top) and compression (bottom) specimen.

## Morphology of Modified Epoxy Grout

FESEM results of all epoxy grouts are presented in Fig. 6. The FESEM test was conducted to study the failure surface of selected tensile samples. As shown in Fig. 6, abundant of graphene nanoplatelets particles can be seen on the failure surface of 0.1% graphene specimen while only few graphene particles was detected on the failure surface for 0.01% sample. This indicates that the amount of graphene may still not up to the maximum quantity as reinforcement for the epoxy grout in tensile specimen. Based on the findings of tensile test and supported by FESEM result, a higher percentage of graphene has the potential to further increase the tensile strength.

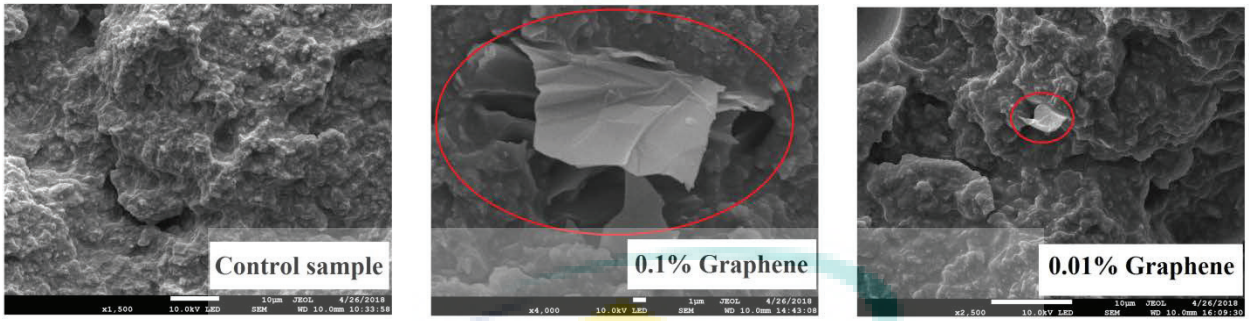


**FIGURE 6.** The failure surface of selected epoxy grouts.

## CONCLUSIONS

Modification of commercially available epoxy grout has been achieved by adding graphene nanoplatelets as reinforcement in order to explore the effect of graphene nanoplatelets towards the tensile and compressive properties. It was found that tensile strength of the modified epoxy grout has been improved up to 50% by adding few percentages of graphene for both mechanical tests. Graphene nanoplatelets show the ability to enhance the strength of both mechanical properties of epoxy grout. In addition, it was found that the all epoxy grouts are brittle type of material under tensile load. The optimum percentage of compressive strength considerably achieved at 0.05% sample of graphene because the strength is slightly dropped at the sample 0.1%.

## ACKNOWLEDGMENTS

The author gratefully acknowledges the financial and technical support provided by Universiti Malaysia Pahang (Grant No. RDU1703239), and Orbiting Scientific & Technology Sdn. Bhd.

## REFERENCES

1. N. Saeed, H. Ronagh and A. Virk, Composites Part B: Engineering, **58**, 605–610 (2014).
2. S. N. F. M. M. Tahir, N. Md Noor, N. Yahaya and K. S. Lim, Asian J. of Scientific Research **8(2),** 205-211 (2015).
3. W. A. Bruce and J. Keifner, "Pipeline Repair Using Full-Encirclement Repair Sleeves", in *Oil and Gas Pipelines: Integrity and Safety Handbook,* edited by R. Winston Reive, (John Wiley & Sons, Inc., New Jersey, 2015), pp. 635-654.
4. S. R. Othman, N. Yahaya, N. Md Noor, K. S. Lim, L. Zardasti and A.S.A. Rashid, J. of Pressure Vessel Technology **139(3),** 031702 (2017).
5. P. H. Chan, K. Y. Tshai, M. Johnson, H. L. Choo, S. Li, K. Zakaria, J. of Composite Materials **49(6),** 749-756 (2015).
6. S. N. F. M. M. Tahir, N. Yahaya, N. Md Noor, K. S. Lim and A. A. Rahman, J. of Pressure Vessel Technology **137(5),** 051701 (2015).
7. M. Shamsuddoha, M. M. Islam, T. Aravinthan, A. Manalo and P. Djukic. AIMS Materials Sciences **3(3),** 823-850 (2016).
8. G. Bernardo, M. Laterza, M. D. Amato, G. Andrisani, D. Diaz and E. Laguna, ELARCH Project : the use of innovative product based on nanotechnologies for the protection of architectural heritage, **October 2016**, 1–10 (2016).
9. S. Haladuick, M. R. Dann, ASCE-ASME J. of Risk and Uncertainty in Eng. Sys., Part A: Civil Engineering, **4(2),** June 2018 (2018).
10. CLOCK SPRING. (2017). Retrieved from CLOCKSPRING.
11. K. S. Lim, S. N. A. Azraai, N. Yahaya, L. Zardasti and N. M. Noor, Jurnal Teknologi (Science & Engineering) **79(1)**, 9-14 (2017).
12. M. Z. A. Jalil, A. Valipour, K. S. Lim, S. N. A. Azraai, L. Zardasti, N. Yahaya and N. Md. Noor, Malaysian J. of Civil Eng., **28(Special Issue No. 2),** 65-72 (2016).

13. A. Diniţă, I. Lambrescu, M. I. Chebakov and Gh. Dumitru, "Finite Element Stress Analysis of Pipelines with Advanced Composite Repair", in *Non-destructive Testing and Repair of Pipelines, Engineering Materials,* edited by E.N. Barkanov *et al.,* (Springer International Publishing, Switzerland, 2018), pp. 289-309.
14. S. Chatterjee, F. Nafazarefi, N. H. Tai, L. Schlagenhauf and B. T. T. Chu, Carbon **50**, 5380-5386 (2012).
15. L. C. Tang, Y. J. Wan, D. Yan, Y. B. Pei, L. Zhao, Y. B. Li and G. Q. Lai, Carbon **60**, 16-27 (2013).
16. R. Atif, I. Shyha and F. Inam, Polymers **8(281),** 1-37 (2016).
17. M. Singhi, Int. J. of Sci. Technology and Management **4(Special Issue 1),** 425–432 (2015).

# Effective Dispersion of Carbon Nanotube in Epoxy Grout for Structural Rehabilitation

*Kar Sing* Lim[1*], *Seng Hai* Kam[1], *Libriati* Zardasti[2], *Nordin* Yahaya[2], *Norhazilan* Md Noor[2]

[1]Faculty of Civil Engineering and Earth Resources, Universiti Malaysia Pahang, Lebuhraya Tun Razak, Gambang, Kuantan, Pahang 26300, Malaysia.

[2]Faculty of Civil Engineering, Universiti Teknologi Malaysia, UTM Skudai, Johor 81310, Malaysia.

**Abstract.** The industry nowadays is incorporating the composite repair system for repairing pipelines rather than the conventional steel repair. The mechanism of this repair method usually consists of three components which are the composite wrapping, infill material and the adhesive. However, there has been very little research on the function of the infill in the repair mechanism. This work is concerning the enhancement of the performance or the strength properties of the infill material in pipeline repair by reinforcing the putty with carbon nanotubes (CNT). The enhancement of the performance of the infill has been carried out by dispersing the CNT into epoxy resin with a three roll mill. In the mechanical properties testing, it is found that the CNT is an effective material to improve the tensile strength of the epoxy grout. However, the CNT-modified samples in the compressive property test show a contrast to the tensile test. All the CNT-modified samples exhibit a lower compressive strength than the control sample and the milled down sample. In conclusion, CNT shows the potential to be a very good material to enhance the mechanical properties of epoxy grout, however, with this specific brand of epoxy grout that contains steel filler in the resin, the CNT only improve the tensile properties but the compressive properties of the epoxy grout has been compromised as compared to the control sample.

## 1 Introduction

Despite the fact that steel pipelines are the most effective and safe ways for oil and gas transportation over a long distance, they are prone to adverse deterioration in the form of corrosion, crack, dents, wearing, buckling, and gouging that may potentially lead to leaking and rupture [1-4]. Repair methods have since then being developed to retrofit damaged pipelines and composite repair method has become more popular in recent years [5-7]. Composite pipeline repair consists of three components which are the composite wrapping, infill material and the adhesive [8-9]. The infill material of composite repair system is neglected in current design codes. However, these past few years the number of pipeline operators using fibre reinforced polymer composite repair system to repair pipelines has

* Corresponding author: limks@ump.edu.my

been swelling. This has caused the recent development of design codes for the design of the repairs of pipelines such as ASME PCC-2 [10] and ISO/TS 24817 [11]. These codes were developed to standardize the design method of composite pipeline repair. This has also made quality control in this field a reality as pipeline operators has increasingly utilizing this method of repair. However, the codes only take into consideration the remaining strength of damaged pipe and the composite wrapping strength in the design without involving the strength of the infill material. This study is only aimed to modifying the commercially available epoxy grout by adding different percentages of carbon nanotubes (CNT).

Theoretically, the CNT will be able to enhance the mechanical properties of the epoxy grout as it exhibits a very high aspect ratio which results in a high specific surface area (SSA) [12]. The issue with CNT is that the interfacial bonding of the nanoparticles is strong and to achieve a proper dispersion of the individual CNTs in the epoxy grout can be difficult. The advantage of reinforcing epoxy grout with CNT can be limited if the linkage between CNTs and the epoxy grout is not sufficient. A three roll mill right now is the most popular dispersion machine out there. The dispersion of the CNT was done by the three roll mill through a calendaring process. The calendaring process of the three roll mill utilized the shear force created between the roller to separate the agglomeration of CNT and dispersing it as evenly as possible. After the dispersion process is completed, the effectiveness of nano-particle CNT as reinforcement in an epoxy grout will be evaluated by determining the mechanical properties of the epoxy grout samples.

## 2 Methodology

The putty used in this study is commercially available steel-filled epoxy grout. The samples are prepared in 5 different variables which is the control sample, a milled down sample, 0.01% CNT sample, 0.05% CNT sample and 0.1% CNT samples. The modification of putty starts with mixing epoxy resin and CNT using planetary centrifugal mixer, the Kakuhunter SK-350TII. CNT was added at different percentage into the epoxy resin and transfer into the Kakuhunter SK-350TII machine for 120 seconds for mixing and degassing purposes. The mixer is capable to accommodate mixing and degassing for various materials regardless of any viscosity to achieve a homogeneous mixing. The mixing process is shown in Fig. 1. The CNT-epoxy resin mixture was then undergoing calendaring process using a three-roll mill, the EXACKT 80E machine to disperse the CNT. A milled down sample where the resin is put through the three roll mill without any CNT added was done because size of the existing filler is bigger than the smallest gap size of the rollers which is 15 µm. Fig. 2 shows the calendaring process of CNT into epoxy resin and Table 1 summarizes the configuration used for the calendaring process. The samples are prepared for two different mechanical properties tests which are the tensile and compression test. The tensile and compressive strength tests were done in accordance to the ASTM D638 and ASTM D695, respectively. A Shimadzu 50kN Universal Testing Machine was utilized for the tests. A Field Emission Scanning Electron Microscopy (FESEM) test is also conducted to find out the nature of the failure of selected samples.

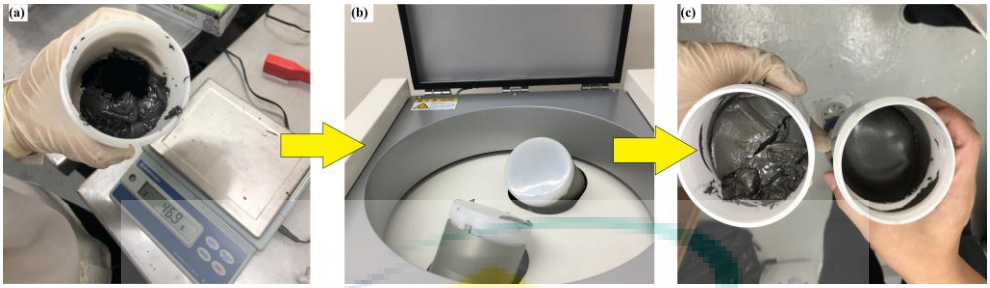


**Fig. 1.** (a) neat resin with CNT particle; (b) mixing process; (c) neat resin (left) and mixed resin-CNT (right).

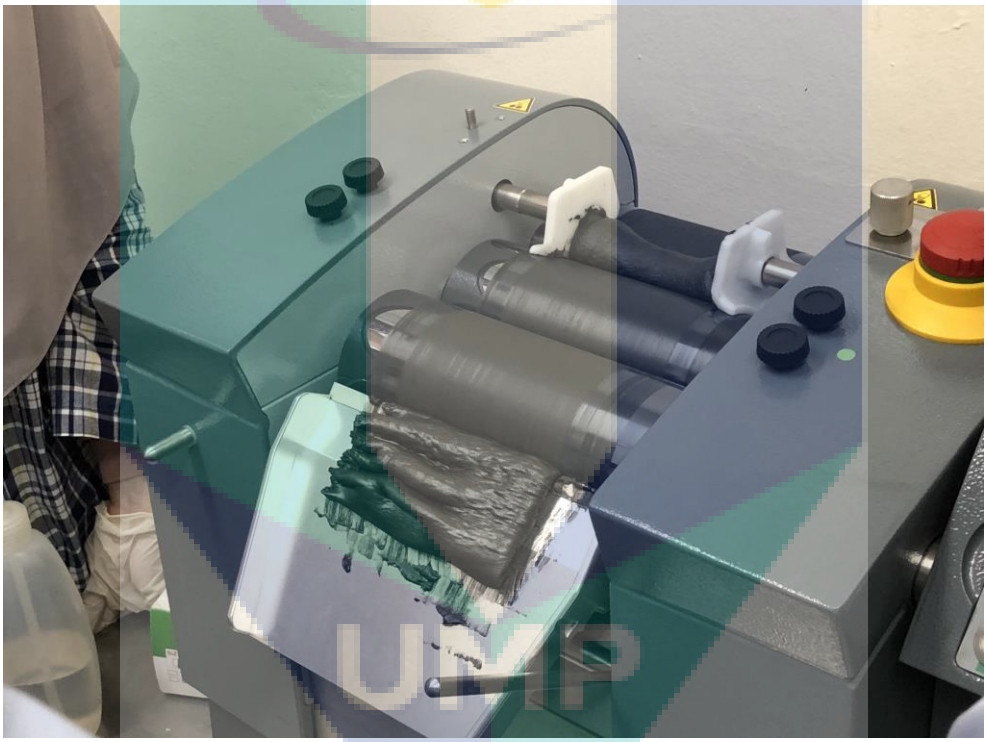

**Fig. 2.** Calendaring process of CNT-resin mixture.

**Table 1.** Three roll mill configuration.

| No of passes | Gap 1 (μm) | Gap 2 (μm) | Roller Speed (rpm) |
|---|---|---|---|
| 1 | 100 | 60 | 200 |
| 2 | 60 | 30 | 200 |
| 3 | 45 | 15 | 350 |

## 3 Results and discussions

The results of tensile test are tabulated in Table 2. The plus and minus sign (±) after average value represents standard deviation of the sample. The tensile test result of the samples in Table 2 shows that the 0.01% CNT samples recorded the highest average tensile strength and the milled down sample has the lowest average tensile strength. Samples with more CNT added has a lower average tensile strength than the 0.01% CNT which is 14.33MPa for the 0.05% CNT sample and 15.56MPa for the 0.1% CNT sample. There is an increase of 62% and 13% of tensile strength from the milled down samples and control sample to the 0.01% CNT added sample, respectively. This shows that CNT is a very effective material to enhance the tensile strength of the epoxy grout. The decrease of the tensile strength for the 0.05% CNT and the 0.1% CNT added can be explained by the optimum amount added to enhance the performance of the epoxy grout. The drop happens after the percentage of weight content added exceeds the optimum percentage [13].

**Table 2.** Tensile test result.

| Sample | Label | Tensile Strength (MPa) | Young's Modulus (GPa) |
|---|---|---|---|
| Control | TC | 15.93 ± 0.36 | 8.65 ± 0.91 |
| Milled Down | TM | 11.09 ± 2.32 | 8.83 ± 2.52 |
| 0.01% CNT | T01C | 17.99 ± 2.60 | 9.91 ± 3.85 |
| 0.05% CNT | T05C | 14.33 ± 1.16 | 7.88 ± 1.90 |
| 0.1% CNT | T10C | 15.56 ± 0.71 | 9.12 ± 0.38 |

Compression strength of the infill material is brought onto action as the infill material act as the load transfer from the pipeline and the composite wrapping. The compression test result are summarised in Table 3. The compression test result in Table 3 shows that the sample with the highest compressive strength is the milled down sample with 71.12MPa and the sample with lowest compressive strength at 61.79MPa is the 0.05% CNT samples. In contrast to the strength, the young's modulus of the milled down sample exhibits the lowest Young's modulus in all the samples at 7.21GPa. The 0.1% CNT sample has the highest compressive strength and Young's Modulus in all the CNT-modified samples at 65.90MPa and 9.24GPa, respectively. Despite expected rise in mechanical properties, the compressive strength of the CNT-modified samples all decrease from the milled down sample where it drops 8.77% from the milled down sample to the 0.01% CNT added, 13.12% for the 0.05% CNT added and 7.33% for the 0.1% CNT added.

**Table 3.** Compression test result.

| Sample | Label | Compressive Strength (MPa) | Young's Modulus (GPa) |
|---|---|---|---|
| Control | CC | 69.19 ± 3.56 | 8.30 ± 1.59 |
| Milled Down | CM | 71.12 ± 5.56 | 7.21 ± 1.89 |
| 0.01% CNT | C01C | 64.88 ± 4.64 | 7.36 ± 1.38 |
| 0.05% CNT | C05C | 61.79 ± 2.49 | 8.62 ± 0.53 |
| 0.1% CNT | C10C | 65.90 ± 8.46 | 9.24 ± 0.88 |

In both the mechanical properties test, the result of the milled down sample differ from the other. This situation is most likely caused by the phase separation of the existing epoxy grout filler in the resin from the resin by the three roll mill (refer Fig. 3). The sizes of the

existing filler in the resin are too big to go through the designated gap of the three roll mill. The milled down sample has the highest compressive strength but the lowest tensile strength. The existing steel filler in the resin are suspected to act as the main tensile strength contributor in the unmodified matrix of the epoxy grout. Hence, with the steel filler which is the tensile strength contributor in the matrix separated from the resin in the milled down sample, the tensile strength drops dramatically from the control sample to the milled down sample. On the other hand, with the tensile strength contributor separated, the compressive strength of the matrix can be improved because the matrix will be denser and without any filler.

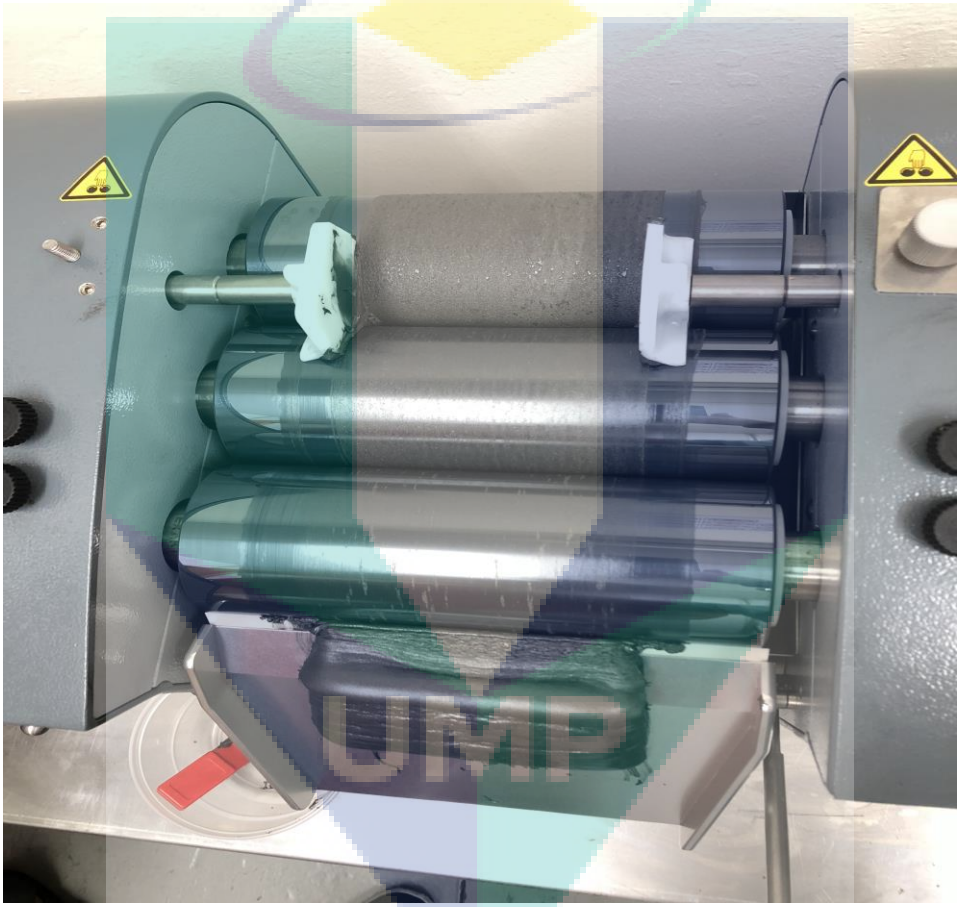

**Fig. 3.** Phase separation of the existing filler on the three roll mill.

Fig. 4 shows the result of the FESEM test on the failure surface of selected samples. The FESEM test conducted shows that the CNT in the 0.1% CNT (T10C-03) is abundant on the failure surface. On the other hand, there is nothing but the epoxy grout on the failure surface of the milled down sample (TM-05). In contrast to the abundant of CNT on the 0.1% CNT, the 0.05% CNT added has very little CNT on the failure surface, hence, the tensile strength of the 0.05% CNT is the lowest. In the control sample (TC), the existing steel filler is present as evident in the FESEM images but absent in the milled down sample which proves the phase separation on the existing steel filler.

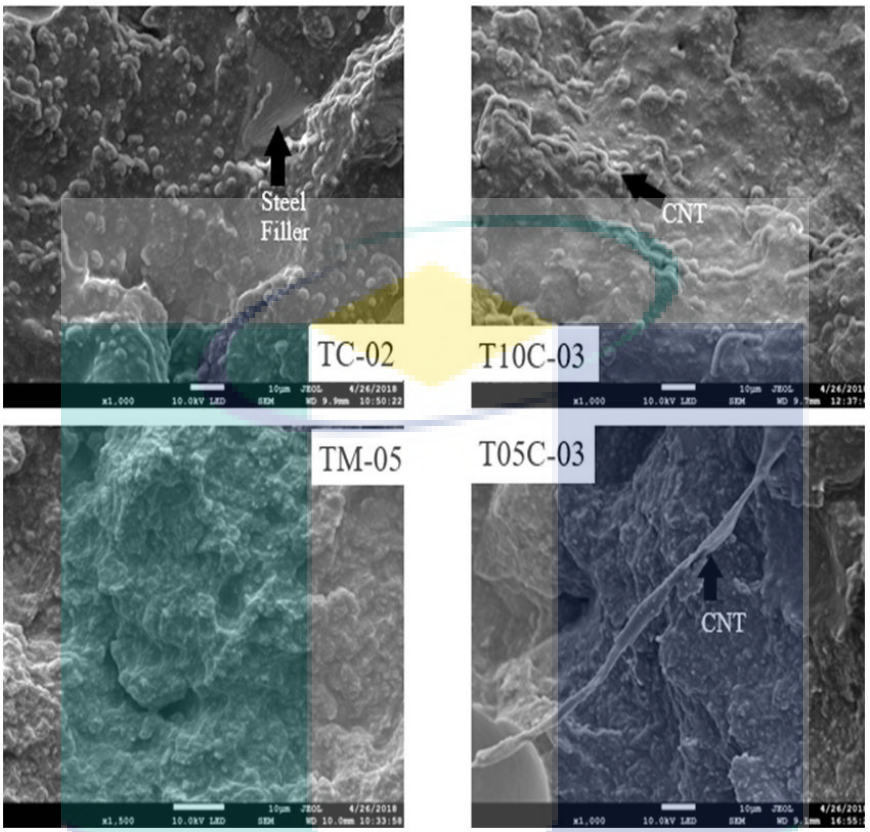


**Fig. 4.** The failure surface of selected samples.

## 4 Conclusions

The tensile strength of the epoxy grout has improved with the addition of CNT into the epoxy matrix but it is the opposite for the compressive strength of the epoxy grout where it decreases with the addition of CNT. In conclusion, CNT can be a very good material to enhance the mechanical properties of epoxy grout, however, with this specific brand of epoxy grout that contains steel filler in the resin, the CNT only improve the tensile properties but the compressive properties of the epoxy grout decrease as compared to the control sample. More percentage variables can be done to get the optimum percentage of CNT to be added. The optimum percentage is important to optimize the amount of CNT used for the enhancement of the performance of the infill material.

The authors gratefully acknowledge the financial and technical support provided by Universiti Malaysia Pahang (Grant No. RDU1703239), Universiti Teknologi Malaysia and Orbiting Scientific & Technology Sdn. Bhd.

## References

1. S. N. F. M. M. Tahir, N. Yahaya, N. Md Noor, K. S. Lim, A. A. Rahman. Journal of Pressure Vessel Technology, **137(5)**, 051701 (2015)

2. M. Shamsuddoha, M.M. Islam, T. Aravinthan, A. Manalo, P. Djukic. AIMS Materials Sciences, **3(3),** 823-850 (2016)
3. S.R. Othman, N. Yahaya, N. Md Noor, K. S. Lim, L. Zardasti, A.S.A. Rashid. Journal of Pressure Vessel Technology, **139(3),** 031702 (2017)
4. X. Liu, J. Zheng, J. Fu, J. Ji, G. Chen. Journal of Natural Gas Science and Engineering, **50**, pp. 64-73 (2018)
5. C. Alexander, B. Vyvial, F. Wilson. *Proceedings of the 2014 10th International Pipeline Conference (IPC 2014). 29th September – 3rd October, 2014. Calgary, Alberta, Canada.* Paper No.: IPC2014-33410 (2014)
6. P.H. Chan, K.Y. Tshai, M. Johnson, H.L. Choo, S. Li, K. Zakaria. Journal of Composite Materials, **49(6),** 749-756 (2015)
7. S. Haladuick, M.R. Dann. ASCE-ASME Journal of Risk and Uncertainty in Engineering Systems, Part A: Civil Engineering, **4, (2),** June 2018 (2018)
8. K. S. Lim, S.N.A. Azraai, N. Yahaya, L. Zardasti, N. Md Noor. Jurnal Teknologi, **79(1),** 9-14 (2017)
9. J.M. Duell, J.M. Wilson, M.R. Kessler. International Journal of Pressure Vessels and Piping, **85,** 782-788 (2008)
10. ASME International. *ASME PCC-2 2011. Repair of Pressure Equipment and Piping.* New York, USA: The American Society of Mechanical Engineers. (2015)
11. ISO. *ISO/TS 2481. Petroleum, Petrochemical and Natural Gas Industries – Composite Repairs of Pipework – Qualification and Design, Installation, Testing and Inspection.* Switzerland: International Organization for Standardization (2006)
12. F.H.Gojny, M.H.G. Wichmann, U. Köpke, B. Fiedler, K. Schulte. Composites Science and Technology, **64(15 SPEC. ISS.),** 2363–2371 (2004)
13. A.M. Rashad. *Construction and Building Materials*, **153,** 81–101 (2017)

**Lim Kar Sing**[1]
Faculty of Civil Engineering and Earth Resources,
Universiti Malaysia Pahang,
Lebuhraya Tun Razak, Gambang,
Kuantan 26300, Pahang, Malaysia
e-mail: limks@ump.edu.my

**Nordin Yahaya**
Faculty of Engineering,
School of Civil Engineering,
Universiti Teknologi Malaysia (UTM),
Skudai 81310, Johor, Malaysia
e-mail: nordiny@utm.my

**Alireza Valipour**
Department of Civil Engineering,
Shiraz Branch,
Islamic Azad University,
Shiraz 71993-3, Iran
e-mail: vali@iaushiraz.ac.ir

**Libriati Zardasti**
Faculty of Engineering,
School of Civil Engineering,
Universiti Teknologi Malaysia (UTM),
Skudai 81310, Johor, Malaysia
e-mail: libriati@utm.my

**Siti Nur Afifah Azraai**
Faculty of Engineering,
School of Civil Engineering,
Universiti Teknologi Malaysia (UTM),
Skudai 81310, Johor, Malaysia
e-mail: snafifah2@live.utm.my

**Norhazilan Md Noor**
Faculty of Engineering,
School of Civil Engineering,
Universiti Teknologi Malaysia (UTM),
Skudai 81310, Johor, Malaysia
e-mail: norhazilan@utm.my

# Mechanical Properties Characterization and Finite Element Analysis of Epoxy Grouts in Repairing Damaged Pipeline

*Oil and gas pipelines are subjected to various types of deterioration and damage over long service years. These damaged pipes often experience loss of strength and structural integrity. Repair mechanisms have been developed in restoring the loading capacity of damaged pipelines, and composite repair systems have become popular over the past few years. The mechanical properties of the putty/grout are critical to their potential application as infill materials in structural repair. In this paper, the compression, tensile, and flexural behavior of four epoxy grouts was investigated through laboratory tests. The stiffness of the grouts for compression, tensile, and flexural was found to be 6 GPa to 18 GPa, 4 GPa to 15 GPa, and 4 GPa to 12 GPa, respectively. The ultimate strength for all grouts was found from 62 MPa to 87 MPa, 18 MPa to 38 MPa, and 34 MPa to 62 MPa under compression, tensile, and flexural tests, respectively. The behavior of all the tested grouts is discussed. A finite element (FE) model simulating a composite-repaired pipe was developed and compared with past studies. The FE results show a good correlation with experimental test with margin of error less than 10%. By replacing the infill properties in FE model to mimic the used of different infill material for the repair, it was found that about 4–8% increment in burst pressure can be achieved. This signifies that the role of infill material is not only limited to transferring the load, but it also has the potential to increase overall performance of composite-repaired pipe.* [DOI: 10.1115/1.4041792]

*Keywords: composite repair, finite element analysis (FEA), infill material, mechanical properties, pipeline*

## 1 Introduction

In the oil and gas industry, a pipeline is regarded as the most economic and safe way of transporting products from one point to another [1–5]. Throughout the service years, these pipelines are subjected to damage and deterioration caused by several factors. These include material and construction defects, natural forces, third party damage, and corrosion [6,7]. A corroded pipeline will reduce its strength and eventually its service life. The deterioration of steel pipelines is a common and serious problem experienced by the industry as this may lead to reduction of life span or a loss of structural integrity. In a pipeline failure investigation report published by Pipeline and Hazardous Materials Safety Administration, a pipeline rupture that occurred on May 2015 has caused an estimated 500 bbl of crude oil to enter the Pacific Ocean. The main culprit of the failure is external corrosion. Even though this incident does not cause any fatalities or injuries, the total cost of property damage and clean-up was about $143 million [8]. In 2014, an explosion of underground pipeline in Kaohsiung, Taiwan killed at least 27 people and injured 286. Initial investigation suggested that the cause of this incident was likely triggered by a leaky underground pipeline owned by a local chemical producer that operates a 4 in propene pipeline [9]. Therefore, corrosion and metal loss cause failures in pipelines and their repair techniques are of interest to researchers all around the world [10–12].

Currently, a wide range of rehabilitation techniques and repair methods are available for onshore and offshore pipelines. Rapid growth has been observed in the development and application of fiber-reinforced polymer (FRP) composites, which are often used to reinforce corroded metallic pipelines [13]. The use of fiber-reinforced polymer composites has been proven effective for repairing steel structures such as risers and pipelines [14–17]. These FRP composite repair systems are specially engineered products consisting of high strength fiber reinforcement in a thermoset polymer resin. The commonly used fibers in FRP composites are glass, carbon, and aramid, in combination with polymer-based thermosetting resins such as epoxy, urethane, and vinyl ester [15,18]. Repair systems using FRP composite can be

[1]Corresponding author.

Contributed by the Pressure Vessel and Piping Division of ASME for publication in the Journal of Pressure Vessel Technology. Manuscript received January 12, 2018; final manuscript received October 12, 2018; published online November 12, 2018. Assoc. Editor: Kiminobu Hojo.

  

categorized as precured layered, flexible wet lay-up, preimpregnated, split composite sleeve, and flexible tape systems. Although the products made by different companies and research institutes around the world have widely different performance, its composite material repair system mainly includes three parts: (i) high strength FRP composite wrap, (ii) adhesive, and (iii) high compressive infill material. Despite many advantages offered by composite repair systems as shown in the past literature, several issues regarding the behavior and overall performance of the composite repair systems are not fully understood. These issues include the complexity of surface preparation, hollowness, delamination and debonding between steel and composite, load transfer mechanism, effect of defect geometries, performance and contribution of infill, and conservativeness in existing closed-form solution [13,19–22]. These are the gaps in current body of knowledge and further investigation is required in order to have better understanding on the behavior of composite-repaired steel pipeline, hence improving the efficiency of composite repair systems. Crude oil price has dropped from July 2014 to early 2016 from an average of USD110 to USD40 per barrel [23]. The global oil price is currently fluctuating between USD50 and USD70, which means a smaller profit margin for oil and gas producers. Therefore, asset integrity management and optimization has become a major concern for oil and gas producers and researchers to save maintenance costs. Owing to that, few researchers have started looking into optimization of composite pipeline repair [24–26].

Grout or putty is usually used as infill material in composite repair systems. The common understanding on the role of grout/putty is to fill the damaged section (i.e., corrosion) and to ensure a smooth bed for the composite wrap. In addition, it also serves as medium for load transfer from the corroded pipe to the composite wrap. This is important to provide a continuous support to minimize the outward distortion of the corroded section. Therefore, the effectiveness of these repair systems largely depends on the performance of the grout. The properties of grout are significant parameters for the numerical simulation or theoretical prediction of the behavior of a repair system to be optimized in terms of repair design. It is therefore essential to characterize the mechanical and thermal properties of epoxy grouts to determine their efficiency as infill materials in composite repair system [11]. However, detailed investigations on the role and contribution of putty are very limited in the previous literature for a composite-repaired pipe due to its assigned limited function in composite repair system. This is also reflected in the codes and standards of current industry practices. The design of composite repair system can be found in ASME PCC-2- Part 4, Non-metallic and Bonded Repairs [27] and ISO/TS 24817, Composite Repairs for Pipework [28]. Duell et al. [29] have investigated the performance of an externally corroded pipeline repaired using composite wrap. The design equation in ASME PCC-2 was used to determine the minimum repair thickness of composite wrap layers. The finding suggests that the existing repair design is overconservative. The repair design in both ASME and ISO codes does not account for the present of infill material, only minimum remaining wall thickness (of the pipe) and additional strength of composite wrap are considered.

It is well known that there are several factors concerning the performance of composite (such as variability in properties, shortage of long-term information, and degradation of material strength over time, loading conditions), therefore a larger safety factor in the design equation is justifiable. However, in order to optimize the current design philosophy, the conservativeness in the existing codes needs to be gradually reduced. The inclusion of strength contribution by the infill could be one of the ways forward in this optimization process. Hypothetically, as the putty acts as part of the repair system, it should somehow affect the overall performance of the repair. However, the evaluation on the effect of infill toward overall repair performance is hardly available in the previous studies. Therefore, this research has taken initial step to investigate the influence of infill materials toward the overall performance of a composite-repaired pipe. Characterization and evaluation of material properties for four commercially available epoxy grouts were carried out. A finite element model was developed and validated based on the experimental data published by

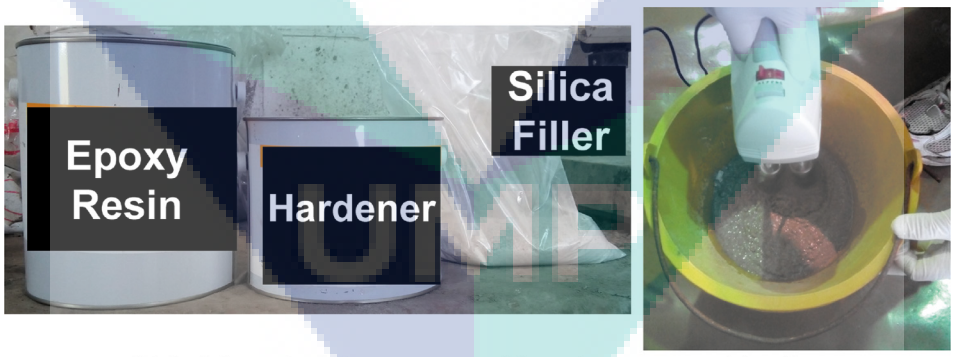


Materials and mixing process of 3-part epoxy grout / putty


Materials and mixing process of 2-part epoxy grout / putty

**Fig. 1 Material preparation**

Duell et al. [29,30]. This model serves as benchmark model in evaluating the influence of different infill properties toward overall repair performance.

## 2 Materials and Methods

Four commercially available epoxy grouts/putties were investigated based on their application and reported properties as per manufacturer's datasheet. Due to commercial confidentiality, the grouts used in this study are named as grouts A, B, C, and D. Grout A is a three-part silica filler reinforced epoxy grout consisting of epoxy resin, hardener, and silica sand. Meanwhile, grouts B, C, and D are two-part epoxy grout consisting of modified epoxy resin and hardener. Grout B is a ferro-silicon filled epoxy resin, grout C is steel reinforced putty, and grout D is ceramic and steel particle reinforced composite. All the fillers for grouts B, C, and D were premixed into the modified epoxy resin, hence the two-parts system.

The preparation of epoxy grouts was carried out as per manufacturer guideline. The epoxy resin, hardener, and silica filler of grout A were weighed based on ratios recommended by the manufacturer datasheet. An electrical mixer was used to thoroughly mix epoxy resin with hardener at low speeds until a smooth consistency was achieved in a clean dry container. It was followed by adding the silica sand filler and mixing all three parts until a homogeneous grout was obtained. Similar to grout A, the epoxy resin and hardener of grouts B, C, and D were weighed according to the manufacturer datasheet. The two parts were then manually mixed on a dry and clean mixing pan until a homogeneous grout was obtained. Figure 1 shows the materials and mixing process for the three-part (top) and two-part (bottom) grouts.

Once the grouts were thoroughly mixed, specially designed steel molds were used in casting the compression, tensile, and flexural test samples for all grouts. The samples were cured at room temperature (about 27 °C) for 24 h prior to testing. All the tests were carried out using an INSTRON 5567 Universal Testing Machine with a capacity of 25 KN. In order to determine Young's modulus, strain gauges for composite (UFLA-5-11-1L) were glued on the surface of compression and tensile specimen. In order to determine flexural modulus and strength, a low voltage displacement transducer was placed at the bottom center of the specimen to measure the deflection of the sample under flexural load. The strain gauges and low voltage displacement transducer were then connected to a data logger so that the strain and deflection can be recorded throughout the testing. Figure 2 shows the mechanical testing for all samples. Table 1 shows a summary of the mechanical properties' tests for all grouts.

In order to investigate the influence of mechanical properties of grouts upon overall repair performance, a finite element (FE) model was developed based on the previously published data. Duell [30] and Duell et al. [29] have carried out a series of experimental studies to investigate the performance of a composite overwrap system used to repair externally corroded pipeline. Different defect geometries (length, width, and depth) and loading conditions (static and cyclic) were simulated in their studies. Since the aim of this study is to investigate the effect of different infill properties toward the overall performance of composite-repaired pipeline, only a case study was chosen. The chosen case was a defective pipe with a 150 mm (6 in) × 150 mm (6 in) × 50% metal loss defect in the center of the pipe and statically pressurized to failure. The pipeline is 168.3 mm (6 in) in diameter with a wall thickness of 7.11 mm (0.28 in), 1.5 m length, ASTM A-106 Grade B, seamless, plain carbon steel. The putty that was used to fill the defect on the pipe is a diglycidyl ether of bisphenol-A based epoxide cured with an aliphatic amine hardener and a thixotropic fumed silica additive. Weave carbon fabric with a similar diglycidyl ether of bisphenol-A epoxy/amine prepolymer resin was used to wrap around the defective pipe and was cured after 24 h to form a rigid composite overwrap. A total of six layers of composite wrap were applied to cover the defect, giving a repair thickness of 3.1 mm. The properties of the pipe, putty, and composite were obtained through tensile (steel and composite wrap) and compression (putty) tests, and are listed in Table 2. The ultimate strength of steel pipe and composite wrap was 570 MPa and 576 MPa, respectively. The experimental burst pressure of the composite-repaired pipe was 43.1 MPa.

ABAQUS v6.12-1 finite element software package was used to create the model, generate meshes, and perform FE calculations to simulate the burst test. The pipe and putty were meshed as eight-nodes linear hexahedron elements, C3D8R, while the carbon composite wrap was meshed using eight-node linear quadrilateral in-plane general-purpose continuum shell element, SC8R. The mesh size at the defect region of steel pipe, putty, and composite was about 4 mm (along axial and hoop directions). Meanwhile at the radial direction (through thickness), steel pipe defect and putty were modeled in three layers, while six layers were modeled for composite wrap to represent the actual number of composite layers used in experimental work. A total of 111,264, 3840, and 38,160 elements are generated for pipe, putty, and composite wrap, respectively.

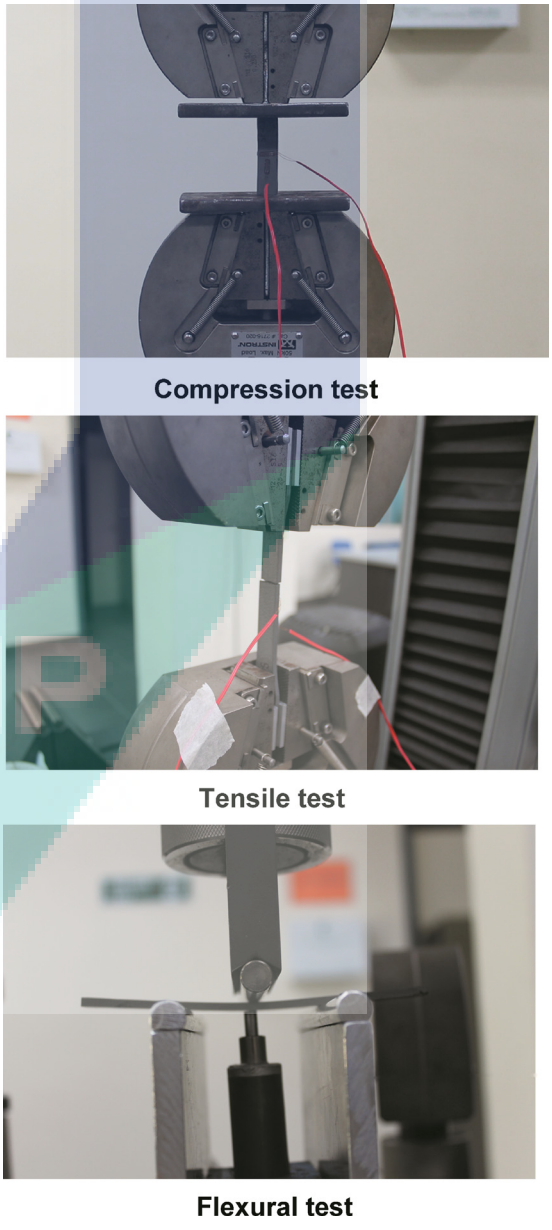


**Fig. 2 Mechanical testing of the grouts**

Figure 3 shows the individual and assembled meshed parts for the composite-repaired pipe model. This is an idealization of the repair where perfect bonding using surface-to-surface tie constraint was assumed between two interfaces which are (i) putty which filled the defect area of steel pipe and (ii) composite wrap which enclosed steel pipe and putty within. This assumption omits the effect such as microvoids at the interfaces of repair which can arise due to variation in material types, curing process, possible shrinkage, and installation technique. Similar assumption has been made by Shouman and Taheri [31] and Chan et al. [16], where the authors found good agreement with measured results. A constant pressure loading condition (slightly higher than the expected failure pressure) was applied incrementally on all of the surface areas of the inside wall of the pipe. Symmetry boundary conditions were applied at both ends of the steel pipe. A von Mises based failure criterion was used to define failure in steel pipe and putty, while maximum stress failure criterion was used for composite wrap. The repaired pipe can be considered as a burst failure when the von Mises equivalent stress in the steel in the finite element analysis (FEA) simulation reaches the ultimate tensile stress and when the maximum stress in the composite exceeds its ultimate tensile strength in one of the principle material directions. The predicted burst pressure from the model will be compared to experimental burst pressure as reported in Duell et al. [29]. Once the developed finite element model was validated with experimental result, a parametric study was carried out by substituting the properties of four tested grouts in this study into the developed finite element model. The burst pressure for all cases will then be compared to evaluate the overall performance with regard to the putty properties.

## 3 Experimental Results and Discussion

**3.1 Compressive Properties.** Adequate compressive strength is required to ensure that the load from the steel pipe can be transferred to the composite overwrap that strengthens the defective pipe. Table 3 shows the summary of compressive properties for all tested grouts. The values in the table represent the average maximum strength prior to sample failure. The value after the ± - sign represents standard deviation. The ultimate compressive strength and Young's modulus were 62.39–87.52 MPa and 6.18–18.93 GPa, respectively. Grout A was found to have highest modulus and strength, while grout B and grout C exhibit lowest modulus and strength, respectively. The strain at ultimate stress of grout A is about half that of the other three grouts, indicating high stiffness behavior of grout A. Three-part epoxy system has silica sand filler compared to other two-part epoxy systems. Thus, three-part silica reinforced epoxy resin gains the advantage and achieved a higher strength and modulus than the two-part epoxy systems used in this study.

Figure 4 shows the typical stress–strain behavior under compression loading for all tested grouts. All grouts show elastic behavior followed by strain softening behavior after ultimate stress. The behavior of grout A was found to be different from other grouts. The stress–strain curve of grout A plummets suddenly beyond ultimate stress region, indicating brittle behavior. The strain at failure for grout A was also the lowest among all tested grouts. The stress–strain relation of three-part epoxy resin is similar to the ideal behavior shown by the fine filled epoxy resin where the stress reduces after maximum stress. This is very similar to compressive behavior of polymer concrete [32]. Grouts B, C, and D show higher reading, two times the strain at failure of grout A. As shown in Fig. 4, the strain softening in the plastic region is more noticeable where grout D exhibits highest plastic deformation. Smooth strain softening beyond ultimate stress is observed in grout B. Chen et al. [33] have defined typical compressive stress strain behavior for polymers into five stages: linearly elastic, nonlinearly elastic, yield-like (peak) behavior, strain softening, and nearly perfect "plastic" flow. The behavior of two-part epoxy systems followed the first four stages in compressive

**Table 1 Summary of test details**

| Tests | Standards | $N$ | Dimensions (mm) | Geometry | Loading rate (mm/min) |
|---|---|---|---|---|---|
| Compressive | ASTM: D695 | 5 | $12.7 \times 12.7 \times 50.8$ | Prismatic | 1.3 |
| Tensile | ASTM: D638 | 5 | $13.0 \times 3.2$ | Dumbbell | 5.0 |
| Flexure (three-point bending test) | ASTM: D790 | 5 | $127 \times 12.7 \times 3.2$ | Prismatic | 1.365 |

**Table 2 Material properties used in finite element model (source: Ref. [29])**

| | Properties | |
|---|---|---|
| Material | Linear (below yield) | Nonlinear (above yield) |
| Steel | Young's modulus, $E = 207$ GPa<br>Poisson's ratio, PR = 0.3 | Yield Stress, $\sigma = 300$ MPa<br>Above yield stress, individual values from the experimental tension tests were used as input for a nonlinear elastic-plastic model |
| Putty | Young's modulus, $E = 1.74$ GPa<br>Poisson's ratio, PR = 0.45 | Yield stress, $\sigma = 33$ MPa<br>Tangent modulus, $E_{tan} = 0.87$ GPa |
| Composite | Young's modulus, $E$<br>$E$ (radial) = 5.5 GPa<br>$E$ (axial) = 23.4 GPa<br>$E$ (hoop) = 49.0 GPa<br>Poisson's ratio, PR<br>$PR_{xy} = 0.430$<br>$PR_{xz} = 0.196$<br>$PR_{yz} = 0.430$<br>Shear modulus, $G$<br>$G_{xy} = 0.69$ GPa<br>$G_{xz} = 29.6$ GPa<br>$G_{yz} = 0.69$ GPa | The nonlinear properties for composite are not available |

Note: The $x$, $y$, and $z$ directions correspond to the radial, axial, and hoop directions, respectively.

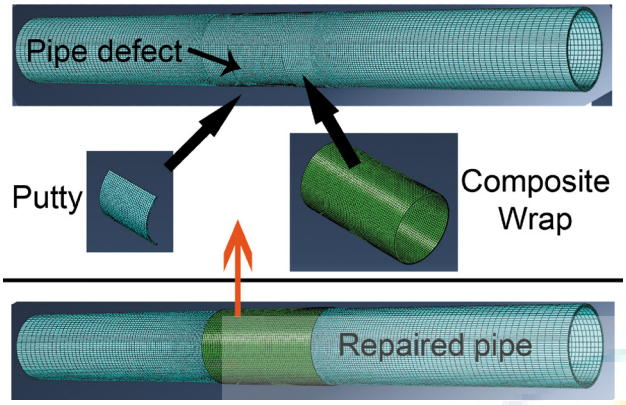


**Fig. 3 Meshed finite element model**

**Table 3 Summary of compression test results**

| Grouts | Young's modulus (GPa) | Ultimate compressive strength (MPa) | Strain at ultimate stress (mm/mm) |
|---|---|---|---|
| A | 18.93 ± 4.78 | 87.52 ± 1.95 | 0.0084 ± 0.0013 |
| B | 6.18 ± 0.39 | 68.07 ± 2.92 | 0.0163 ± 0.0015 |
| C | 7.28 ± 0.63 | 62.39 ± 4.49 | 0.0152 ± 0.0005 |
| D | 6.77 ± 0.80 | 74.86 ± 9.91 | 0.0171 ± 0.0024 |

stress–strain behavior. This behavior is often observed for polymer material under compression loading.

Figure 5 shows the typical failure pattern for all tested grouts. Distinctive failure pattern was found between three-part and two-part epoxy systems. Grout A exhibits brittle failure behavior without any noticeable deformation prior to ultimate stress. A vertical split crack propagating along the center of the sample was observed beyond the ultimate stress. An "explosion" like sound was heard and the stress suddenly plummets sharply when failure had occurred. On the other hand, all two-part epoxy systems (grouts B, C, and D) show noticeable malleability (ductility) behavior. Malleability and ductility are a material's ability to deform under compressive and tensile stress, respectively. These mechanical properties are aspects of plasticity, the extent to which a solid material can be plastically deformed without fracture. Under compression, all two-part grouts exhibit noticeable deformation after the initial elastic stage. Buckling and initial cracks (perpendicular to loading direction) were observed at top and bottom part of the sample where the maximum stress occurred. It was then followed by gradual reduction in stress prior to failure.

**3.2 Tensile Properties.** A summary of tensile test results is tabulated in Table 4. As seen in Table 4, Young's modulus is ranged from 4.66 GPa to 15.38 GPa, while the recorded ultimate tensile strength ranged from 18.90 MPa to 38.94 MPa. Grout A had the highest stiffness and lowest tensile strength. Meanwhile, for two-part epoxy systems, grout B shows lowest stiffness and strength, while highest tensile modulus and strength was recorded for grout D. Modulus of grout A is about two times higher than grout D. On the other hand, the strength of grout D is about two-fold that of grout A. The ultimate tensile strength and strain at ultimate stress show an increase manner from grout A to grout D. Strain of grout A is about 4–5 times lower than other grouts, indicating high stiffness nature of grout A. All grouts show much lower ultimate strength where grout A was about 4.5 times lower while grouts B, C, and D are 2–3 times lower than their respective compressive strength. One has to remember that the fracture in tension is affected by crack propagation. Meanwhile in compression, flaws tend to close and stop propagation, hence the higher strength in compression [34]. The silica sand filler in grout A has larger particle than the filler in grouts B, C, and D. As reported in Shamsuddoha et al. [11], filler with larger particle tends to lower the tensile strength. The matrix-filler interface that experienced de-bonding can reduce the strength of a material.

Figure 6 shows the stress–strain curve for all grouts under uniaxial tensile test. All grouts exhibit much lower ductility under tension as compared with their compression behavior. In addition, the ultimate strength in tension is much lower than those exhibited under compression. As shown in Fig. 6, all grouts exhibit a brittle behavior where no plastic deformation was detected in the stress–strain curve. Linear and slightly nonlinear behavior was observed for all grouts. No noticeable strain hardening or softening behavior can be seen in the graph. Grouts B, C, and D show relatively prolonged deformation as compared to grout A. All samples failed due to splitting, perpendicular to the loading direction when it reached peak stress. Figure 7 shows the fractured sample of all grouts for tensile test. No noticeable deformation such as necking was observed in all samples. Suwanprateeb [35] discussed the failure mechanism of fine calcium carbonate in polyethylene composite. The effect of coarse filler in the resin matrix can be explained in two different ways. First opinion is that the aggregate may be strong enough to provide sufficient

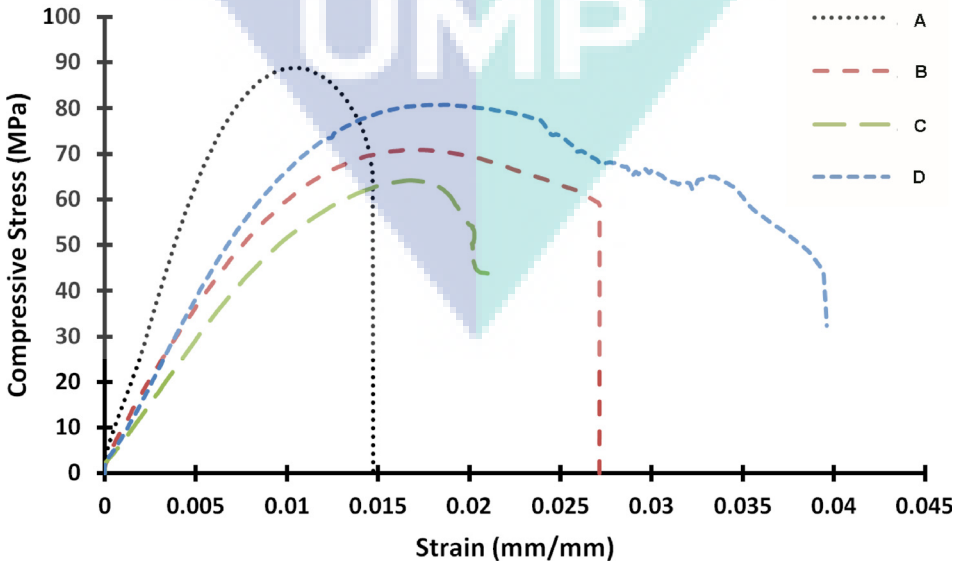


**Fig. 4 Stress–strain behavior of all grouts under compression loading**

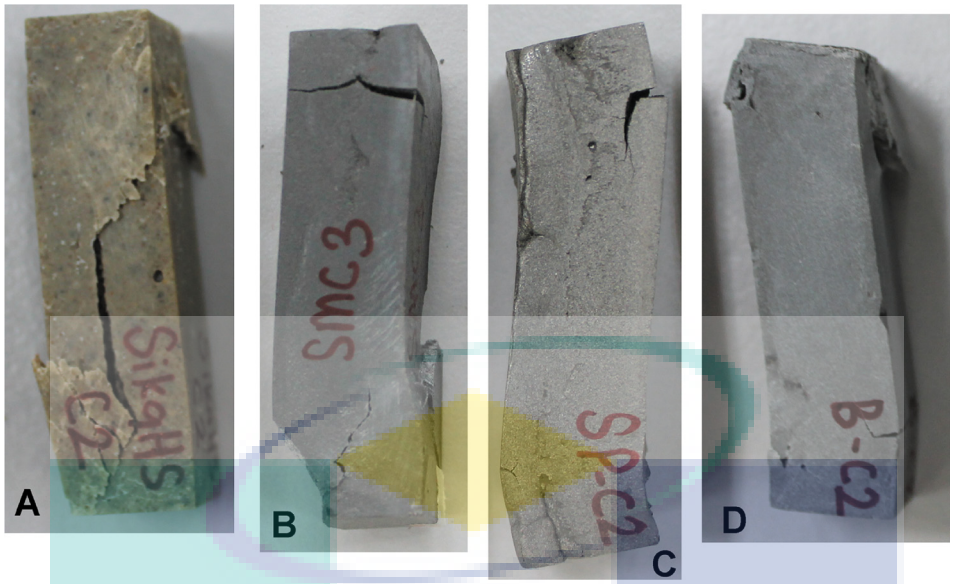


Fig. 5 Failure pattern of compression sample

Table 4 Summary of tensile test results

| Grouts | Young's modulus (GPa) | Ultimate tensile strength (MPa) | Strain at ultimate stress (mm/mm) |
|---|---|---|---|
| A | 15.38 ± 1.26 | 18.90 ± 4.62 | 0.00096 ± 0.00033 |
| B | 4.66 ± 0.30 | 24.55 ± 4.12 | 0.00442 ± 0.00095 |
| C | 6.10 ± 0.27 | 28.92 ± 7.22 | 0.00474 ± 0.00188 |
| D | 8.06 ± 0.19 | 38.94 ± 8.97 | 0.00510 ± 0.00150 |

resistance against failure where the failure occurs at the interfaces of the resin matrix and the aggregate, provided the matrix is also stronger than the interface bonding energy. The second possibility may be that the aggregate is weaker than both the resin matrix and the interface bond. These rigid fillers can act as defects in the composites if the filler is weak or the interface adhesion between fillers and matrix is not strong, which is the case for silica filled epoxy grouts in the present study. This behavior justifies the reduction of strength in the tensile specimens in grout A. Similarly, relative ductility that is seen in grouts B, C, and D which comes from the resin is also reduced. Hence, the stiffness has increased in the coarse filled grout [11].

**3.3 Flexural Properties.** Table 5 summarizes the flexural properties of all grouts under a three-point bending test. Similar to tensile properties, grout A has the highest stiffness (12.643 GPa) and the lowest flexural strength (34.575 MPa) of all grouts. On the other hand, grout B shows lowest stiffness (4.561 GPa) and strength (41.365 MPa), while the highest tensile modulus (6.979 GPa) and strength (61.955 MPa) is recorded for grout D among two-part epoxy systems. The flexural strength of grouts A, B, C, and D is about 40%, 60%, 70%, and 80% of its compression strength, respectively. All grouts showed higher strength but lower modulus as compared to their tensile properties.

The stress–strain response of all grouts under flexural loading is illustrated in Fig. 8. The flexural behavior of all grouts is comparable to their respective tensile behavior. Linear and slightly nonlinear behavior can be seen for all grouts where grouts B, C, and D exhibit prolonged deflection under flexural loading. Grout A

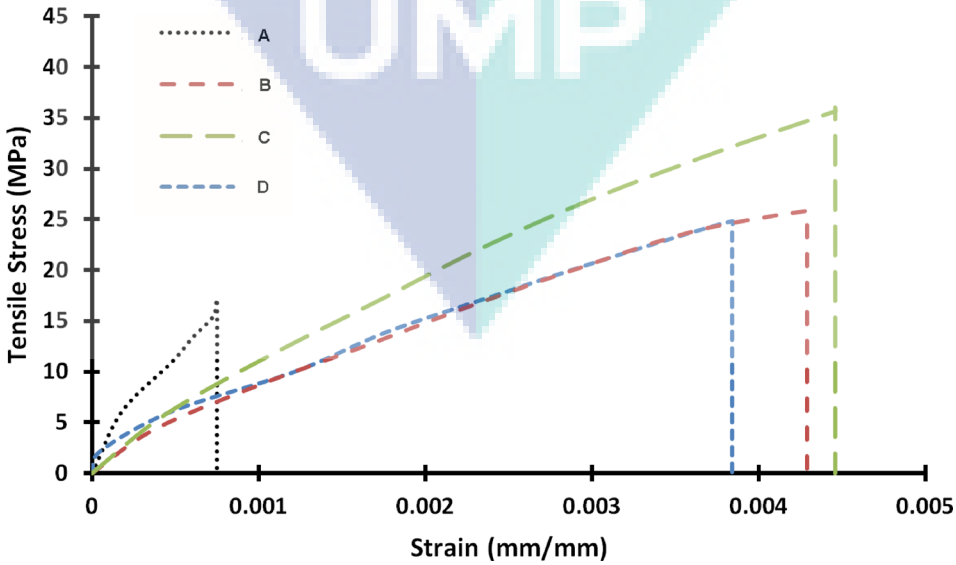


Fig. 6 Stress–strain behavior of all grouts under tensile loading

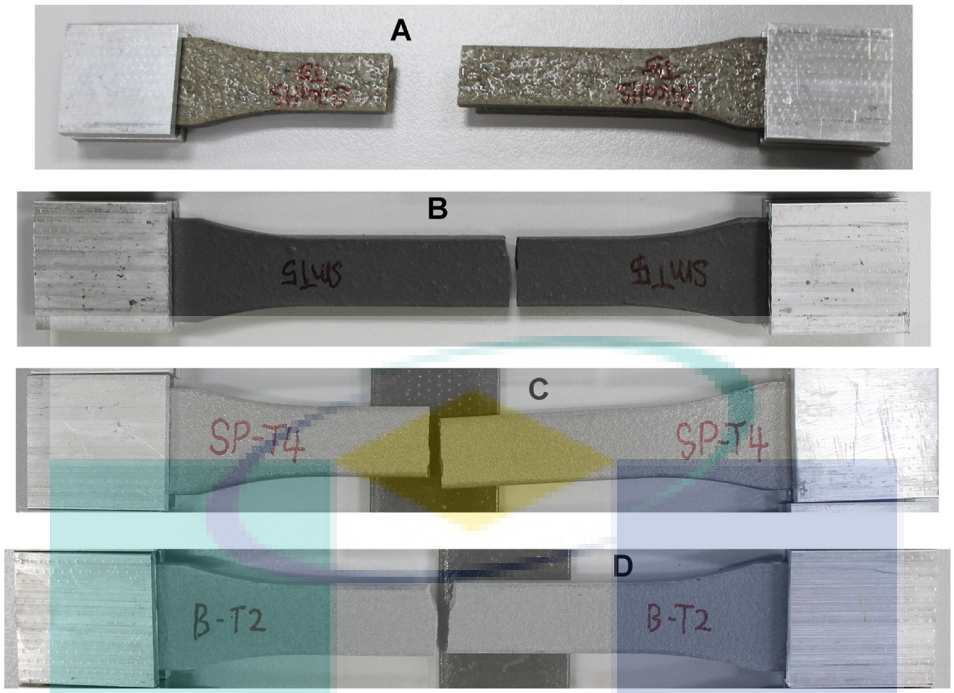


**Fig. 7 Failure pattern of tensile test sample**

**Table 5 Summary of flexural test result**

| Grouts | Young's modulus (GPa) | Ultimate flexural strength (MPa) | Strain at ultimate stress (mm/mm) |
|---|---|---|---|
| A | 12.643 ± 0.464 | 34.575 ± 2.399 | 0.00250 ± 0.00033 |
| B | 4.561 ± 0.349 | 41.365 ± 2.768 | 0.00936 ± 0.00019 |
| C | 4.979 ± 0.290 | 46.086 ± 3.438 | 0.01020 ± 0.00117 |
| D | 6.979 ± 0.478 | 61.953 ± 4.991 | 0.01029 ± 0.00098 |

shows relatively low strain (about four times lower) at ultimate stress where failure occurred. The brittleness of all grouts is indicated by their stress–strain behavior where no plastic deformation was observed beyond ultimate stress, as shown in Fig. 8. The typical failure pattern of all grouts is presented in Fig. 9. As mentioned earlier, all grouts fail in a brittle manner. During the test, a very low deflection was observed in grout A while noticeable bending occurred for grouts B, C, and D under flexural loading. This shows that grout A is relatively less flexible as compared to other grouts. Close examination of the failure surface found that the formation of crack is almost perpendicular to the length of grout A. On the other hand, the cracks for grouts B, C, and D deviated from the tension zone at the bottom of sample and propagate toward compression zone, causing a small wedge at the middle of the sample. The formation of this compression wedge can be related to the increment of strength. It is also noticed that high tensile properties resulted in higher flexural properties as well. These phenomena are discussed by Shamsuddoha et al. [11] where the authors carried out detail characterization of mechanical properties of five epoxy grouts.

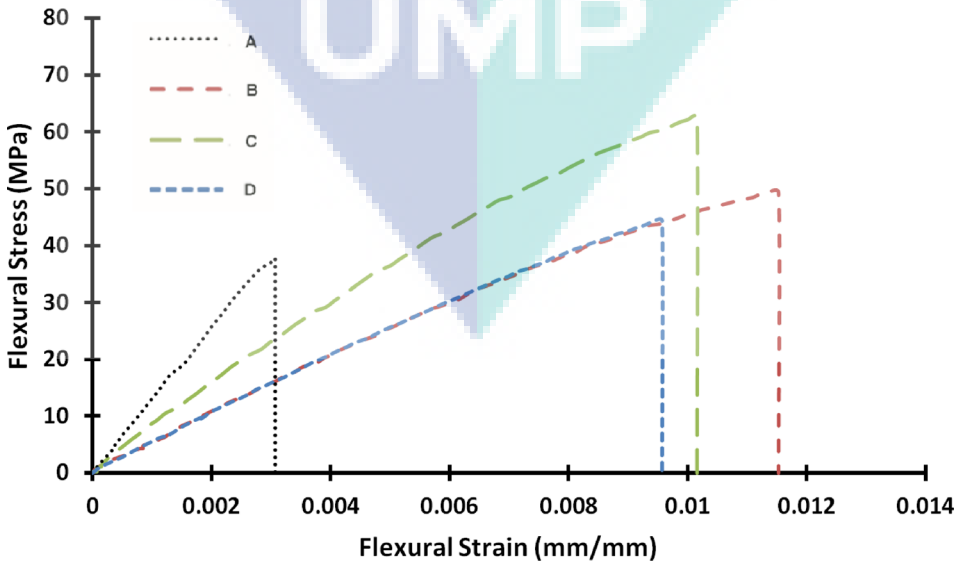


**Fig. 8 Stress–strain behavior of all grouts under flexural loading**

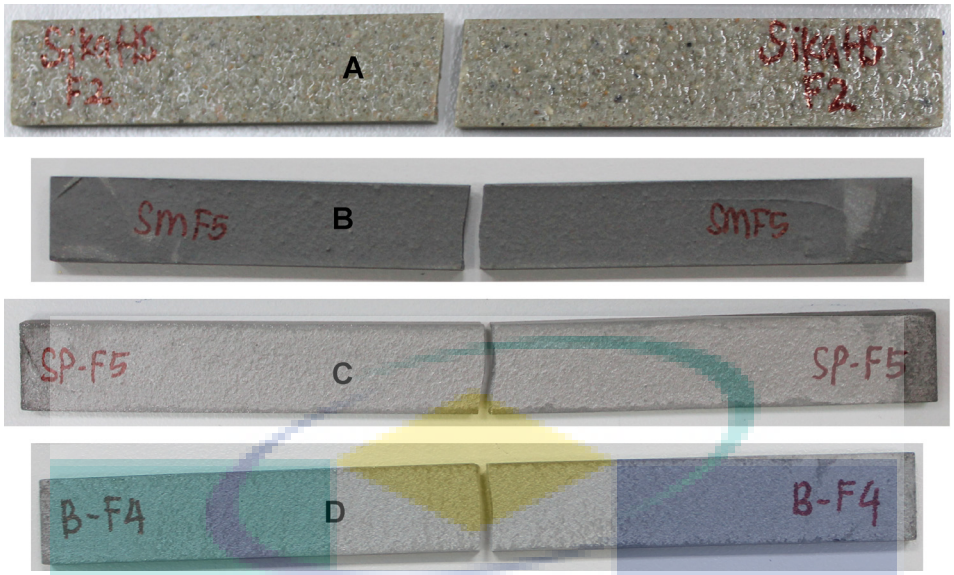


**Fig. 9 Failure pattern of flexural test samples**

**3.4 Finite Element Analysis.** Representative finite element simulation results at the failure pressure are shown in Figs. 10 and 11. The predicted burst pressure of the benchmark model was 38.9 MPa. The margin of error between the benchmark model and the experimental result is 9.7%. Chan et al. [16] investigated the performance of carbon fiber reinforced polyethylene strip for repairing externally corroded defective pipeline. The authors found a good agreement between the simulated and experimental results with margin of error less than 10%. A variation of 10% difference between the simulated and the experimental burst pressure is regarded as acceptable [16,31]. As seen in Fig. 11, highest stress concentration was observed near the edge of the defect region of steel pipe as shown by the arrow. This is the predicted failure location in the model and matches the failure location in the experimental test conducted by Duell et al. [29]. As seen in Fig. 10, at the initial loading stage, the stress of steel pipe was found relatively higher than composite and putty. This phenomenon can be linked to the stiffness of all components. The stiffness of steel pipe (207 GPa) is relatively higher than putty (1.74 GPa) and composite (49 GPa). At this elastic zone, the higher the stiffness, the higher the resultants stress. At this stage, the deformation (bulging) is restricted, and therefore, only small portion of load is being transferred to other components. As the pressure continues to increases beyond the yield stress of the pipe, the stress rate of steel pipe has decreased as indicated by the gradient of the stress-pressure curve. This signifies that the stress of pipe is being largely transferred and shared out to other components. At pressures beyond 29 MPa, the stress in composite has surpassed the stress in steel. As the pressure continues to increase to about 38 MPa, the composite has reached its ultimate stress (576 MPa). At the same applied pressure, a sudden increase of stress was observed in steel pipe (from around 410 MPa to 570 MPa), indicating that the failure in steel pipe has occurred. This can be explained as the additional strength provided by the composite is

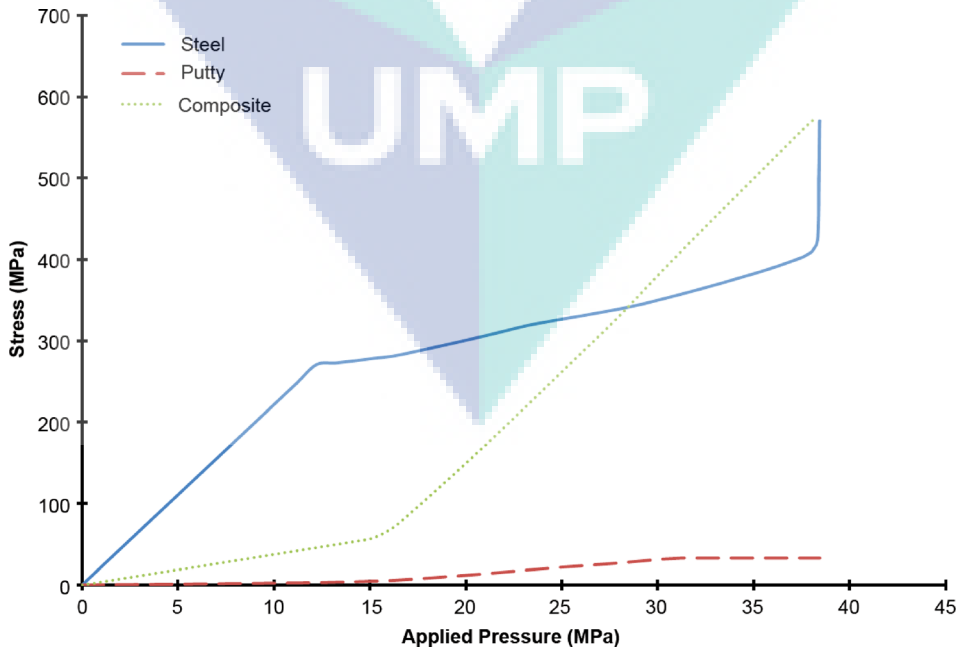


**Fig. 10 Stress versus applied pressure of benchmark model**

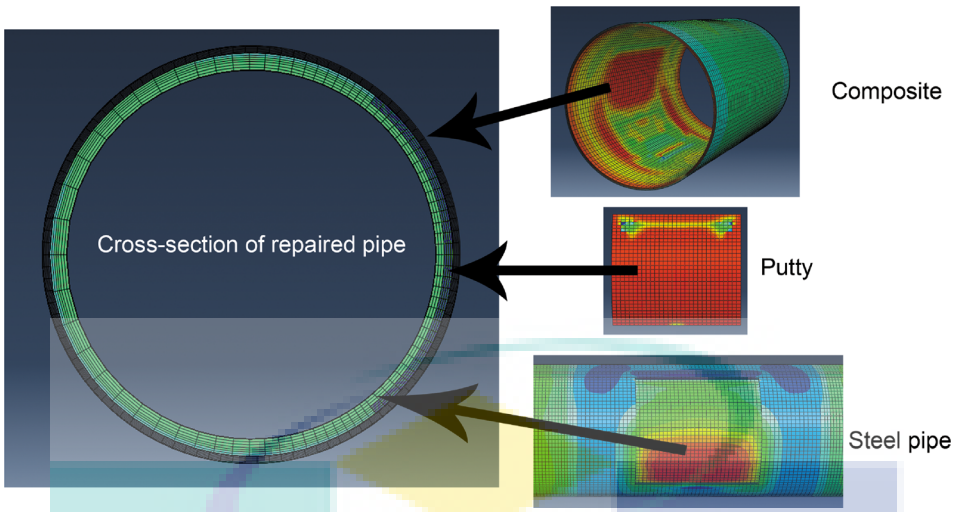


**Fig. 11 Stress contour of finite element model**

**Table 6 Results of FEA**

| Model | FEA burst pressure (MPa) | Percentage difference (%) |
|---|---|---|
| Duell et al. [29], $E = 1.74$ GPa | 38.9 | N/A |
| Grout A, $E = 18.93$ GPa | 41.9 | 7.7 |
| Grout B, $E = 6.18$ GPa | 40.7 | 4.6 |
| Grout C, $E = 7.28$ GPa | 41.3 | 6.2 |
| Grout D, $E = 6.77$ GPa | 41.1 | 5.7 |

Note: Model Duell et al. [29] serves as benchmark model for percentage difference.

taken away, the pipe is the only component bearing the load, and hence, the instant increase of stress, consequently leading to the failure of the repaired pipe.

The results of parametric study using the putty properties that have been characterized in this study are tabulated in Table 6. The predicted burst pressure of benchmark model is regarded as benchmark in evaluating the performance of other putties. As seen in Table 6, the burst pressure has increased by 4.6–7.7%. Grout A and grout B have recorded the highest and lowest increment in burst pressure, respectively. Meanwhile, burst pressure has increased from 38.9 MPa to 41.3 MPa and 41.1 MPa for grout C and grout D, respectively. This result shows an interesting

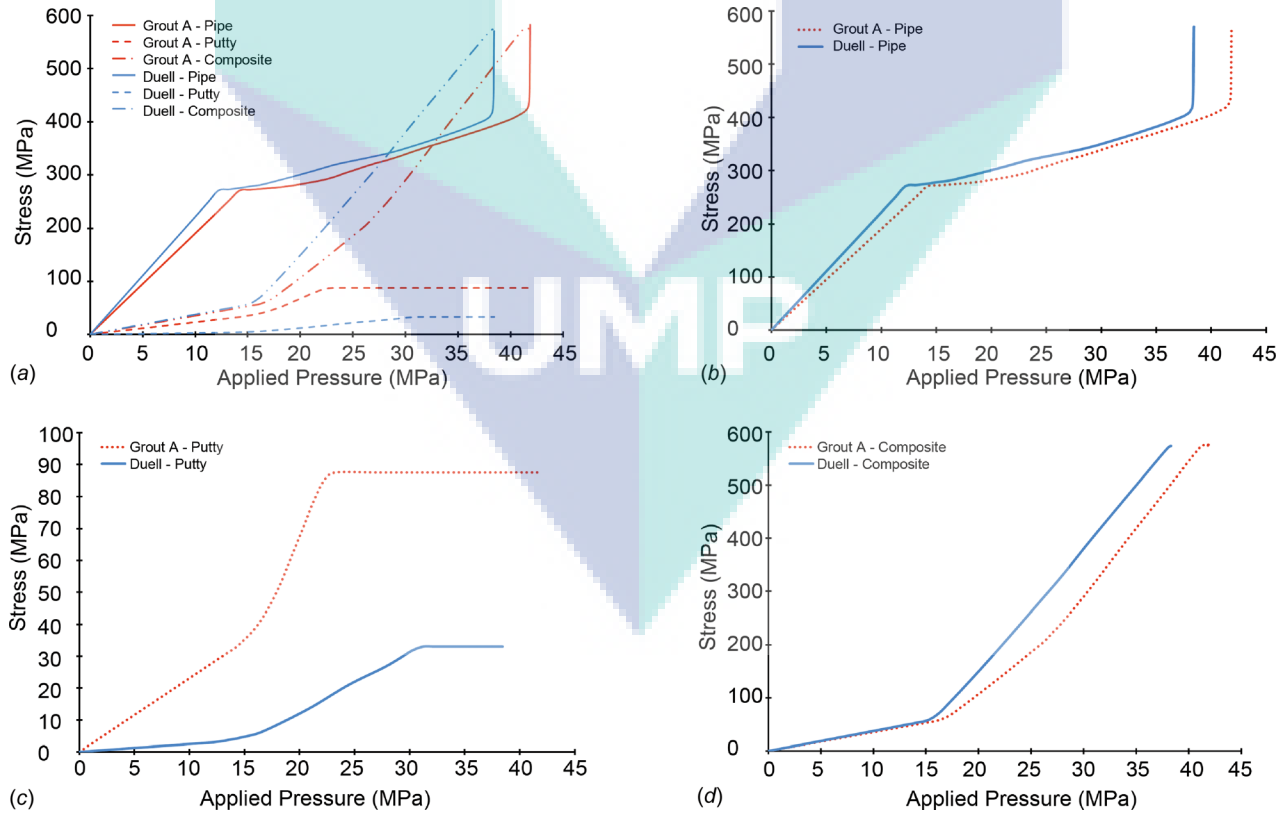


**Fig. 12 Comparison of FEA predicted stress as a function of applied internal pressure in steel pipe for benchmark model and grout A model: (*a*) stress-pressure curve in pipe, putty and composite, (*b*) stress-pressure curve in pipe, (*c*) stress-pressure curve in putty, and (*d*) stress-pressure curve in composite**

indication, where the higher the Young modulus of the grouts, the higher the predicted burst pressure.

In order to provide additional information, a comparison of stresses in composite-repaired pipes corresponding to the increment of applied pressure for benchmark model and grout A model is presented in Fig. 12. Figure 12(*a*) shows the stresses in all components for both models. It was found that the benchmark model has failed at a lower pressure as compared to grout A model. Figures 12(*b*)–12(*d*) illustrate a clearer picture where comparison between stresses in pipe, putty, and composite for benchmark model and grout A model is presented. A comparable stress-pressure pattern can be seen in both models for all components. The result showed that the yield stress was reached first in benchmark model (at applied pressure around 12 MPa) where around 14 MPa of applied pressure was required to cause yielding in grout A model, as illustrated in Fig. 12(*b*). Meanwhile, Fig. 12(*c*) depicts that the stress of putty in grout A model is higher than the benchmark model. The rate of stress development for benchmark model is relatively lower than grout A model, as indicated by a less steep gradient in the stress-pressure curve. In addition, putty in grout A model reaches ultimate stress at a much lower pressure (about 23 MPa) as compared to benchmark model (about 30 MPa). The possible explanation for this phenomenon is that the stiffness and strength of grout A putty is much higher than the benchmark model, thus it experienced a higher stress at lower pressure. As reported in Sec. 3.1, grout A is relatively brittle than two-part grouts; therefore, this result seems reasonable where the behavior of putty used in benchmark model is closer to two-part grouts (low stiffness, hence prolonged deformation). Figure 12(*d*) shows the stress response in composites for both models. Similar to Fig. 12(*b*), stress in grout A model is lower beyond the pressure that caused yielding of steel pipe. As a result, grout A model is able to withstand higher pressure prior to failure. Overall, this parametric study shows that the higher the additional stiffness provided by the grouts, the higher the burst pressure can be obtained, hence the improvement in overall repair performance can be achieved. However, experimental test to further validate the FEA results and provide better understanding in regard to the role of putty toward overall repair performance will be essential.

## 4 Conclusion

Four epoxy grouts were tested to study the behavior under compression, tensile, and flexural loading. Grout A recorded the highest compressive strength, while grout D shows the highest strength under both tensile and flexural test. Meanwhile, grout A was found to be the stiffest material, recording the highest modulus under all loading conditions. On the other hand, grout B shows the lowest stiffness under all tests. All the properties were then used in parametric study to evaluate its effect on composite-repaired pipe via finite element study. A finite element model of externally corroded steel pipe repaired using composite wrap was developed and validated based on a published experimental data. This validated model served as benchmark model. The evaluation of the influence of different infill properties was achieved through replacing the material properties in the present study with the putty properties used in the benchmark model. This is to mimic a scenario if the same repair is to be carried out in the industry, what is the effect of using different putties toward repair performance. If there are any influence that can be determined, it might help the engineer in designing and selecting the most suitable putty so that an optimum result can be achieved. The results show by only changing the properties of infill, about 4–8% increase in burst pressure can be achieved. In addition, this study revealed that a higher pressure is needed to cause yielding at the defect area of steel pipe if stiffer putty is used. It is worth to note that the repair materials (putty and composite wrap) come with wide range of performance (in terms of strength and stiffness). The contribution of high performance putty might be more significant if a lower strength and thickness composite wrap is to be used. Since the results are only gained through numerical study, experimental tests are suggested to further validate this finding. If the contribution of infill can be proven, it is suggested to take this into account in future practice for designing pipeline composite repair. This can help in optimizing the repair design by reducing the conservativeness, which may reduce the cost of pipeline composite repair systems in the future.


## Acknowledgment

The authors would like to specially thank Professor Michael R. Kessler for sharing master thesis of Mr. Joshua Michael Duell that provided detail material properties for the development of finite element model in this study.

## Funding Data

- Universiti Malaysia Pahang (RDU1703239).
- Universiti Teknologi Malaysia (02K77 and 13H27).


## References


[1] Kishawy, H. A., and Gabbar, H. A., 2010, "Review of Pipeline Integrity Management Practices," Int. J. Pressure Vessels Piping, **87**(7), pp. 373–380.

[2] Li, Y., Li, T. X., Cai, G. W., and Yang, L. H., 2013, "Influence of AC Interference to Corrosion of Q235 Carbon Steel," Corros. Eng. Sci. Technol., **48**(5), pp. 322–326.

[3] Tahir, S. N. F. M. M., Noor, N. M., Yahaya, N., and Lim, K. S., 2015, "Relationship Between In-Situ Measurement of Soil Parameters and Metal Loss Volume of X70 Carbon Steel Coupon," Asian J. Sci. Res., **8**(2), pp. 205–211.

[4] Tahir, S. N. F. M. M., Yahaya, N., Noor, N. M., Lim, K. S., and Rahman, A. A., 2015, "Underground Corrosion Model of Steel Pipelines Using In Situ Parameters of Soil," ASME J. Pressure Vessel Technol., **137**(5), p. 051701.

[5] Othman, S. R., Yahaya, N., Noor, N. M., Lim, K. S., Zardasti, L., and Rashid, A. S. A., 2017, "Underground Modeling of External Metal Loss for Corroded Buried Pipeline," ASME J. Pressure Vessel Technol., **139**(3), p. 031702.

[6] CONCAWE, 2013, "Performance of European Cross-Country Oil Pipelines: Statistical Summary of Reported Spillages in 2009 and Since 1971," CONCAWE, Brussels, Belgium, Report No. 3/11.

[7] Lim, K. S., Azraai, S. N. A., Yahaya, N., and Noor, N. M., 2015, "Comparison of Mechanical Properties of Epoxy Grouts for Pipeline Repair," Res. J. Appl. Sci. Eng. Technol., **11**(12), pp. 1430–1434.

[8] United State Department of Transport, 2016, "Plains Pipeline, LP—Failure Investigation Report Santa Barbara County, California Crude Oil Release—May 19, 2015," U.S. Department of Transportation, Washington, DC.

[9] Hsu, J. W., and Liu, F., 2014, "Taiwan Gas Blasts Likely Caused by Faulty Pipe," Wall St. J. (epub).

[10] Shamsuddoha, M., Islam, M. M., Aravinthan, T., Manalo, A., and Lau, K. T., 2013, "Effectiveness of Using Fibre-Reinforced Polymer Composites for Underwater Steel Pipeline Repairs," Compos. Struct., **100**, pp. 40–54.

[11] Shamsuddoha, M., Islam, M. M., Aravinthan, T., Manalo, A., and Lau, K. T., 2013, "Characterization of Mechanical and Thermal Properties of Epoxy Grouts for Composite Repair of Steel Pipelines," Mater. Des., **52**, pp. 315–327.

[12] Azraai, S. N. A., Lim, K. S., Yahaya, N., and Noor, N. M., 2015, "Infill Materials of Epoxy Grout for Pipeline Rehabilitation and Repair," Malays. J. Civ. Eng., **27**(1), pp. 162–167.

[13] Lim, K. S., Azraai, S. N. A., Noor, N. M., and Yahaya, N., 2016, "An Overview of Corroded Pipe Repair Techniques Using Composite Materials," Int. J. Mater. Metall. Eng., **10**(1), pp. 19–25.

[14] da Costa Mattos, H. S., Reis, J. M. L., Paim, L. M., da Silva, M. L., Amorim, FC., and Perrut, V., 2014, "Analysis of a Glass Fibre Reinforced Polyurethane Composite Repair System for Corroded Pipelines at Elevated Temperatures," Compos. Struct., **114**, pp. 117–123.

[15] Alexander, C., 2014, "The Role of Composite Repair Technology in Rehabilitating Piping and Pipelines," ASME Paper No. PVP2014-28257.

[16] Chan, P. H., Tshai, K. Y., Johnson, M., Choo, H. L., Li, S., and Zakaria, K., 2015, "Burst Strength of Carbon Fibre Reinforced Polyethylene Strip Pipeline Repair System—A Numerical and Experimental Approach," J. Compos. Mater., **49**(6), pp. 749–756.

[17] Khan, V. C., Bagalanesan, G., Pradhan, A. K., and Sivakumar, M. S., 2017, "Nanofillers Reinforced Polymer Composites Wrap to Repair Corroded Steel Pipe Lines," ASME J. Pressure Vessel Technol., **139**(4), p. 041411.

[18] Kopple, M. F., Lauterbach, S., and Wagner, W., 2013, "Composite Repair of Through-Wall Defects in Pipework—Analytical and Numerical Models With Respect to ISO/TS24817," Compos. Struct., **95**, pp. 173–178.

[19] Ma, W. F., Luo, J. H., and Cai, K., 2011, "Discussion About Application of Composite Repair Technique in Pipeline Engineering," Adv. Mater. Res., **311–313**, pp. 185–188.

[20] Shamsuddoha, M., Islam, M. M., Aravinthan, T., Manalo, A., and Lau, K. T., 2012, "Fibre Composites for High Pressure Pipeline Repairs, In-Air and

Subsea—An Overview," Third Asia-Pacific Conference on FRP in Structures (APFIS 2012), Feb. 2–4, Paper No. T1A05.
[21] Farrag, K., 2013, "Selection of Pipe Repair Methods," Final Report GTI -Project Number 21087, Gas Technology Institute, Illinois.
[22] Saeed, N., 2015, "Composite Overwrap Repair System for Pipelines—Onshore and Offshore Application," Ph.D. thesis, University of Queensland, Brisbane, Australia.
[23] Dev, R., and Chaubey, D. S., 2016, "World's Oil Scenario—Falling Oil Prices Winners and Losers: A Study on Top Oil Producing and Consuming Countries," Imp. J. Interdiscip. Res., **2**, pp. 378–383.
[24] Haladuick, S., and Dann, M. R., 2018, "Decision Making for Long-Term Pipeline System Repair or Replacement," ASCE-ASME J. Risk Uncertain. Eng. Syst. Part A, **4**(2), p. 04018009.
[25] Barkanov, E. N., Lvov, G. I., and Akishin, P., 2018, "Optimal Design of Composite Repair Systems of Transmission Pipelines," *Non-Destructive Testing and Repair of Pipelines*, Barkanov, E. N., Dumitrescu, A., and Parinov, I. A., eds., Springer, Cham, Switzerland, pp. 387–398.
[26] Dinita, A., Lambrescu, I., Chebakov, M. I., and Dumitru, G., 2018, "Finite Element Stress Analysis of Pipelines With Advanced Composite Repair," *Non-Destructive Testing and Repair of Pipelines*, Barkanov, E. N., Dumitrescu, A., and Parinov, I. A., eds., Springer, Cham, Switzerland, pp. 289–309.
[27] ASME, 2012, "ASME PCC-2 Repair of Pressure Equipment and Piping," American Society for Testing and Materials, New York.
[28] ISO, 2006, "Petroleum, Petrochemical and Natural Gas Industries—Composite Repairs of Pipework—Qualification and Design, Installation, Testing and Inspection," International Organization for Standardization, Geneva, Switzerland, Switzerland, No. ISO/TS 24817.
[29] Duell, J. M., Wilson, J. M., and Kessler, M. R., 2008, "Analysis of a Carbon Composite Overwrap Pipeline Repair System," Int. J. Pressure Vessels Piping, **85**(11), pp. 782–788.
[30] Duell, J. M., 2004, "Characterization and FEA of a Carbon Composite Overwrap Repair System," M.Sc. thesis, University of Tulsa, Tulsa, OK.
[31] Shouman, A., and Taheri, F., 2011, "Compressive Strain Limits of Composite Repair Pipelines Under Combined Loading States," Compos. Struct., **93**(6), pp. 1538–1548.
[32] Chow, T. S., 1991, "Prediction of Stress-Strain Relationships in Polymer Composites," Polymer, **32**(1), pp. 29–33.
[33] Chen, W., Lu, F., and Cheng, M., 2002, "Tension and Compression Tests of Two Polymers Under Quasi-Static and Dynamic Loading," Polym. Test., **21**(2), pp. 113–121.
[34] Ram, A., 1997, *Fundamentals of Polymer Engineering*, Springer Science+Business Media, New York.
[35] Suwanprateeb, J., 2000, "Calcium Carbonate Filled Polyethylene: Correlation of Hardness and Yield Stress," Composites, Part A, **31**(4), pp. 353–359.

Thin-Walled Structures 139 (2019) 321–333

Contents lists available at ScienceDirect

Thin-Walled Structures

journal homepage: www.elsevier.com/locate/tws

Full length article

# Behaviour of steel pipelines with composite repairs analysed using experimental and numerical approaches

Kar Sing Lim[a,*], Siti Nur Afifah Azraai[b], Nordin Yahaya[b], Norhazilan Md Noor[b], Libriati Zardasti[b], Jang-Ho Jay Kim[c]

[a] Faculty of Civil Engineering and Earth Resources, Universiti Malaysia Pahang, Lebuhraya Tun Razak, Gambang, Kuantan, Pahang 26300, Malaysia
[b] Faculty of Civil Engineering, Universiti Teknologi Malaysia, UTM, Skudai, Johor 81310, Malaysia
[c] Department of Civil and Environmental Engineering, Yonsei University, 50 Yonsei-ro, Sinchon-dong, Seodaemun-gu, Seoul, South Korea

ARTICLE INFO

*Keywords:*
Burst test
Composite repair
Finite element analysis
Mechanical properties
Pipeline

ABSTRACT

Over long service periods, pipelines are subjected to deterioration and damage, which can reduce their strength and structural integrity. Repair mechanisms have been developed for restoring the loading capacity of damaged pipelines; in this context, composite-repair systems have become popular over the past few years. The material properties of the repair system components (putty and composite wrap) are critical in designing the repair and understanding the behaviour of a composite-repaired pipe. In this study, the mechanical properties of steel pipe, putty, and composite wrap were investigated individually through laboratory tests. The behaviour of all the materials is discussed to understand their response under various loading conditions. The steel pipes showed the highest tensile strength and modulus. The composite wrap shows better performance during tensile testing than during compression testing. Meanwhile, the putty recorded superior compressive properties as compared to its tensile and flexural properties. The steel pipe shows ductile behaviour while the putty and composite wrap exhibit brittle behaviour. The study was then followed by full-scale pipeline burst tests and finite element analyses on a defective pipe and a composite-repaired pipe. The results show that the burst pressure of the composite-repaired pipe increased by 23% and it experienced significantly reduced strain in the defect region. Detailed information on the burst pressure and strain reading over the entire applied pressure range was recorded for all the components of the burst-test specimens and their behaviour is discussed to achieve a better understanding of composite-repaired pipes. These findings can be very useful in the optimising the existing composite repair design procedures.

## 1. Introduction

Pipelines with a total length of over one million kilometres are laid around the world to transport products, such as oil and natural gas, and new pipelines are expected to be installed in the near future. Among all the countries, the United States of America owns the longest span of pipelines, followed by Russia, Canada, and China with a length of over 50,000 km per country [1]. Despite the fact that steel pipelines are the most effective and safe means for oil and gas transportation over long distances, they are prone to deterioration in the form of corrosion, cracks, dents, wearing, buckling, and gouging, which may potentially lead to leaking and rupture [2–4]. The deterioration of steel pipelines is a common and serious problem experienced by the industry and it may lead to a reduction in the lifespan of the pipeline or a loss in its structural integrity [5,6]. According to Ref. [7], more than 60% of the world's oil and gas transmission pipelines are over 40 years old. Most of these pipelines are in urgent need of rehabilitation in order to function at their desired operating capacity. Therefore, pipeline failures due to corrosion and metal loss and their repair techniques are of intense research interest [8–11].

A wide range of rehabilitation techniques and repair methods are available for onshore and offshore pipelines. In recent years, it has been observed that there is a rapid growth in the development and application of fibre-reinforced polymer (FRP) composites; these composites have been proven to be effective for repairing steel structures, such as risers and pipelines [12–15]. Although products made by different companies and research institutes exhibit a widely varying performance, in general, a composite material repair system includes the following three parts: (i) a high-strength FRP composite wrap/clamp, (ii) a high-performance adhesive, and (iii) a high-compressive infill

* Corresponding author.
*E-mail address:* limks@ump.edu.my (K.S. Lim).

https://doi.org/10.1016/j.tws.2019.03.023
Received 24 July 2018; Received in revised form 16 December 2018; Accepted 8 March 2019

material. FRP composites have been chosen to repair steel pipelines due to their lightweight, high strength and stiffness, excellent fatigue properties, and good corrosion resistance. Despite the many advantages offered by composite repair systems, several issues regarding the behaviour and overall performance of composite repair systems are not yet fully understood. These issues include delamination and de-bonding between the steel pipe and composite material, comprehensive behavioural analysis of the composite-repaired pipe, performance and contribution of the infill, load-transfer mechanism, effect of defect geometries, and conservativeness in the existing closed-form solutions [7,8,16,17]. These gaps in the current body of knowledge demand further investigation in order to achieve a better understanding of the behaviour of composite-repaired steel pipelines and subsequently improve the efficiency of composite repair systems.

Crude oil price has dropped from July 2014 to early 2016 from an average of USD110 to USD40 per barrel. This trend is likely to continue [18], which means a smaller profit margin for oil and gas producers. Therefore, asset integrity management and optimisation has become a major concern for oil and gas producers to save maintenance costs. Grout or putty is usually used as an infill material in composite repair systems. It is generally understood that grout/putty fills the damaged sections (i.e., external corrosion) and provides a smooth bed for the composite wrap instead of serving as a secondary layer of protection and sharing the load. In addition, putty also serves as a medium for load transfer from the corroded pipe to the composite wrap. This is important to provide a continuous support to minimise outward distortion of the corroded section. Therefore, the effectiveness of these repair systems largely depends on the performance of the grout [19–21]. Grout properties are significant parameters in numerical simulations and the theoretical prediction of the behaviour of a repair system. It is therefore essential to characterise the properties of epoxy grouts to determine their efficiency as infill materials in composite repair systems [20]. However, detailed studies on the properties, role, and contribution of putty to composite-repaired pipes are very few in number (both experimental and numerical simulations) due to its assigned limited function in composite repair systems. This lack of information limits the effort to optimise the design of composite repair systems.

Previous studies on composite-repaired pipelines mainly focused on the performance of the composite wrapper instead of the performance of the putty. In most of the past literature, detail information of infill material in a composite repaired pipe is hardly available, such as in the works done by Refs. [10,22,23]. [22] Conducted experimental burst tests and finite element analysis on carbon fibre-reinforced polymer composites strengthened damaged pipes. The pipeline is 168.3 mm diameter with a wall thickness of 7.11 mm, 1.5 m length, ASTM A-106 Grade B, seamless, plain carbon steel, repaired using epoxy putty with carbon fibre reinforced polymer (CFRP) composite overwrap. Simulated defects were machined into the pipe wall to mimic external corrosion with a longitudinal length of 152.4 mm and a depth of 50% wall thickness. For the first specimen, the hoop dimension defect length was 152.4 mm. For the second specimen, the hoop dimension defect length was completely around the circumference (axisymmetric defect). Six layers of composite wrap were applied to cover the defect, giving a repair thickness of 3.1 mm. The properties of the pipe, putty and composite were obtained through laboratory test and were used to develop finite element models. Two specimens were hydrostatically tested in this study. The specimens were pressurised to rupture pressure. The repaired specimen burst violently as the composite wrap segment exploded apart with a longitudinal crack running the full length of the defect region. The recorded burst pressure for first and second specimens was 43.1 MPa and 43.8 MPa, respectively. This information was used to validate the developed finite element model. Results obtained from the numerical modelling using the ANSYS finite element software package were in good agreement with experimental results. Two additional finite element models with a defect of 25.4 mm and 76.2 mm in the hoop direction were developed to study the effect of defect length on hoop direction. The predicted burst pressure for 25.4 mm and 76.2 mm specimens was 43.8 MPa and 44.8 MPa, respectively. A comparison of repair thickness using a design code based on ASME PCC-2 was performed for evaluation purposes [24]. Based on a burst pressure of 44 MPa, the minimum repair thickness of composite wrap was calculated as 4.57 mm. This is higher than the 3.1 mm of composite wrap used in the FEA model with a similar predicted burst pressure. The author pointed out possible reasons for the ASME standard over predicting minimum repair thickness. These include the strain hardening of steel after yielding, defect geometry, and the presence of putty are not considered in the closed-form solution. The authors concluded that defect length in the hoop direction had little impact on failure pressure under monotonic loading. This study compares the burst pressure of experimental test and numerical simulations. The strain reading for the steel, putty, and composite is not reported; hence comparison is not feasible to validate the behaviour of the repaired pipes. It is also noted that compressive properties were used as input in a bilinear material model for putty. It is understandable that compressive properties is required to transfer the load from the damaged pipe to the composite wrap, however, the main stress for a pressurised pipe is hoop stress and is commonly associated with tensile properties. Furthermore, the bilinear material model used in this study does not account for the failure limit of the putty. Therefore, the additional reinforcement provided by the putty in this simulation might differ from its actual behaviour.

Due to the nature of operational requirement, cyclic loads are often experienced by pipelines [23]. conducted experimental tests to compare the effectiveness of composite repair and steel sleeves. Steel pipe specimens of grade X42, with a diameter of 12.75-inchs and a thickness 0.753-inchs were used to produce 75% corrosion samples with an 8-inch and 6-inch defect in the axial and hoop directions, respectively. A 4-inch diameter with a 15% dent was introduced onto the external wall of a grade X42, 12.75-inch diameter, and 0.188 inch thickness pipe. All samples for each defect cases were repaired using E-glass FRP composite wrap, Type A and Type B steel sleeves. The defect region was filled with incompressible load transfer putty. The repair thickness of the composite wrap was 0.625-inch (10 layers) based on design calculations performed prior to the repair. Strain gauges were installed onto the defect surface and external composite layer to monitor strain during testing. Fatigue and burst tests were conducted for all samples. The burst test results revealed that the performance of the composite wrap was comparable to Type A and Type B steel sleeves as the specimens failed outside the repaired region. This indicates that the repair was not only able to restore the damaged pipe to its original performance, but has also exceeded the original strength of the pipe. In another word, the repair might be over designed. In addition, composite repaired corrosion samples was observed able to reduce the hoop strain levels to those similar to steel sleeve repairs at the pressure correspond to 72% Specified Minimum Yield Strength (SMYS) of the pipe. On the other hand, under cyclic test, the composite repaired sample failed at 198550 and 149913 cycles for the corrosion and dent samples, respectively. No failure occurred for steel sleeve repaired samples indicating the effectiveness of steel sleeves reinforcement in withstanding cyclic load. The author also performed calculation to estimate the remaining life of the pipes, subjected to similar fatigue cycle. It was reported that composite repaired corrosion and dent samples could last for 58 and 594 years, respectively. Even though performance was lower than steel sleeve repair, it is regarded as adequate for most operating scenarios. Thus the author concluded that composite repair could be a viable means of repairing pipeline defects such as corrosion and dent when properly designed.

In a recent study [10], investigated the performance of carbon fibre reinforced polyethylene strip for repairing externally corroded defective pipeline. In order to achieve the objective, experimental test was carried out and supported by finite element analysis. API 5L X52 steel pipeline with a dimension of 219 mm diameter and 12.7 mm thickness

was machined with a 50% wall loss to simulate external corrosion. The defect was 622 mm in axial direction and over the full circumferential (hoop direction). The defect was filled with epoxy grout before the composite strip was installed. Finite element model of the composite strip repaired pipeline was developed with ABAQUS software. The material properties of the steel pipe were extracted from previous published work by Ref. [25]. On the other hand, the input of epoxy grout was taken from measured data where only the elastic properties (Young's modulus) of putty was used in the model. Several assumptions and theories were applied when deriving the orthotropic properties of composite strip due to insufficient measured data. The ASME PCC-2 standard was used to design the thickness of the composite strip. A limit state analysis technique known as double elastic curve was employed in this study to determine the maximum allowable hoop strain correspond to the design pressure and burst pressure. Three models were developed and analysed for a (a) bare pipe; (b) corroded pipe, and (c) composite repaired corroded pipe. The results were reported in good agreement with experimental test and numerical simulation for composite repaired corroded pipe. As no experimental test was conducted for the other two cases, the author compared the burst pressure with industry standard. It was observed that the repaired pipe showed a higher burst pressure than the bare pipe, indicating the capability of the composite strip in restoring strength, similar to the result as reported in Ref. [23]. However, the failure patterns for both studies were different, as the failure in this study occurred within the repaired region, which is closer to the failure pattern as seen in work done by Ref. [22]. Therefore [10], suggested studies on the sensitivity of different variables that govern the repair can be conducted in future.

A group of researcher have spent considerable time and effort in characterisation and the failure pressure estimation of composite repaired pipeline [26–29]. [26] Investigated with an alternative repair system using two grout systems: silicon steel alloy filled polymers and oligomers, and epoxy resins with aluminium powder. The compressive strengths of the materials were 56 and 104 MPa while tensile strengths were 59 and 67 MPa, respectively. It was also suggested to apply the above mentioned materials and then to cover using a composite material sleeve to assure a satisfactory level of structural integrity. About four years later [27], has carried out burst test and long-term pressure test on produced water pipelines containing through-thickness defect that were repaired with epoxy system (without composite wrap). A year later [28], has published another study on failure estimation of localized corroded pipelines. In year 2016 [29], has extended the methodology used in Refs. [27,28] to propose a simple methodology to predict the failure pressure of a reinforced pipeline with arbitrary geometry of the corroded region and considering any composite repair system. These researchers utilized a set elasto-plastic constitutive equations for thin-walled metallic pipe for pressure estimation for all works in Refs. [27–29]. It was concluded that with a simple algebraic expression, a reasonable estimate for the failure pressure of a corroded thin-walled pipe reinforced with an arbitrary composite glove can be obtained. This estimate only requires the knowledge of the elastic modulus of the composite in the circumferential direction and of the ultimate stress of the pipe material obtained in a tensile test, besides a few information about the geometry (composite thickness, pipe inner diameter and wall thickness and the average geometry of the defect). Indeed, these works have provided essential information on the estimation of failure pressure for undamaged, localized corrosion and composite repaired pipe. On the other hand [11,20], carried out detailed characterisation of the infill material (epoxy grouts) to explore the potential of these grouts being used as infill for pipeline repair. They found that three grouts have the potential to be used for pipeline repair when comparing the tested mechanical properties to some other literature. However, no repair work was carried out, owing to which a complete evaluation of these infill materials in composite repair systems was not feasible.

In most of the experimental burst tests conducted in previous investigations, strain gauges were used to record the strain experienced by the repaired pipe. The effectiveness of a repair system in reducing strain is considered important for battling deformation, such as the bulging and buckling of a repaired pipe. Previous studies reported strain readings only for the steel pipe and composite wrap. These readings were used as an indicator to evaluate the performance a particular repair system. However, the strain experienced by the putty was not monitored and hence the contribution of the infill could be evaluated. Because information on the actual properties of all the materials used in composite-repaired pipes is lacking, the behaviour of composite-repaired pipes is not yet fully understood. Therefore, in this study, we take an initial step to investigate the overall behaviour of a composite-repaired pipe through comprehensive experimental tests and numerical analysis. Detailed material characterisation of all the components used in the composite repair system was carried out followed by experimental burst tests and finite element analysis (FEA). Strain reading of each component was recorded during the burst tests and compared with the FEA results to achieve a comprehensive understanding of the overall behaviour of composite-repaired pipes.

## 2. Materials and methods

### 2.1. Material characterisation

Three types of materials were used in this study: a segment of a steel pipe, an epoxy grout/putty, and a pre-impregnated FRP composite wrap. API 5L Grade B steel pipe (6 m in length) with dimensions of 168.3 mm (outer diameter) and 7.11 mm (wall thickness) was used in this study. The tensile properties together with stress-strain curve of a steel pipe are very important in determining its load-carrying capacity and critical for both theoretical calculations as well as numerical simulations. In order to determine the tensile properties of the pipe, dumbbell-shaped sheet-type tensile specimens were machined from the pipe segment in accordance with ASTM E8 guidelines [30]. The width of the narrow section was 12.5 mm and the overall length of the specimen was 200 mm. The width and thickness of the specimen were measured and recorded. Tensile tests based on ASTM E8 were conducted to determine the Young's modulus and strength of the steel pipe. In addition, two burst-test specimens were also produced from the same pipe segment, namely defective pipe and composite-repaired pipe. This is to minimise possible variations in the properties of tensile and burst-test specimens.

A commercially available pre-impregnated FRP composite wrap was used to repair one of the defective pipes. The composite wrap is made from a 0°/90° bi-directional E-glass fibre impregnated with a specially formulated epoxy resin manufactured by a company in Malaysia. Eight specimens were produced for each direction (hoop and axial) to determine the tensile and compressive properties corresponding to the loading directions. The samples were cured at room temperature for five days according to the manufacturer's guidelines. Tensile and compression tests were conducted on the composite wrap according to the ASTM D3039 [31] and ASTM D6641 [32] guidelines, respectively. The putty used to fill the defect is a commercially available three-part silica filler-reinforced epoxy grout. It consists of an epoxy resin, a hardener, and silica sand. An electric mixer was used to thoroughly mix the epoxy resin, hardener, and silica filler until a homogeneous grout was obtained. Once the grouts were thoroughly mixed, specially designed steel moulds were used to cast the compressive, tensile, and flexural test samples for all grouts. The samples were cured at room temperature (about 27 °C) for 24 h prior to testing. Compressive, tensile, and flexural tests were carried on the epoxy grout according to the ASTM D695 [33], ASTM D638 [34], and ASTM D790 [35] guidelines,

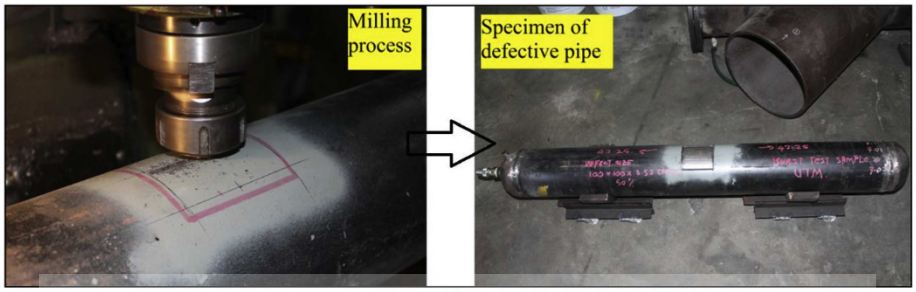


Fig. 1. Machining defects on steel pipes.

respectively.

Mechanical testing of all the materials was conducted on an INSTRON 25 KN universal testing machine. In order to calculate the Young's modulus, strain gauges were installed on the compression and tensile samples and a linear variable displacement transducer (LVDT) was used on the flexural samples (epoxy grout) to record strain and deflection, respectively. A data logger was used to continuously record the readings of the strain gauges and LVDT until the samples failed. The objective of conducting these tests is to provide a fundamental understanding of the mechanical-failure behaviour of composite repair systems, such as brittleness or ductility, subjected to the aforementioned loadings. Furthermore, this information would be used as input for FEA at a later stage.

### 2.2. Experimental pipeline-burst tests

Two burst-test specimens were used in this study – defective pipe and repaired pipe. Defects of 100 mm × 100 mm × 3.555 mm were machined on their external surfaces at mid length to simulate 50% volumetric surface defects due to corrosion. The machining process was carried in a controlled manner using milling machine in order to achieve a uniform defect. The defect was measured using a digital calliper to ensure the dimension of the defect is as desired. This is the common practice in simulating external corrosion effect on a pipeline. The defect-machining process is shown in Fig. 1. Two spherical end caps of a high strength were used to cover both ends of the pipe. A fitting for the pressure inlet and "bleeding point" was welded onto one of the end caps. The function of the "bleeding point" is to remove any trapped air bubbles in the pipe to prevent pressure inconsistencies during the burst test. The end caps were then welded to the steel pipe.

One of the defective pipes was repaired using the composite wrap and putty at zero pressure. Waterproof strain gauges were installed at various locations on the pipe, including the centre and edge of the defect. Epoxy grout was used to cover the whole region of the defect and a smooth surface was formed. The putty was allowed to cure for 24 h at room temperature before the composite wrap was applied. Composite-wrap repair was carried out after 24 h when the grout was considered fully cured. Waterproof strain gauges were installed on the surface of the cured putty. The locations of the installed strain gauges are similar to those installed on the defect surface. A primer, which was supplied with the composite wrap, was used as an adhesive to bond the pipe with the composite wrap. The wrapping process was carried out layer by layer. The process was conducted manually and the composite was wrapped by hand around the pipe. After the first layer was almost fully wrapped, a steel roller was used to remove air bubbles along the axial and hoop directions throughout the repair region. The process was repeated until a total of three layers (representing a thickness of 3 mm) of composite wrap were applied. The repaired pipe was then cured for five days prior to burst testing. The process of wrapping is depicted in Fig. 2.

An electric hydraulic pump with a maximum pressure capacity of approximately 70 MPa was used to pressurise the pipes. The pump was connected to the pressure inlet attached to the end cap. A pressure gauge was installed to record the pressure experienced by the pipe throughout the burst test. The readings of the pressure gauge were recorded in a video format to enable the analysis of pressure over time. The strain gauges were then connected to a data logger to record strain readings at various locations before the burst test was conducted. The burst test was conducted according to the procedure followed by Ref. [23]. The burst-test procedure was similar for all the specimens and included the following steps.

1. Take a photo of the specimen before testing.
2. Start the data logger in order to record the strain reading.
3. Increase the pressure at an approximate rate of 0.1 MPa per second.
4. Increase the pressure up to approximately 72% of the specified minimum yield strength (SMYS) and hold for 5 min.
5. Continue to increase the pressure up to approximate 100% of SMYS and hold for another 5 min.
6. Increase pressure until failure occurs.
7. Take a photo of the failed specimen.

The burst pressure and strain reading were recorded for analysis at a later stage.

### 2.3. Finite element analysis

ABAQUS® v6.12-1 finite-element software package was used to create the model, generate meshes, and perform finite element (FE) calculations to simulate the burst tests. The pipe and putty were meshed as reduced integration, 8-nodes linear brick elements of type C3D8R, while the composite shell was modelled as a reduced integration, 4-nodes shell element of type S4R. A total of 121,968 and 2268 elements were generated for the steel pipe and putty, respectively. The elements of the steel pipe were connected by 153,953 nodes, while 3248 nodes connected the elements of the putty. On the other hand, 12,432 elements connected by 12,580 nodes were generated for the composite shell. The analysis duration was set to 500 s with a linear increase in pressure to 50 MPa, which simulates a loading rate of 0.1 MPa/s. The non-linear effects concerning large displacement have been considered in this analysis.

Fig. 3 shows the meshed defective pipe, putty, composite, and repaired pipe. This is an idealisation of the repair process, where perfect bonding is assumed between the two interfaces, which are the i) putty filling the defect area and the steel pipe and ii) composite wrap, which encloses the steel pipe and putty within. This assumption does not take into account the effect of micro-voids at the interfaces of repair; voids can arise due to variations in the material type, curing processes, possible shrinkage, and installation techniques. Similar assumptions were made by Refs. [10,36]; these authors found a good agreement between

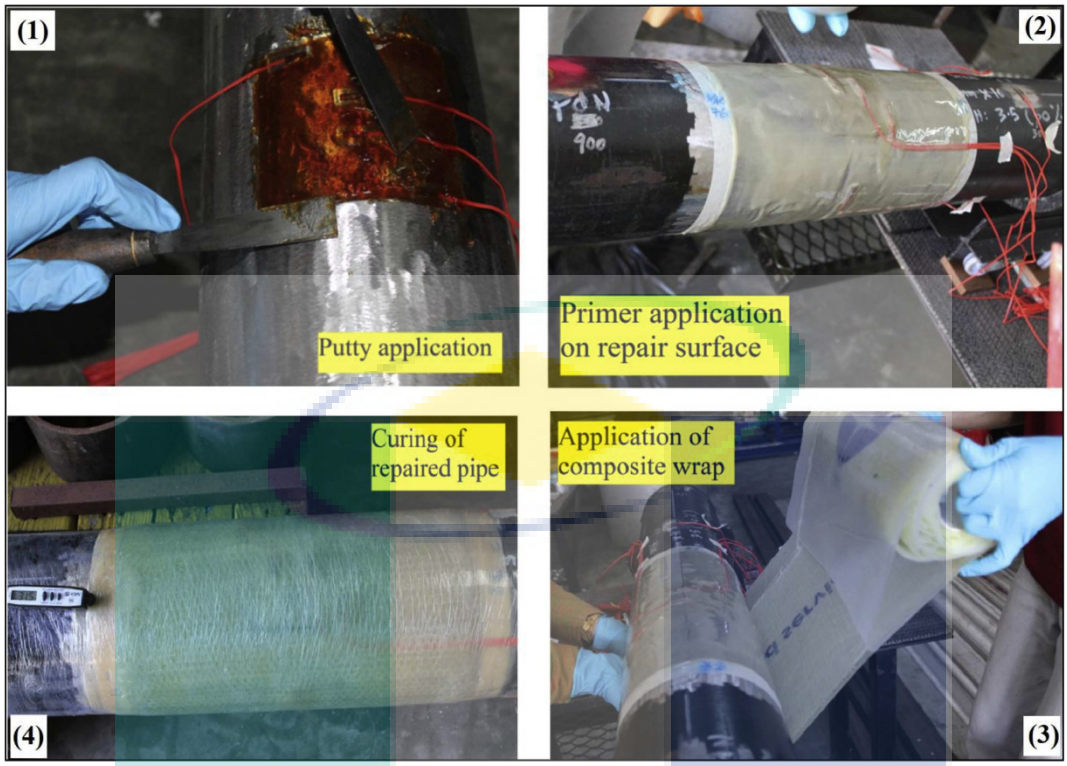


**Fig. 2.** Application of composite wrap on the defective pipe.

the simulated and experimental results. A constant pressure-loading condition (slightly higher than the expected failure pressure) was applied incrementally on all of the surfaces of the inside wall of the pipe. A von Mises-based failure criterion was used to define failure in the steel pipe and putty, while Hashin failure criteria was used for the composite wrap. The von Mises criterion is often used in determining whether an isotropic and ductile metal (in this case, the steel pipe) will yield when subjected to a complex loading condition while the Hashin

**Table 1**
Tensile properties of the API 5L Grade B steel pipe.

| API 5L Grade B Steel Pipe | Young's Modulus (GPa) | Ultimate Tensile Strength (MPa) | Yield Strength (MPa) |
|---|---|---|---|
| Tensile Properties | 221.37 | 480.13 | 293.27 |

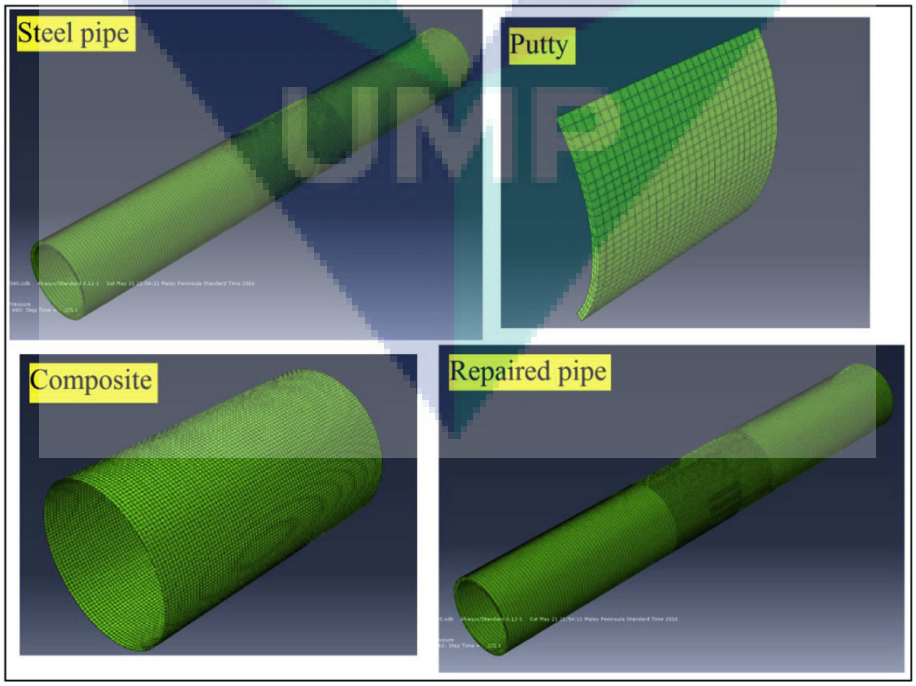


**Fig. 3.** Meshed models of the steel pipe, putty, composite, and repaired pipe.

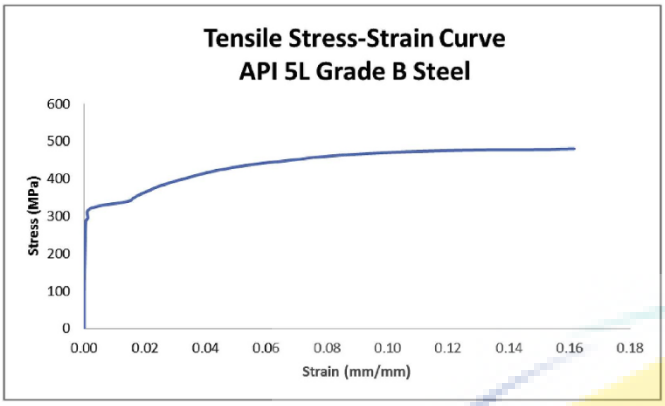


Fig. 4. Stress-strain curve of the steel pipe.

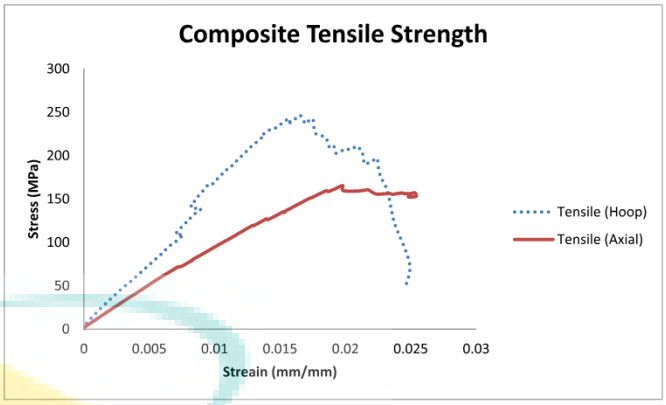


Fig. 5. Tensile stress-strain behaviour of the composite wrap.

failure criterion is suitable to capture the progressive failure of a FRP composite.

## 3. Results and discussion

### 3.1. Material characterisation

#### 3.1.1. Steel pipe

Table 1 shows the tensile properties of the steel pipe specimens. It can be seen that the Young's modulus, ultimate tensile strength, and yield strength were 221.37 GPa, 480.13 MPa, and 293.27 MPa, respectively. The tensile stress-strain curve of the steel pipe is shown in Fig. 4. Linear-elastic behaviour can be observed in the early loading stage followed by plastic deformation and strain hardening. The obtained curve is typical of ductile materials in the tensile mode. In the elastic zone, due to the high stiffness of steel, deformation was relatively small. When the stress was increased to the yield stress, plastic deformation was observed, followed by strain hardening before sample failure.

#### 3.1.2. Composite wrap

Table 2 summarises the tensile test results corresponding to the composite wrap. The values in the table represent the average maximum strength prior to sample failure. The value after the ± sign represents standard deviation. The Young's modulus and ultimate tensile strength were found to be 14.34 GPa and 241.27 MPa, respectively, in the hoop direction. In the axial direction, the modulus and ultimate strength were 10.09 GPa and 169.43 MPa, respectively. The strength and modulus of the composite wrap in the hoop direction were about 40% higher than those in the axial direction. The hoop-direction samples show a slightly lower strain at the peak stress compared to axial samples. The strains at failure for both samples were about the same, as depicted in Fig. 5. However, the stress-strain characteristics of the samples were different. In the case of the hoop sample, in the elastic zone, strain increased with stress up to the peak stress. Beyond the ultimate stress, a progressive failure resembling a non-smooth strain-softening behaviour was observed. Meanwhile, as seen in the same figure, in the axial sample, strain continued to increase without any increase in stress, even beyond the peak stress, before sample failure occurred. During testing, a glass-breaking sound followed by a shattering sound corresponding to the glass fibres was heard when the sample experienced peak stress.

**Table 2**
Tensile properties of the composite wrap.

| Tensile | Young's Modulus (GPa) | Ultimate Tensile Strength (MPa) |
|---|---|---|
| Hoop | 14.32 ± 1.14 | 241.27 ± 11.32 |
| Axial | 10.09 ± 0.73 | 169.43 ± 9.40 |

**Table 3**
Compression properties of the composite wrap.

| Compression | Young's Modulus (GPa) | Ultimate Compressive Strength (MPa) |
|---|---|---|
| Hoop | 11.47 ± 1.32 | 55.55 ± 6.02 |
| Axial | 11.60 ± 2.08 | 80.78 ± 7.48 |

The compression test results of the composite wrap in the hoop and axial directions are listed in Table 3. The Young's moduli of both sets of samples were found to be comparable. A higher compressive strength was observed in the axial sample. The Young's moduli of the hoop and axial samples were 11.47 GPa and 11.60 GPa, respectively. Meanwhile, the hoop sample recorded a 55.55 MPa ultimate strength and the measured compressive strength of the axial sample was 80.78 MPa, which is approximately 45% higher than that of the hoop sample. These observations do not agree with the tensile test results, where the strength of the hoop sample was found to be ~40% higher than that of the axial sample. The stress-strain behaviour of the hoop and axial samples is illustrated in Fig. 6. A similar behaviour was observed; both samples failed in a brittle manner as depicted by a sharp drop in stress at the ultimate stress. The failure strain of the hoop sample was about one order lower than that of the axial sample; this behaviour is different from its tensile behaviour.

#### 3.1.3. Putty

Table 4 shows a summary of the mechanical properties of the tested putty after curing for 24 h. The ultimate strength values corresponding to compression, tensile, and flexural tests were 87.52 MPa, 18.90 MPa, and 34.58 MPa, respectively. Meanwhile, the Young's moduli during compression, tensile, and flexural tests were 18.93 GPa, 15.38 GPa, and

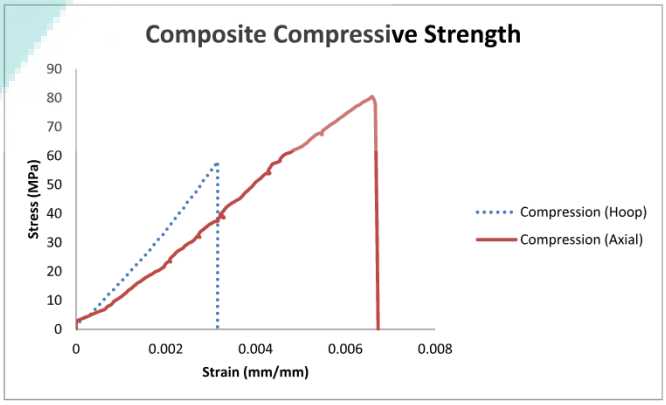


Fig. 6. Compression stress-strain behaviour of the composite wrap.

**Table 4**
Mechanical properties of the putty.

| Properties | Ultimate Strength (MPa) | Young's Modulus (GPa) |
|---|---|---|
| Compression | 87.52 ± 1.95 | 18.93 ± 4.78 |
| Tensile | 18.90 ± 4.62 | 15.38 ± 1.26 |
| Flexural | 34.58 ± 2.40 | 12.64 ± 0.46 |

12.64 GPa, respectively. Fig. 7 shows the stress-strain curves of the tested putty under compression, tensile, and flexural conditions. A linear and slightly non-linear behaviour was observed in the tests. No noticeable strain hardening or softening could be observed in the graphs. The stress-strain curve plummeted suddenly beyond the ultimate stress region, which indicates brittle behaviour. This is very similar to the compressive behaviour of polymer concrete. Fig. 8 shows the typical failure patterns of the tested putty. The putty exhibits brittle failure behaviour without any noticeable deformation prior to ultimate stress. During compression testing, a vertical crack propagating along the centre of the sample was observed beyond the ultimate stress. An 'explosion'-like sound was heard and the stress plummeted sharply when failure occurred. No noticeable deformation, such as necking or bending, was observed during tensile and flexural tests [37]. discussed the failure mechanism of fine calcium carbonate in polyethylene composites. The effect of fillers in the resin matrix can be explained in two different ways. According to the first theory, the filler may be strong enough to provide sufficient resistance against failure when failure occurs at the interface of the resin matrix and filler, provided the matrix is stronger than the interface. The second possibility may be that the filler is weaker than the resin matrix and interface. In this case, the rigid fillers act as defects in the composites, which is the case for silica-filled epoxy grouts in the present study. This behaviour justifies the reduction in strength in the tensile specimens of the putty. The highest strength and modulus were recorded under compression testing. The tensile strength of the putty is about 20% of its compressive strength, which indicates a low tensile-compression ratio. This indicates that the tested

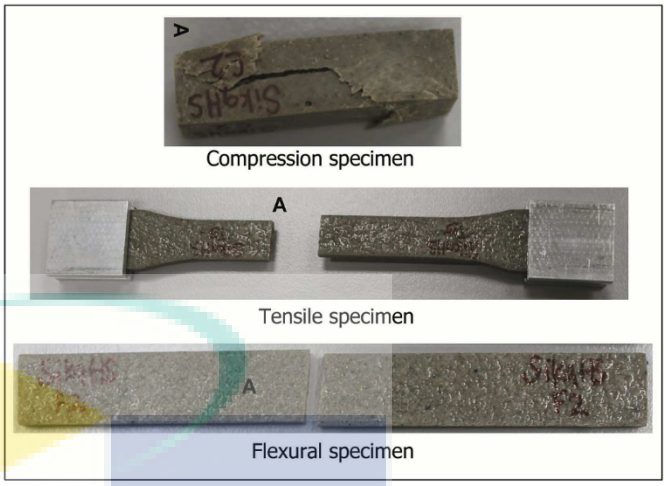


**Fig. 8.** Failure patterns of putty under various loading conditions.

putty is more suitable for combined loading systems that require a high compressive strength but only a low tensile strength. As stated by Ref. [21], the load transfer between the infill and pipe wall plays an important role, especially in reducing the stress level in the defect area.

### 3.2. Pipeline-burst tests

#### 3.2.1. Defective pipe

The first burst test was conducted on a pipe simulating a 100 mm × 100 mm defect with 50% wall loss due to external corrosion. It was expected that failure would occur at the defect region due to metal loss. Strain gauges were installed at three different locations, one at the middle of the defect, one near the edge of the defect, and one in the non-defect region at a length approximately one-fourth of the total length of the pipe. The recorded burst pressure for this specimen was 26.8 MPa. Fig. 9 depicts the pressure-strain curve recorded for the

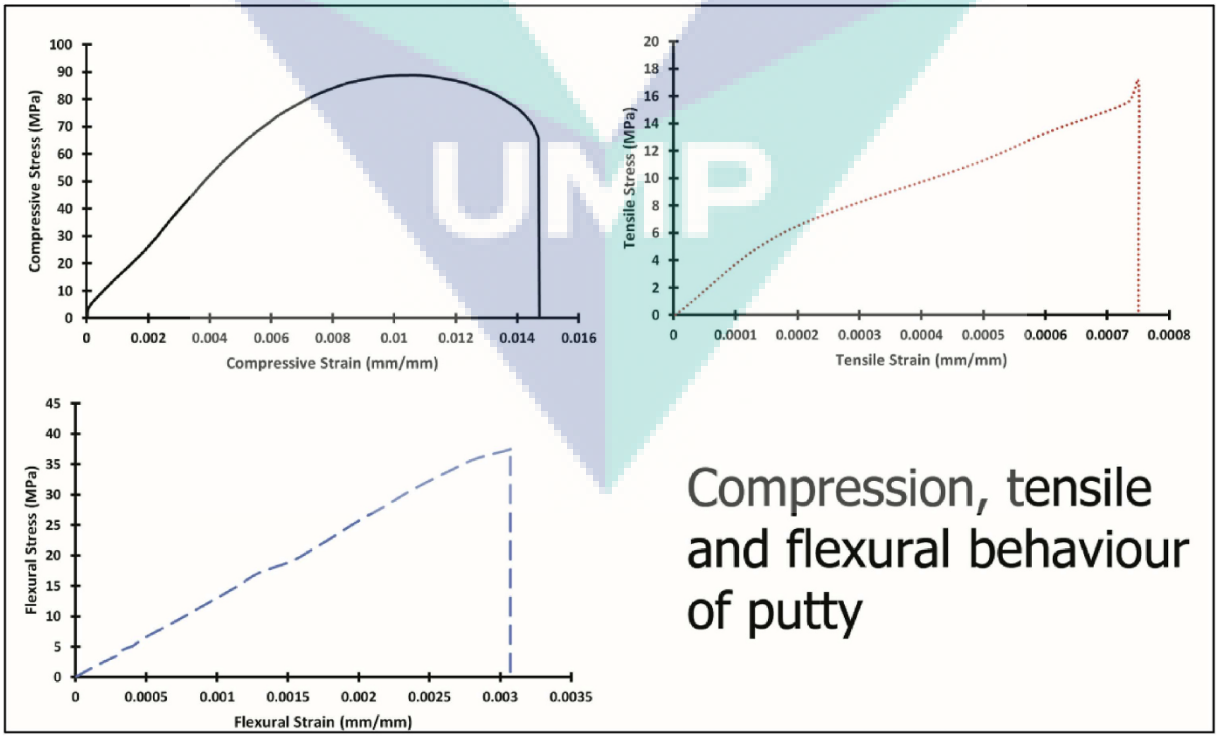


**Fig. 7.** Stress-strain behaviour of putty under various loading conditions.

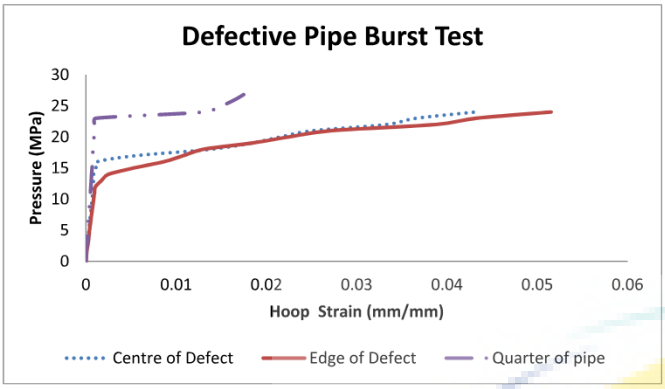


**Fig. 9.** Pressure-strain curve of the defective pipe.

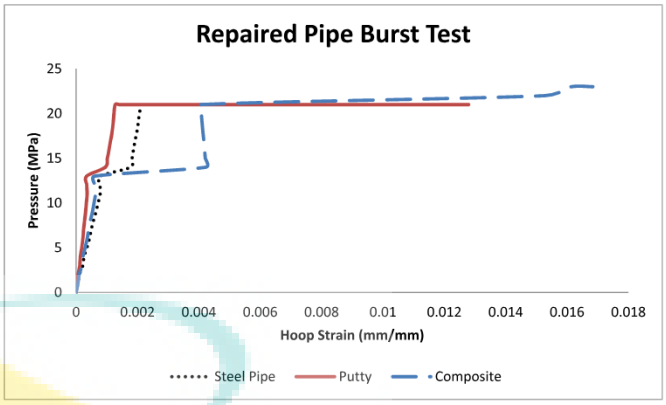


**Fig. 11.** Pressure-strain curve of the repaired pipe.

defective pipe. The strain readings in the defect region of the pipe were recorded up to a pressure of 24 MPa only due to the failure of the strain gauges beyond this pressure. This may be due to a bulging effect, which broke the strain gauges. As expected, strain in the non-defect region (quarter length of the pipe) was relatively lower than that in the defect region, signifying a relatively lower stress as compared to the defect region. The pressure-strain behaviour at all locations shows a comparable pattern at the beginning of the pressure load. Yielding at the edge of the defect was observed at the lowest pressure followed yielding in the middle of the defect and the non-defect region. The yield pressures of the edge of the defect, middle of the defect, and non-defect regions were about 12 MPa, 15 MPa, and 22 MPa, respectively. The pressure-strain behaviour corresponding to the middle and edge of the defect was comparable at pressures beyond 17 MPa. The edge of the defect recorded a higher strain than the middle of the defect, which indicates that larger deformation occurred near the edge of the defect. On the other hand, the strain reading of the non-defect region was three times lower than that of the defect region at the burst pressure. Fig. 10 shows the failed defective pipe. Failure was observed near the edge of the defect with a crack running along the axial direction of the pipe. This failure pattern also matched the pressure-strain behaviour, where a larger deformation was observed near the edge of the defect.

### 3.2.2. Composite-repaired pipe

The second burst test was conducted on a similar defective pipe repaired using the composite wrap and putty. The objective of this test is to study the behaviour of composite-repaired pipes to determine the additional strength provided by the composite wrap and putty. It was found that composite repair successfully strengthened the defect region, resulting in a higher burst capacity compared to the defect pipe. The burst pressure of the repaired pipe was 33 MPa, which is 23% higher than that of the defective pipe. Strain gauges for all the components failed much earlier than the repaired pipe. Strain gauge readings for the steel pipe and putty could be recorded only up to 21 MPa, while the strain reading for the composite wrap could be recorded up to 23 MPa.

The pressure-strain curves of all the components of the repaired pipe are shown in Fig. 11. These curves were used to study the behaviour of all the components with respect to deformation and applied pressure. As can be seen in Fig. 11, at the initial stage of loading, the strain reading of all the components exhibits a small linear increment. When the pressure was increased to 13 MPa and held for 5 min, the strain in the composite increased significantly. On the other hand, strain in the steel pipe and putty increased by only a small amount. It is also observed that strain variation occurred in each component, signifying differences in the deformation experienced by each component. As mentioned in previous studies, a high stiffness is crucial for preventing pipe deformation. According to the results of material characterisation, the stiffness of the composite wrap is lower than that of the steel pipe and putty; hence, a larger deformation in the composite is justifiable. Considering the larger deformation, the strain gauge placed at the middle of the putty might have been crushed due to internal pressure causing bulging; this might have compressed the strain gauge towards the inner surface of the composite wrap. The tensile strength of the putty is relatively low compared to the tensile strengths of the steel pipe and composite wrap. A part of the putty might have failed under the application of hoop stress during the 5-min it was held at pressure of 13 MPa. During this time, the putty loses its stiffness. This hypothesis is supported by the strains recorded for the putty; strain reading at the centre of the putty surface could only be recorded up to 13 MPa. The failure pattern for the repaired pipe is shown in Fig. 12. Failure occurred near the edge of the defect region; this region is enlarged in the figure for a better view. A close examination of the failure region revealed that the putty was brittle and broke into multiple pieces.

As mentioned in previous studies, putty with a high compressive modulus might increase the overall repair performance of a composite repair system [21,22,38]. The additional stiffness provided to the

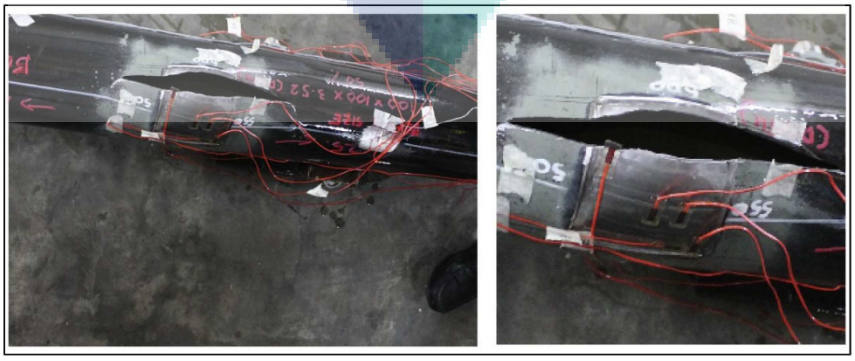

**Fig. 10.** Failure pattern of the defective pipe.

**Fig. 12.** Failure pattern of the repaired pipe.

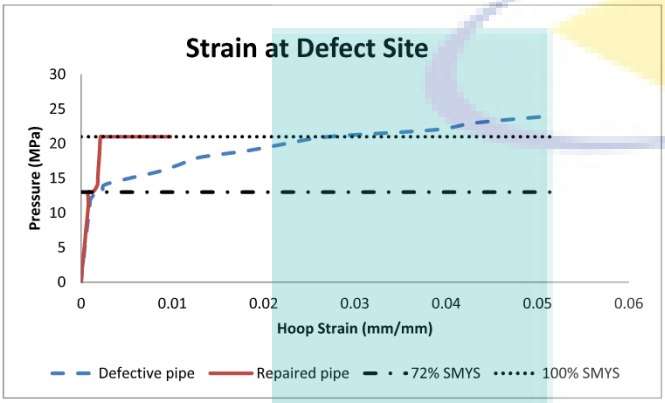


**Fig. 13.** Comparison of strains in the defective and repaired pipes.

damaged pipe is deemed important as it can help in reducing the strain on the pipe, thus preventing early yielding of the damaged section [9]. It is often desired that a composite repair system, in addition to increasing the ultimate burst capacity, should reduce the strain on a pipe to ensure that integrity is restored to the damaged section [9]. Fig. 13 illustrates the pressure-strain curves of the defective and repaired pipes. These curves are used to investigate the performance of the composite-repair system in reducing strain on the defect surface. Pressures corresponding to approximately 72% SMYS and 100% SMYS of the pipes are also shown in the figure for a discussion on strain reduction. As shown in Fig. 13, at a pressure of 13 MPa (corresponding to 72% SMYS), the strain readings of the defective and repaired pipes were recorded as 0.002427 mm/mm and 0.001259 mm/mm, respectively. The repaired pipe shows a lower strain than the defective pipe, which indicates a strain reduction on the defect surface. When the pressure is further increased to 21 MPa (corresponding to 100% SMYS), strain in the defective pipe increased significantly to 0.027109 mm/mm, which signifies that the damaged section yielded, which in turn induced a large deformation. Meanwhile, for a similar pressure differential, only a small increment was observed in the strain of the repaired pipe. The recorded strain for the repaired pipe was 0.002119 mm/mm. This indicates that during the pressure increment process, the composite repair system successfully restrained deformation in the damaged section. In addition, the strain at 100% SMYS of the repaired pipe is still lower than the strain at 72% SMYS of the defective pipe. This is an extremely significant observation and it gives us to understand that the integrity of the damaged section was successfully restored in the repaired pipe.

The thickness of the composite wrap used in the current study was 3 mm for the repaired pipe. The burst pressure was recorded as 33 MPa for the repaired pipe. If a similar pressure is used in accordance with ASME-PCC2, a minimum thickness of about 8 mm is required. This is about 2–3 times higher than the repair thickness used in the current study, indicating the conservative nature of the current design codes. Similar findings can be found in the works of [23]. This conservativeness is also highlighted by Refs. [17,22]. [9] Justifies this conservativeness in terms of the shortage of data on the long-term performance of the composite wrap. The author stated that the polymer-based composite wrap might potentially experience a loss of strength over time; hence, a large safety margin is needed to accommodate this degradation as well as the uncertainties. However, in order to optimise the current design philosophy, this conservativeness needs to be gradually reduced [17,39]. As putty is a part of the composite repair system, the inclusion of its strength contribution should be considered in the closed-form solution of composite-repair design. Thus, the optimisation process can be started by including the putty's contribution into the existing closed-form solution. This can be done through a parametric study by changing the properties of the putty and determining the changes in the burst capacity. Under these circumstances, an increment or reduction in the burst capacity might be quantified, thus opening a window of opportunity to improve the current design codes. Therefore, a comprehensive study to investigate the effect of putty towards the overall repair performance is needed to provide a better understanding of the role of putty in composite-repaired pipes.

### 3.3. Finite element analysis

#### 3.3.1. Finite element analysis of the defective pipe

After the material properties for FEA were determined, a model to simulate the burst test of the defective pipe was created. The accuracy and efficiency of FEA largely depends on the meshing size of the model. Therefore, mesh convergence analysis was conducted to determine the optimal mesh size; it ranged from 24 mm to 1.7775 mm. The results of the mesh convergence are tabulated in Table 5. The total number of elements exponentially increased beyond the 7.11 mm mesh size while the predicted burst pressure gradually decreased as the mesh size was reduced. A percentage difference between mesh sizes was calculated based on the reduction of a particular mesh size. For example, the percentage difference between the 24 mm and 12 mm mesh sizes is 0.23% and the difference between the 7.11 mm and 3.55 mm mesh sizes is 0.14%. As the mesh size was reduced to 2.37 mm, the number of elements increased by 3.4 times, but the difference for predicted burst pressure between the 3.55 mm and 2.37 mesh sizes is less than 0.05%. As the mesh size is further reduced to 1.7775 mm, the predicted burst pressure remained the same. Therefore, with consideration towards the

**Table 5**
Results of mesh convergence study.

| Mesh Size (mm) | No. of Element | Predicted Burst Pressure (MPa) | Percentage Difference (%) |
|---|---|---|---|
| 24 | 1200 | 42.05 | – |
| 12 | 4400 | 41.95 | 0.23 |
| 7.11 | 12096 | 41.92 | 0.07 |
| 3.55 | 94640 | 41.86 | 0.14 |
| 2.37 | 321816 | 41.85 | 0.04 |
| 1.7775 | 757120 | 41.85 | 0 |

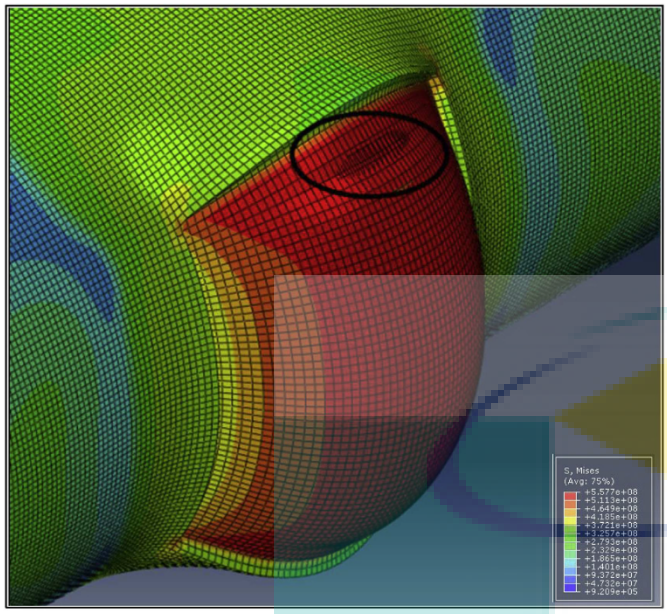


**Fig. 14.** Stress contour and failure at the defect region of the defective pipe model.

accuracy and efficiency of analysis time, mesh size of 3.55 mm was selected for the numerical simulation. As the defect region is the predicted critical stress concentration region, a denser mesh with a smaller element size (1.7775 mm) was used to generate the mesh of this area. The pipe and putty were meshed as reduced integration, 8-nodes linear brick elements of type C3D8R with a total of 121,968 elements and 153,953 nodes. The predicted burst pressure of the defective pipe model was 28.78 MPa, which is about 7.39% higher than the 26.8 MPa burst pressure recorded in experimental studies. It is noted that the strain readings in the experimental tests are available only up to pressures of 24 MPa and hence comparisons beyond this pressure are not feasible.

Fig. 14 illustrates the stress contour plot of the defect region of the defective pipe. This figure was enlarged to show the details of the predicted failure location. As seen in Fig. 14, bulging occurred at the defect region and caused failure along the axial direction of the pipe, similar to the failure pattern and location observed in experimental tests. Fig. 15 depicts the pressure-strain curves obtained using FEA and experimental tests. As seen in Fig. 15, the experimental results in the defect region were reasonably well predicted by the FEA model. The two lines show linear-elastic behaviour with small increments in strain at pressures lower than 13 MPa. In addition, strain readings for the

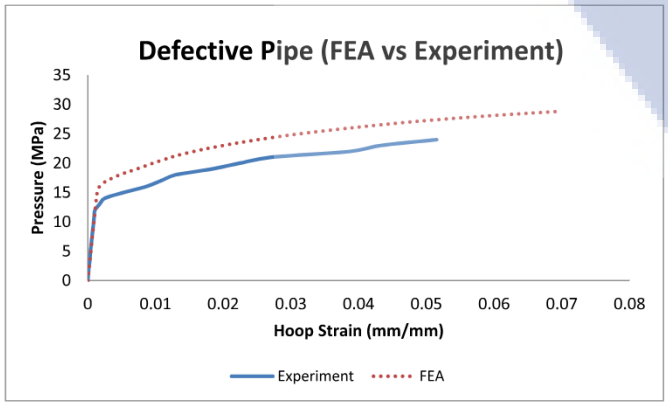


**Fig. 15.** Comparison between the experimental and FEA results of the defective pipe.

**Table 6**
Model study of the putty material for the repaired pipe.

| Material Model | Burst Pressure (MPa) | Accuracy (%) |
|---|---|---|
| Elastic only | 40.13 | 22.15 |
| Bilinear-compression | 38.54 | 16.79 |
| Bilinear-tensile | 36.86 | 11.70 |
| Tensile elastic-perfectly plastic | 31.77 | 3.73 |

elastic zone were almost accurately predicted by the model. A large deformation was observed in the experimental results beyond a pressure of 13 MPa, indicating that yielding occurred at this pressure. Meanwhile, FEA predicted yielding at a pressure of 15 MPa. It was found that the FEA model slightly over predicted the performance of the defective pipe with lower strains at a similar applied pressure when compared to the experimental results. This may due to the FEA assumes a perfect condition of pipeline concerning the material properties while in reality, the material properties of the pipe might slightly varies as throughout the pipe body. Therefore, based on comparison of predicted burst pressure, pressure-strain curve, and failure location, the capability of the developed defective pipe model in simulating the test conditions of a real environment is confirmed.

### 3.3.2. Finite Element Analysis of the Repaired Pipe

There is very limited information available on the numerical simulations of putty. Owing to this limitation, some putty properties were either extracted from secondary sources or only the elastic modulus was considered. Different material models in numerical simulations were proposed by different researchers [10,22,36,40]. This indicates mixed opinions on the modelling of putty behaviour. In addition, there is a discrepancy in property (compression, tensile, or flexural) selection. This makes a comparison between experimental results and numerical simulations less comprehensive. Thus, in this study, we make an attempt to develop a material model good enough to be used for modelling the putty for composite-repaired pipes.

Four finite element models were developed using different material models for the putty and their predicted burst pressures are presented in Table 6. From the results, it was found that only the tensile elastic-perfectly plastic model was a good predictor, with an error margin of 3.73%, when the burst pressure of the repaired pipe is considered (the experimental burst pressure is 33 MPa). All other models were found to over predict the burst pressure by 12%–22%. To further confirm the accuracy of the chosen tensile elastic-perfectly plastic material model for putty, the pressure-strain curve of this model was compared with the experimental results. However, the strain reading for the experimental test was not fully recorded due to the failure of some strain gauges. Experimental strain readings are only available up to 21 MPa (pipe and putty) and 23 MPa (composite) of the applied pressure. Hence, only these data sets were compared.

Fig. 16 compares the experimental and FEA-predicted pressure-strain curves corresponding to the surface of the pipe defect (top left), putty (top right), and composite (bottom left). As can be seen in Fig. 16, the experimental and FEA strain readings of the pipe defect were similar to each other up to 18 MPa, indicating that the simulated result is good up to this point. When the applied pressure exceeded 18 MPa, the FEA model predicted a slightly higher strain than the experimental results, which signifies that the FEA slightly underestimated the performance of the pipe up to a pressure of 21 MPa. Fig. 16 (top right) depicts the comparison between the experimental and FEA results corresponding to the putty. Similarly, with respect to the steel pipe, it was found that the FEA model marginally under-predicted the performance of the putty, which was reflected by a higher strain reading at an equivalent applied pressure. On the other hand, the FEA model was found to slightly overestimate the performance of the composite, as can be seen in the bottom left portion of Fig. 16. The experimental and FEA

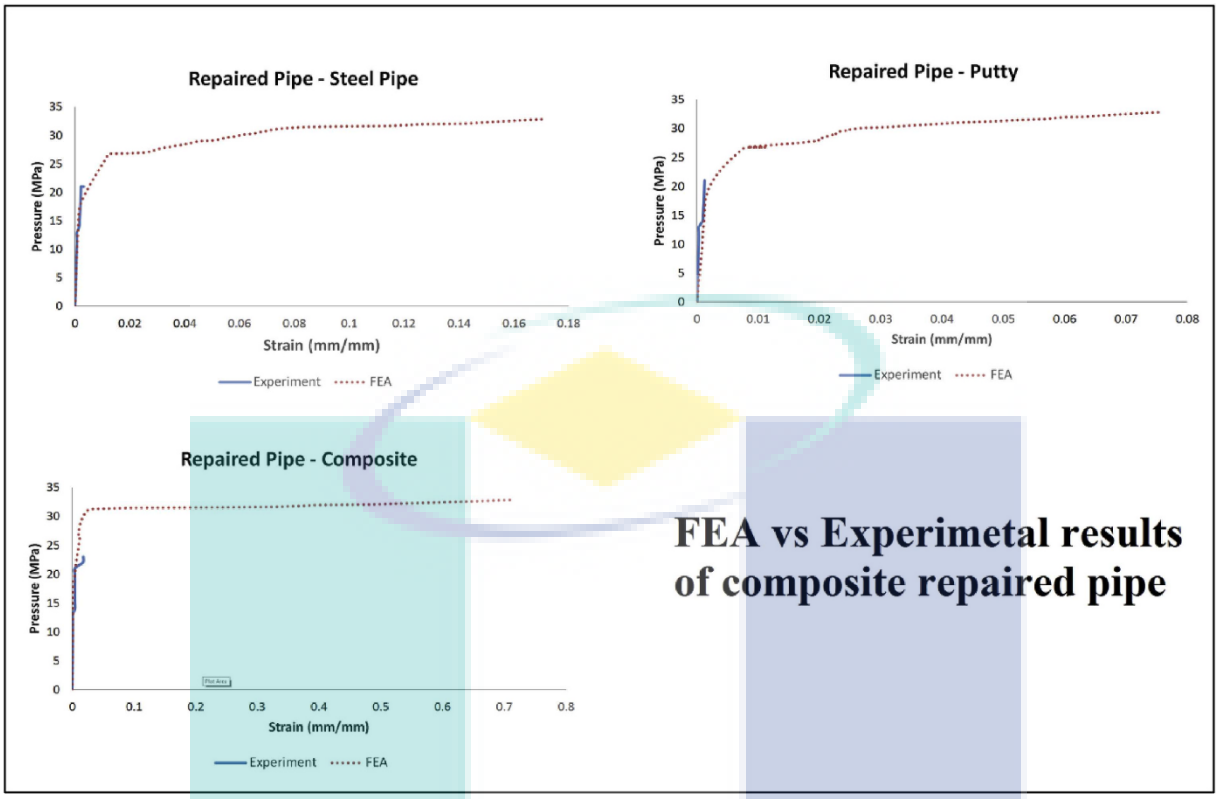


**Fig. 16.** Comparison between the experimental and FEA results for the repaired pipe.

strain readings were similar up to an applied pressure of 21 MPa. Meanwhile, the FEA strain readings were slightly lower than the experimental readings at similar pressures. Overall, the FEA model of the repaired pipe shows good agreement with the experimental pressure-strain curves for all the components (pipe, putty, and composite). This gives an indication of the suitability of tensile elastic-perfectly plastic model as putties.

Fig. 17 shows the stress contour plot for the entire repaired pipe-model, with all components enlarged to examine the stresses experienced in different parts. The image at the top represents the full model, followed by the steel pipe, putty, and composite wrap. When a pipe is pressurised internally, three principal stresses are generated – hoop stress, axial stress, and radial stress. When the ratio of the pipe diameter to thickness is greater than 20 ($D/t > 20$), the pipe can be considered as a thin-wall structure [41]. The pipe used in this study has a diameter of 168.3 mm and thickness of 7.11 mm. The calculated D/t ratio is 23.67; therefore, the thin-wall assumption was adopted to determine the stresses.

It is well known that the greatest stress experienced by a pressurised pipe is the hoop stress [42]; thus, only one stress contour plot is presented for the steel pipe. The highest stress concentrations were observed at the edges of the defect region along the axial direction. This is the failure location predicted by the model and it matches the experimental failure location, where stress at the centre of the defect was lower than that at the edge of the defect along the axial direction. On the other hand, the stresses experienced by the putty in a composite-repaired pipe are not completely understood. As the focus of this study is to comprehensively analyse the behaviour of a composite-repaired pipe, a detailed investigation was carried out on the stresses experienced by the putty in the radial, hoop, and axial directions. The stress contours of the putty in the radial (left), hoop (middle), and axial (right) directions are presented in the same figure (Fig. 17). It was found that compressive (blue colour) and tensile (red colour) stresses were experienced by the putty in all directions. The highest tensile stress was found at the edges of the putty, while a compressive stress was observed at the centre of the putty. The predicted maximum tensile stresses are 87 MPa, 101 MPa, and 96 MPa in the radial, hoop, and axial directions, respectively. On the other hand, the compressive stress was relatively small, with maximum predicted stresses of 21 MPa, 10 MPa, and 15 MPa in the radial, hoop, and axial directions, respectively. The highest tensile stress was found along the hoop direction at the edge of defect area underneath the composite wrap. Again, from the results on the predicted burst pressures, pressure-strain curves, and failure locations, it can be confirmed this model shows a good corroboration with the experimental results.

## 4. Conclusions

The present paper carried out detailed material characterisation on the steel pipe, putty, and composite wrap in order to gain fundamental understanding on the properties and behaviour of the tested materials. It was followed by experimental burst test and numerical simulation to evaluate and investigate the comprehensive behaviour of a composite repaired pipeline. The results indicate a ductile behaviour for the steel pipe with high tensile strength and modulus. On the other hand, the putty and composite wrap showed brittle behaviour under compressive, tensile, and flexural loads. The composite wrap exhibited the lowest modulus, while the putty recorded lowest tensile strength. This information was later used to analyse the behaviour of a composite-repaired pipe. Burst tests were conducted on a defective pipe and a composite-repaired pipe and the results were compared. The objective is to comprehensively evaluate the performance and behaviour of composite repair systems and composite-repaired pipes. The results show that composite repair successfully increased the burst pressure and reduced strain on the pipe. The burst pressure was increased by about 23%, while the strain at 100% SMYS of the composite-repaired pipe is still lower than the strain at 72% SMYS of the defective pipe, indicating significant strain reduction after repair. The pressure-strain

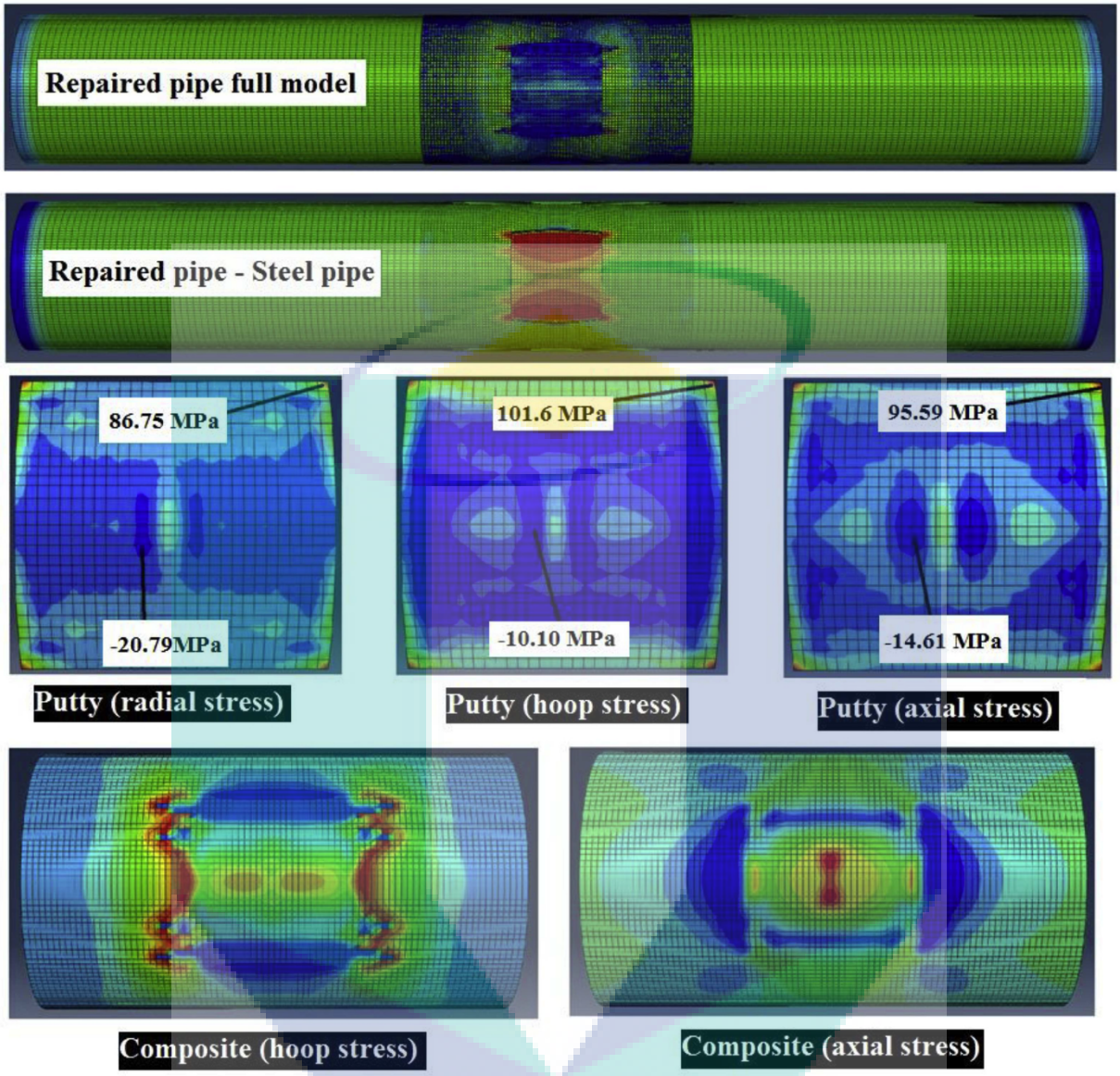


Fig. 17. Stress contour plots for the repaired-pipe model.

curves of all the components (steel pipe, putty, and composite wrap) were presented and discussed. It was observed that strain varied in each component, signifying differences in the deformation experienced by each component. Detailed material characterisation provides useful information on the properties of all the materials that are commonly used in composite repair systems. The characterisation results provide crucial inputs for understanding composite-repaired pipes. In addition, detailed material properties are essential for numerical simulations, such as finite element analysis. As a conclusion, comprehensive understanding on the behaviour of composite repaired pipeline has been achieved through this study and the findings of this study have a significant impact towards improving the fundamental understanding of the behaviour of composite-repaired pipes and can help in the optimisation of composite-repair design in the future.

## Acknowledgement

The authors gratefully acknowledge the financial and technical support provided by Universiti Malaysia Pahang (Grant No. RDU1703239), Universiti Teknologi Malaysia (Grant No. 13H27), and Ministry of Higher Education, Malaysia, MOHE (Grant No. 4F882).

## References

[1] Central Intelligence Agency, The World Fact book Field Listing: Pipelines, Retrieved from the Central Intelligence Agency, 2013, https://www.cia.gov/library/publications/the-world-factbook/fields/2117.html , Accessed date: 26 October 2013.
[2] S.R. Othman, N. Yahaya, N.M. Noor, K.S. Lim, L. Zardasti, A.S.A. Rashid, Modeling of external metal loss for corroded buried pipeline, J. Press. Vessel Technol. 139 (2017) 031702.
[3] S. Haladuick, M.R. Dann, Decision making for long-term pipeline system repair or replacement, ASCE-ASME J. Risk Uncertain, Eng. Syst. Part A: Civil Eng. 4 (2018).
[4] X. Liu, J. Zheng, J. Fu, J. Ji, G. Chen, Multi-level optimization of maintenance plan for natural gas pipeline systems subject to external corrosion, J. Nat. Gas Sci. Eng. 50 (2018) 64–73.
[5] S.N.F.M.M. Tahir, N. Yahaya, N.M. Noor, K.S. Lim, A.A. Rahman, Underground corrosion model of steel pipelines using in situ parameters of soil, J. Press. Vessel Technol. 137 (2015) 051701.
[6] M. Elchalakani, A. Karrech, H. Basarir, M.F. Hassanein, S. Fawzia, CFRP strengthening and rehabilitation of corroded steel pipelines under direct indentation, Thin-Walled Struct. 119 (2017) 510–521.
[7] N. Saeed, H. Ronagh, A. Virk, Composite repair of pipelines, considering the effect of live pressure - analytical and numerical models with respect to ISO/TS 24817 and ASME PCC-2, Composites Part B 58 (2014) 605–610.
[8] M. Shamsuddoha, M.M. Islam, T. Aravinthan, A. Manalo, K.T. Lau, Effectiveness of using fibre-reinforced polymer composites for underwater steel pipeline repairs, Compos. Struct. 100 (2013) 40–54.

[9] C. Alexander, The role of composite repair technology in rehabilitating piping and pipelines, Proceedings of the ASME 2014 Pressure Vessels & Piping Conference (PVP 2014). 20-24 July 2014. Anaheim, California, USA, 2014 Paper No.: PVP2014-28257.
[10] P.H. Chan, K.Y. Tshai, M. Johnson, H.L. Choo, S. Li, K. Zakaria, Burst strength of carbon fibre reinforced polyethylene strip pipeline repair system – a numerical and experimental approach, J. Compos. Mater. 49 (2015) 749–756.
[11] M. Shamsuddoha, M.M. Islam, T. Aravinthan, A. Manalo, P. Djukic, Effect of hygrothermal conditioning on the mechanical and thermal properties of epoxy grouts for pipeline rehabilitation, AIMS Mater. Sci. 3 (2016) 823–850.
[12] A.Y.L. Leong, K.H. Leong, Y.C. Tan, P.F.M. Liew, C.D. Wood, W. Tian, K.A. Kozielski, Overwrap composite repairs of offshore risers at topside and splash zone, Proceedings of 18th International Committee on Composite Materials (ICCM-18). 21st – 26th August 2011. Jeju Island, Korea, 2011.
[13] L.P. Djukic, W.S. Sum, K.H. Leong, W.D. Hillier, T.W. Eccleshall, A.Y.L. Leong, Development of a fibre reinforced polymer composite clamp for metallic pipeline repairs, Mater. Des. 70 (2015) 68–80.
[14] H. Zarrinzadeh, M.Z. Kabir, A. Deylami, Crack growth and debonding analysis of an aluminum pipe repaired by composite patch under fatigue loading, Thin-Walled Struct. 112 (2017) 140–184.
[15] E. Mahdi, E. Eltai, Development of cost-effective composite repair system for oil/gas pipelines, Compos. Struct. (2018), https://doi.org/10.1016/j.compstruct.2018.04.025.
[16] K.S. Lim, S.N.A. Azraai, N. Yahaya, L. Zardasti, N.M. Noor, Strength development of epoxy grouts for pipeline rehabilitation, J. Technol. 79 (2017) 9–14.
[17] Gh Zecheru, Gh Dumitru, A. Dinita, P. Yukhymets, Design of composite repair systems, in: E.N. Barkanov, A. Dumitrescu, I.A. Parinov (Eds.), Non-destructive Testing and Repair of Pipelines, Springer, 2018, pp. 269–285.
[18] R. Dev, D.S. Chaubey, World's oil scenario – falling oil prices winners and losers: a study on top oil producing and consuming countries, Imp. J. Interdiscip. Res. 2 (2016) 378–383.
[19] K. Farrag, Selection of Pipe Repair Methods. Final Report GTI - Project Number 21087, Gas Technology Institute, 2013.
[20] M. Shamsuddoha, M.M. Islam, T. Aravinthan, A. Manalo, K.T. Lau, Characterization of mechanical and thermal properties of epoxy grouts for composite repair of steel pipelines, Mater. Des. 52 (2013) 315–327.
[21] A. Dinita, I. Lambrescu, M.I. Chebakov, Gh Dumitru, Finite element stress analysis of pipelines with advanced composite repair, in: E.N. Barkanov, A. Dumitrescu, I.A. Parinov (Eds.), Non-destructive Testing and Repair of Pipelines, Springer, 2018, pp. 289–309.
[22] J.M. Duell, J.M. Wilson, M.R. Kessler, Analysis of a carbon composite overwrap pipeline repair system, Int. J. Pres. Vessel. Pip. 85 (2008) 782–788.
[23] C. Alexander, B. Vyvial, F. Wilson, Pipeline repair of corrosion and dents: a comparison of composite repairs and steel sleeves, Proceedings of the 2014 10th International Pipeline Conference (IPC 2014). 29th September – 3rd October, 2014. Calgary, Alberta, Canada, 2014 Paper No.: IPC2014-33410.
[24] ASME International, ASME PCC-2-2011 - Repair of Pressure Equipment and Piping, The American Society of Mechanical Engineers, New York, USA, 2011.
[25] C. Ruggieri, D. Fernando, Numerical modelling of ductile crack extension in high pressure pipeline with longitudinal flaws, Eng. Struct. 33 (5) (2011) 1423–1438, https://doi.org/10.1016/j.engstruct.2011.01.001.
[26] H.S. da Costa Mattos, J.M.L. Reis, R.F. Sampaio, V. Perrut, An alternative methodology to repair localized corrosion damage in metallic pipelines with epoxy resins, Mater. Des. 30 (2009) 3581–3591.
[27] H.S. da Costa Mattos, L.M. Paim, J.M.L. Reis, Analysis of burst tests and long-term hydrostatic tests in produced water pipelines, Eng. Fail. Anal. 22 (2012) 128–140.
[28] M.L. da Silva, H.S. da Costa Mattos, Failure pressure estimations for corroded pipelines, Mater. Sci. Forum 758 (2013) 65–76.
[29] H.S. da Costa Mattos, J.M.L. Reis, L.M. Paim, M.L. da Silva, R. Lopes Junior, V.A. Perrut, Failure analysis of corroded pipelines reinforced with composite repair systems, Eng. Fail. Anal. 59 (2019) 223–236.
[30] ASTM International, E8/E8M – 13a, Standard Test Methods for Tension Testing of Metallic Materials, American Society for Testing and Materials, West Conshohocken, USA, 2013.
[31] ASTM International, D3039 – 14, Standard Test Method for Tensile Properties of Polymer Matrix Composite Materials, American Society for Testing and Materials, West Conshohocken, USA, 2014.
[32] ASTM International, D6641/D6641M-14, Standard Test Method for Compressive Properties of Polymer Matrix Composite Materials Using a Combined Loading Compression (CLC) Test Fixture, American Society for Testing and Materials, West Conshohocken, USA, 2014.
[33] ASTM International, D695 – 10, Standard Test Method for Compressive Properties of Rigid Plastics, American Society for Testing and Materials, West Conshohocken, USA, 2010.
[34] ASTM International, D638 – 10, Standard Test Method for Tensile Properties of Plastics, American Society for Testing and Materials, West Conshohocken, USA, 2010.
[35] ASTM International, D790 – 10, Standard Test Methods for Flexural Properties of Unreinforced and Reinforced Plastics and Electrical Insulating Materials, American Society for Testing and Materials, West Conshohocken, USA, 2010.
[36] A. Shouman, F. Taheri, Compressive strain limits of composite repaired pipelines under combined loading states, Compos. Struct. 93 (2011) 1538–1548.
[37] J. Suwanprateeb, Calcium carbonate filled polyethylene: correlation of hardness and yield stress, Composites Part A 31 (2000) 353–359.
[38] J.M. Duell, Characterization and FEA of A Carbon Composite Overwrap Repair System, Master of Science The University of Tulsa, Oklahoma, 2004.
[39] K.S. Lim, S.N.A. Azraai, N.M. Noor, N. Yahaya, An overview of corroded pipe repair techniques using composite materials, Int. J. Chem. Mol. Nucl. Mater. Metall. Eng. 10 (2016) 19–25.
[40] J.L.F. Freire, R.D. Vieira, J.L.C. Diniz, L.C. Meniconi, Effectiveness of composite repairs applied to damaged pipeline, Experimental Techniques September/October, 2007, pp. 59–66.
[41] G.A. Antaki, Piping and Pipeline Engineering: Design, Construction, Maintenance, Integrity, and Repair, Marcel Dekker, Inc., New York, U.S.A, 2003.
[42] H. Liu, Pipeline Engineering, Lewis Publishers, New York, U.S.A, 2003.

*Materials Science Forum*
*ISSN: 1662-9752, Vol. 962, pp 242-248*
*doi:10.4028/www.scientific.net/MSF.962.242*

*Submitted: 2018-12-05*
*Accepted: 2018-12-17*
*Online: 2019-07-12*

# Mechanical Properties of Graphene Nanoplatelets-Reinforced Epoxy Grout in Repairing Damaged Pipelines

Lim Kar Sing[1,a], Libriati Zardasti[2,b], Norhazilan Md Noor[2,c] and Nordin Yahaya[2,d]

[1]Faculty of Civil Engineering and Earth Resources,
Universiti Malaysia Pahang, Lebuhraya Tun Razak, Gambang, Kuantan,
Pahang 26300, Malaysia.

[2]School of Civil Engineering, Faculty of Engineering, Universiti
Teknologi Malaysia, UTM Skudai, Johor 81310, Malaysia.

[a]limks@ump.edu.my, [b]libriati@utm.my, [c]norhazilan@utm.my, [d]nordiny@utm.my

**Keywords:** epoxy grout; graphene nanpplatelets; mechanical properties; pipeline repair

**Abstract.** The use of Fibre Reinforced Polymer (FRP) composites together with infill grout has been proven effective for repairing damaged steel pipelines. This paper study the mechanical properties of epoxy grouts where an amount of 0.2% and 0.8% of graphene nanoplatelets particles were added to commercial epoxy resin to evaluate their behaviour regarding neat epoxy resin. Compressive tests, tensile tests and flexural tests were conducted to study the effect of graphene nanoplatelets towards neat epoxy resin. By comparing graphene-modified grouts and neat epoxy grout, there is no increment of strength under compression and tensile test due to poor dispersion of graphene nanoplatelets. Nevertheless, the addition of graphene has produced a noticeable improvement in flexural properties. This signifies that with the inclusion of graphene nanoplatelets, the properties of epoxy grout can be improved if a better dispersion can be achieved.

## Introduction

Pipelines system is one of the most important parts of energy transportation infrastructure to many countries [1,2]. Pipeline in oil and gas industry are being used to transport products such as oil and gas across various soil environment and from offshore to onshore plant [3,4]. However, steel pipes that are laid underground can go through adverse deterioration in the form of corrosion, crack, dents, wearing, buckling, gouging, leaks and rupture [5,6]. Pipelines surface that exposed to the water and soil environment will have higher corrosion risk due to active chemical reaction by are surrounding environment [7]. A corroded pipeline will reduce its strength and eventually reduce service life [8,9]. Hence, corrosion and metal loss cause failures in pipelines and their repair techniques is one of the prime interests of the researchers all over the world [10,11].

Several literatures have shown that fibre-reinforced polymer (FRP) composites can be effectively used for the construction and retrofit of marine and underground structures [12-14]. The acceptance of composite based materials as an alternative to conventional repair materials is evidenced through the recent development of several codes and standards, including ASME PCC-2 [15] and ISO/TS 24817 [16]. In repairing a defective pipeline, the combination of FRP composite layer and infill material is normally used in the oil and gas industry. Epoxy grouts are usually used as infill material to ensure a smooth bed for the composite layer. More importantly, the infill grout fills the damaged profile caused by corrosion and provides a continuous support to minimize the outward distortion. Therefore, epoxy grouts play a key role of transferring the load from pipe to the composite repair and to increase the load resistance of the structure [17,18].

In order to predict the behaviour of a repair system for an optimum design, the properties of the infill material play a significant parameter. Repair efficiency may be increase with the high performance infill material if it can be serve as second protection layer if failure of composite occurs. This situation has been made convenient by the recent development of nano-particle reinforced polymer composites. Since the discovery of graphene nanoplatelets, it have been widely used and

proven effective in improving the mechanical properties of epoxy grout [19]. A good infill has the potential to increase the efficiency and performance of overall repair system and reduce the total cost by minimizing the used of composite sleeve. Hence, this study aims to investigate the compressive, tensile and flexural properties of graphene-modified epoxy grout to be used as infill material.

## Materials and Methods

The epoxy resin used in this study is a commercially available three-part pourable grout consisting of epoxy resin, hardener, and silica sand. The graphene nanoplatelets were added to unmodified Grout A in 0.2% and 0.8% to the weight of unmodified Grout A. The 0.2% and 0.8% graphene-modified grouts were named as Grout A (G-0.2) and Grout A (G-0.8), respectively. The graphene nanoplatelets in powder form were supplied by a local company. According to the products technical datasheet, the average thickness and particle diameter of this product was 0.68-3.41nm and 1-4nm, respectively [20]. For sample preparation, the graphene nanoplatelets were weighed according to their proposed percentages. It was then dispersed in an acetone solution using an ultrasound sonicator for one hour. The dispersed graphene-acetone solution was then cooled at room temperature while allowing the remaining acetone to evaporate. When the acetone fully evaporated, the resin, hardener and silica filler were prepared according to the unmodified ratio. For the first step, graphene nanoplatelets was added to hardener and mixed with electrical mixes at low speeds. Resin was then added and the mixing process continued for at least two minutes to evenly disperse the graphene nanoplatelets into the matrix. Finally, the silica filler was added and the grout was continuously mixed until a homogeneous grout was achieved. Once the grouts were thoroughly mixed, specially designed steel moulds were used to cast the compressive, tensile and flexural test samples for all grouts. All grouts were cured at room temperature (about 30°C) for 24 hours prior to testing. Table 1 shows a summary of the mechanical properties tests for all grouts. All the tests were carried out using an INSTRON 5567 Universal Testing Machine with a capacity of 25KN. 5 samples of each grout were tested for each properties. These laboratory tests investigated the strength, modulus, and behaviour of all grouts under various loading conditions including compression, tension, and flexural. The information gathered in this stage provides a fundamental understanding of the behaviour such as brittleness or ductility of the grouts when subjected to aforementioned loadings.

Table 1 Summary of mechanical properties test details

| Tests | Standards | *N* | Dimensions (mm) | Geometry | Loading rate (mm/min) |
|---|---|---|---|---|---|
| **Compressive** | ASTM: D695 | 5 | 12.7 x 12.7 x 50.8 | Prismatic | 1.3 |
| **Tensile** | ASTM: D638 | 5 | 13.0 x 3.2 | Dumbbell | 5.0 |
| **Flexure** | ASTM: D790 | 5 | 127 x 12.7 x 3.2 | Prismatic | 1.365 |

## Results and Discussion

**Compression Properties.** In current practice of pipeline repair using composite material, infill material is commonly regarded as load transfer medium. This infill that is confined in between damaged pipe and composite wrap is expected to undergo compressive stress. Therefore, it is important to understand the compressive properties of infill materials. Table 2 shows the summary of compressive properties of the neat epoxy grout and graphene-modified grouts. The strength and modulus values presented in Table 2 to Table 4 are the average maximum strength, modulus and strain at ultimate stress before sample failure. The plus and minus sign (±) after average value represents standard deviation of the sample. The range of the ultimate compressive strength and Young's modulus were 56MPa to 87.52MPa and 12.67GPa to 18.93GPa, respectively. Grout A

(G-0%) was found to have the highest modulus and strength while Grout A (G-0.8%) and Grout A (G-0.2%) exhibit the lowest modulus and strength, respectively. The results of compressive properties of graphene-modified grouts show a reduction in both strength and stiffness as compared to the unmodified Grout A.

Fig. 1 (left) shows the typical stress-strain behaviour under compression loading for all tested grouts. Grout A (G-0.2%) shows elastic behaviour followed by slight strain softening beyond its ultimate stress while there was no any noticeable strain softening behaviour was observed for the neat epoxy grout and the 0.8% graphene-modified grout. The curve of Grout A (G-0.8%) and Grout A (G-0.8%) plummeted suddenly at ultimate compressive stress, indicating brittle behaviour. A close examination of the failure pattern of all grouts showed no noticeable deformation prior to ultimate stress, as shown in Fig. 1 (right). A vertical crack parallel to the loading direction was observed for both samples as they reached ultimate stress. An "explosion" like sound was heard and stress suddenly plummets sharply when failure had occurred. These results signify the brittle nature of all tested grouts.

Table 2 Compressive properties of all grouts

| Grouts | Young's Modulus (GPa) | Ultimate Compressive Strength (MPa) |
|---|---|---|
| **A (G-0%)** | 18.93 ± 4.78 | 87.52 ± 1.95 |
| **A (G-0.2%)** | 14.35 ± 1.66 | 56.00 ± 11.29 |
| **A (G-0.8%)** | 12.67 ± 2.51 | 72.63 ± 14.66 |

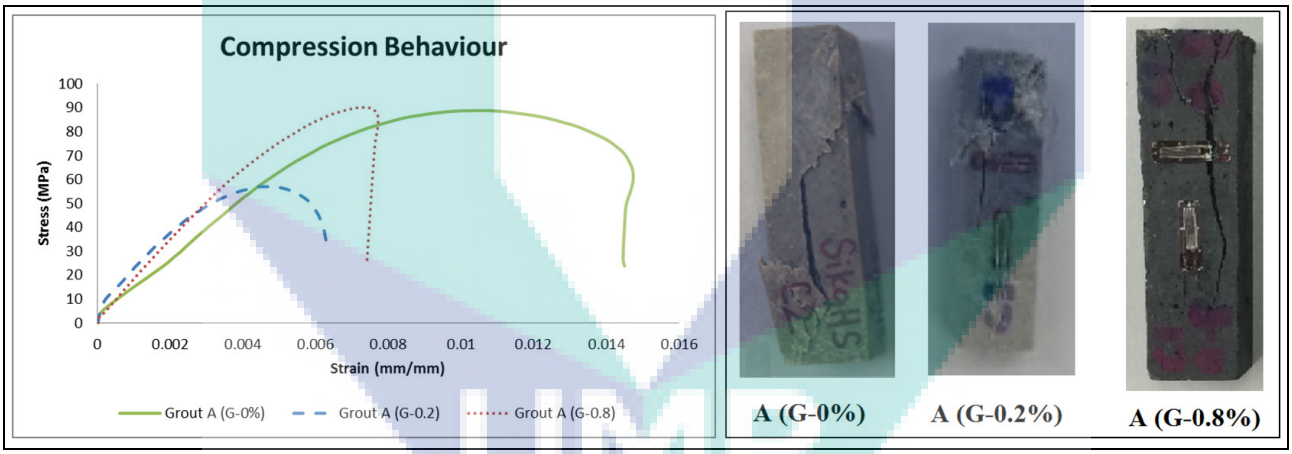


Figure 1 Stress-strain behaviour (left) and failure pattern (right) of compression sampels

**Tensile Properties.** It is well known that pressurized pipe will experience stresses in hoop, axial, and radial directions [21,22]. Hoop stress is most critical stress for a pipe that is subjected to internal pressure. This stress will cause failure of pipe in tension mode. Therefore, tensile properties are considered as most important properties to be understood. A summary of the tensile test results is tabulated in Table 3. As seen in Table 3, Young's modulus is ranged from 15.38GPa to 19.48GPa while the recorded ultimate tensile strength ranged from 13.81MPa to 18.90MPa. Similar to its compressive properties, Grout A (G-0.2%) was found to have a higher modulus but lower strength than Grout A (G-0.8%). As expected, Grout A (G-0.8%) with lower stiffness recorded higher strain at its ultimate stress than Grout A (G-0.2%). Grout A (G-0.8%) showed comparable performance to unmodified Grout A in terms of tensile stiffness and strength. In addition, the ultimate strength in tension for all grouts is much lower than that exhibited under compression. The ultimate tensile strength of Grout A (G-0%) is about 4.5 times lower while graphene-modified grouts is about four times lower than their respective compressive strength.

Fig. 2 (left) shows the stress-strain curve for all tested grouts under uniaxial tensile test. All grouts exhibited much lower ductility under tension as compared with their compression behaviour. As

shown in Fig. 2 (left), all grouts exhibit a brittle behaviour without any plastic deformation detected in the stress-strain curve. Linear and slightly nonlinear elastic behaviour was observed for all grouts. No noticeable strain hardening or softening behaviour can be seen in the graph. All samples failed due to splitting, perpendicular to the loading direction during peak stress. Fig. 2 (right) shows the fractured sample for all grouts in the tensile test. No noticeable deformation such as necking was observed in all samples, which indicates a brittle failure pattern.

Table 3 Tensile properties of all grouts

| Grouts | Young's Modulus (GPa) | Ultimate Tensile Strength (MPa) |
|---|---|---|
| **A (G-0%)** | 15.38 ± 1.26 | 18.90 ± 4.62 |
| **A (G-0.2%)** | 19.48 ± 3.32 | 13.81 ± 3.56 |
| **A (G-0.8%)** | 15.54 ± 2.73 | 18.87 ± 2.36 |

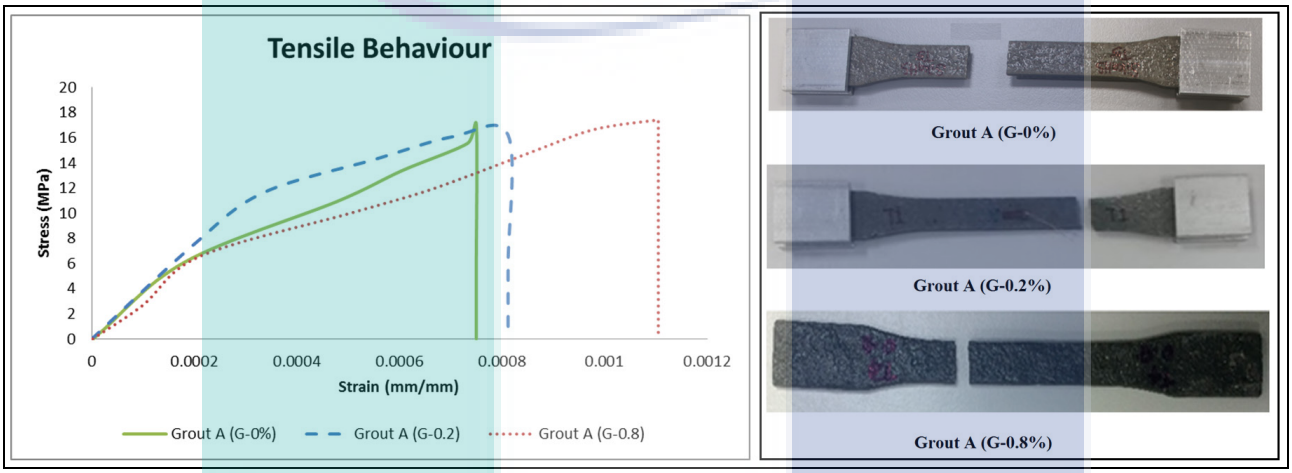


Figure 2 Stress-strain behaviour (left) and failure pattern (right) of tensile sampels

**Flexural Properties.** Other than internal pressure, pipelines are sometimes subjected to other loadings such as bending force. When bending force is present in a pipeline, high flexural strength and stiffness is required to prevent failure of the pipe. Table 4 presents the summary of flexural properties for all grouts. Neat epoxy grout has recorded the lowest strength (34.575MPa) and modulus (12.643GPa) while both graphene-modified grouts shows show comparable performance in terms of stiffness and ultimate flexural strength. Grout A (G-0.2%) shows a slightly lower modulus (14.92GPa) and flexural strength (36.32MPa) than Grout A (G-0.8%). Grout (G-0.8%) recorded 15.93GPa for Young's modulus and 37.44MPa for flexural strength. When compared to unmodified Grout A, the inclusion of graphene nanoplatelets slightly increased stiffness and modulus under flexural loading.

The stress-strain curve for the graphene-modified grouts is shown in Fig. 3 (left). Both grouts exhibit comparable behaviour where only linear elastic behaviour was observed before sample failure, indicating the brittleness of the grouts. This is in agreement with the failure patterns as shown in Fig. 3 (right). A vertical crack running through the thickness of the sample, which is perpendicular to the loading direction, was observed in the middle of the sample where failure occurred. In order to study the effect of the graphene nanoplatelets towards mechanical properties of modified grouts, FESEM test was conducted to provide additional information on the failure surface of graphene-modified grout. The flaky shape of graphene nanoplatelets is highlighted in the rectangular box as shown in Fig. 4. Based on the FESEM results, layers of flaky graphene filler were found stacked together in one location to form a thicker layer of graphene nanoplatelets. This signifies the poor dispersion of graphene nanoplatelets filler in the sample. However, considering the randomness of the filler orientation, some of the graphene filler is anticipated to fill the grout that is aligned with the thickness direction of the sample. Under flexural load, these flaky graphene nanoplatelets might

potentially reinforce the grout to sustain higher flexural load and reduce the deflection, thus increasing the stiffness of the grouts. This finding is in-line with the work done by Chatterjee *et al.* [23] where the authors reported improved flexural properties was achieved with the inclusion of graphene nanoplatelets. The large flakes support crack deflection, thus resulting improvement in stiffness. In addition, these graphene nanoplatelets also function as crack bridging element that increases the strength by reducing the crack propagation.

Table 4 Flexural properties of all grouts

| Grouts | Young's Modulus (GPa) | Ultimate Flexural Strength (MPa) |
|---|---|---|
| **A (G-0%)** | 12.643 ± 0.464 | 34.575 ± 2.399 |
| **A (G-0.2%)** | 14.92 ± 1.50 | 36.32 ± 1.60 |
| **A (G-0.8%)** | 15.93 ± 0.96 | 37.44 ± 3.38 |

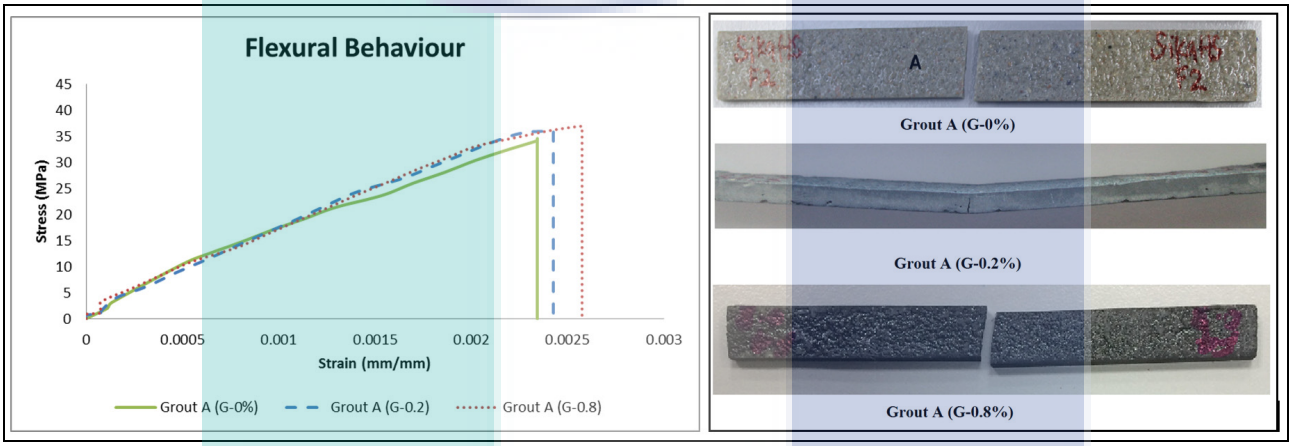


Figure 3 Stress-strain behaviour (left) and failure pattern (right) of flexural sampels

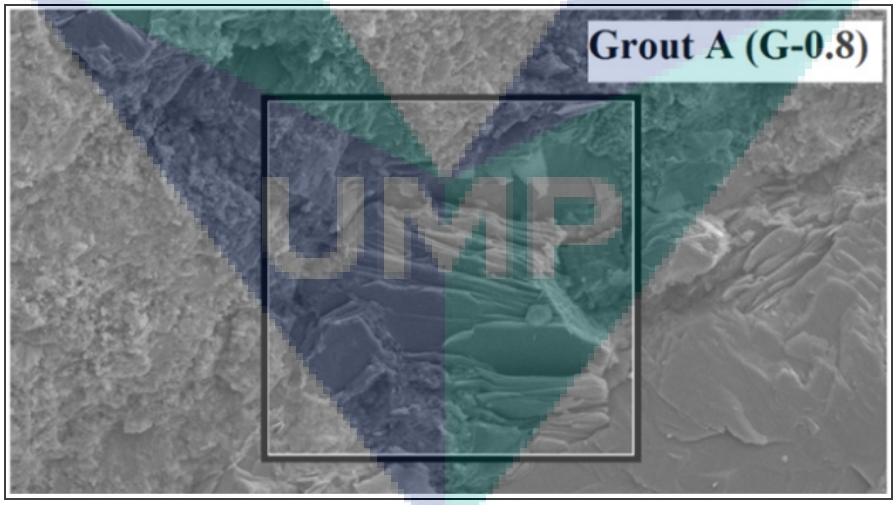


Figure 4 FESEM result of graphene-modified grout

## Conclusion

The modification of the mechanical properties of epoxy grout was successfully conducted by adding graphene nanoplatelets into unmodified Grout A. As a summary, graphene-modified grouts do not show any increase in strength under compression and tensile load when compared with unmodified Grout A. Result of FESEM test indicates poor dispersion of graphene nanoplatelets in the epoxy grouts. This may be the reason why the graphene-modified grouts failed to act as reinforcement to improve the compression and tensile properties. Despite the poor performance of graphene modified grouts in compressive and tensile properties, with the inclusion of 0.2% and 0.8% graphene

nanoplatelets, a noticeable improvement in flexural properties was achieved. The flexural strength has increased about 8% while flexural modulus shows an increment of 26%. In order to gain the advantages of graphene nanoplatelets, a proper dispersion procedure should be used. Dispersion of graphene nanoplatelets is recommended to be carried out by a three-roll mill calendaring process.

**Acknowledgement**

The author gratefully acknowledges the financial and technical support provided by Universiti Malaysia Pahang (UMP) through grant RDU1703239 and RDU171122 as well as Universiti Teknologi Malaysia (UTM) for facilitating in accomplishing this research.

**References**

[1] Bruce, W. A., and Keifner, J. (2015). *Pipeline Repair Using Full-Encirclement Repair Sleeves*. In Winston Reive, R. (Ed.). *Oil and Gas Pipelines: Integrity and Safety Handbook*. New Jersey: John Wiley & Sons, Inc. pp. 635-654.

[2] Salim, U.S., Valipour, A., Azraai, S.N.A., Lim, K.S., Zardasti, L., Noor, M.N., and Yahaya, N. (2016). Compressive, flexural and tensile properties of graphene modified grouts for pipeline rehabilitation, *Malaysian Journal of Civil Engineering*, 28-Special Issue (2), 102-111.

[3] Li, Y., Li, T. X., Cai, G. W., Yang, L. H. (2013). Influence of AC interference to corrosion of Q235 carbon steel. *Corrosion Engineering, Science and Technology,* 48(5), 322-326.

[4] Othman, S.R., Yahaya, N., Noor, M.N., Lim, K.S., Zardasti, L., and Rashid, A.S.A. (2017). Modelling of external metal loss for corroded buried pipeline. *Journal of Pressure Vessel Technology*, 139(3), 031702.

[5] Tahir, S.N.F.M.M., Noor, M.N., and Yahaya, N., and Lim, K.S. (2015). Relationship between in-situ measurement of soil parameters and metal loss volume of x70 carbon steel coupon. *Asian Journal of Scientific Research*, 8(2), 205-211.

[6] Haladuick, S., and Dann, M.R. (2018). Decision making for long-term pipeline system repair or replacement. *ASCE-ASME Journal of Risk and Uncertainty in Engineering System, Part A: Civil Engineering*, 4(2), 04018009.

[7] Bernardo, G., Laterza, M., D'Amato, M., Andrisani., G., Diaz, A., and Laguna, E. (2016). ELARCH Project: the use of innovative product based on the nanotechnologies for the protection of architectural heritage. *Proceeding of the XII Congresso International Sobre Patologia e Reabilitacao de Estruturas*, 26th – 29th October 2016, Portugal.

[8] Tahir, S.N.F.M.M., Yahaya, N., Noor, M.N., Lim, K.S., and Rahman, A.A. (2015). Underground corrosion model of steel pipelines using in-situ parameters of soil. *Journal of Pressure Vessel Technology*, 137(5), 051701.

[9] Pereira, J. C. R., de Jesus, A. M. P., Fernandes, A. A., and Varelis, G. (2016). Monotonic, low-cycle fatigue, and ultralow-cycle fatigue behaviors of the X52, X60, and X65 piping steel grades. *Journal of Pressure Vessel Technology*, 138(3), 031403.

[10] Shamsuddoha, M., Islam, M.M., Aravinthan, T., Manalo, A., and Lau, K.T. (2013). Effectiveness of using fibre-reinforced polymer composites for underwater steel pipeline repairs. *Composite Structures*, 100,40-54.

[11] Saeed, N., Ronagh, H., and Virk, A. (2014). Composite repair of pipelines, considering the effect of live pressure - Analytical and numerical models with respect to ISO/TS 24817 and ASME PCC-2. *Composites: Part B,* 58, 605-610.

[12] Duell, J.M., Wilson, J.M., and Kessler, M.R. (2008). Analysis of a carbon composite overwrap pipeline repair system. *International Journal of Pressure Vessels and Piping*, 85, 782-788.

[13] Leong, A.Y.L., Leong, K.H., Tan, Y.C., Liew, P.F.M., Wood, C.D., Tian, W. and Kozielski, K.A. (2011). Overwrap composite repairs of offshore risers at topside and splash zone. *Proceedings of 18th International Committee on Composite Materials (ICCM-18)*. 21st - 26th August 2011. Jeju Island, Korea.

[14] Chan, P.H., Tshai, K.Y., Johnson, M., Choo, H.L., Li, S., and Zakaria, K. (2015). Burst strength of carbon fibre reinforced polyethylene strip pipeline repair system – A numerical and experimental approach. *Journal of Composite Materials,* 49(6), 749-756.

[15] ASME International. (2011). *ASME PCC-2-2011. Repair of Pressure Equipment and Piping.* New York, USA: The American Society of Mechanical Engineers.

[16] ISO. (2006). ISO/TS 2481. *Petroleum, Petrochemical and Natural Gas Industries – Composite Repairs of Pipework – Qualification and Design, Installation, Testing and Inspection.* Switzerland: International Organization for Standardization.

[17] Farrag, K. (2013). *Selection of Pipe Repair Methods.* Final Report GTI - Project Number 21087, Gas Technology Institute.

[18] Lim, K.S., Azraai, S.N.A., Yahaya, N., Zardasti, L., and Noor, M.N. (2017). Strength development of epoxy grouts for pipeline rehabilitation. *Jurnal Teknologi (Science & Engineering)*, 79(1), 9-14.

[19] Tang, L. C., Wan, Y. J., Yan, D., Pei, Y. B., Zhao, L., Li, Y. B., and Lai, G. Q. (2013). The effect of graphene dispersion on the mechanical properties of graphene/epoxy composites. *Carbon*, 60, 16-27.

[20] Ugent Tech Sdn. Bhd. (2014). Graphene Nanoplatelets UG Pro 680 technical data sheet.

[21] Antaki, G. A. (2003). *Piping and Pipeline Engineering: Design, Construction, Maintenance, Integrity, and Repair.* Marcel Dekker, Inc., New York, U.S.A.

[22] Liu, H. (2003). *Pipeline Engineering*. Lewis Publishers, New York, U.S.A.

[23] Chatterjee, S., Nafazarefi, F., Tai, N.H., Schlagenhauf, L., and Chu, B.T.T. (2012). Size and synergy effects of nanofiller hybrids including graphene nanoplatelets and carbon nanotubes in mechanical properties of epoxy composites. *Carbon,* 50, 5380-5386.

# CHAPTER 7

## 7.0 Conclusion

Effect of graphene as reinforcement in epoxy grout has been successfully investigated where the findings show the graphene filler has increases the strength of epoxy grout under tensile and compression test. Modified epoxy grout at 0.1% had recorded the highest tensile strength but the lowest Young's Modulus under tensile test compared to milled-down sample. However, the compression test with 0.05% sample graphene added recorded the highest compressive strength. This shows that the graphene is a good reinforcement to increase strength for tensile test. In addition, the tensile test result shows that there was improvement made in the tensile strength of the epoxy grout with the addition of CNT. However, the expected outcomes were not fully in-line with hypothesis as the result of the compressive strength test of the CNT-modified samples decrease from the control sample and the milled down sample. In the result, it is found that CNT help improve the tensile strength of the epoxy grout as evident in the 62% increase of tensile strength from the milled down samples to the 0.01% CNT samples but the compressive strength decrease 8.77% from the milled down sample to the 0.01% CNT added, 13.12% for the 0.05% CNT added and 7.33% for the 0.1% CNT added.

In conclusion, graphene nanoplatlets and CNT can be a very good material to enhance the mechanical properties of epoxy grout, however, with this specific brand of epoxy grout that contains steel filler in the resin, the CNT only improve the tensile properties but the compressive properties of the epoxy grout decrease as compared to the control sample.

## 7.1 Recommendations

CNT and graphene nanoplatlets was proven to be a good material for the enhancement of mechanical properties of epoxy grout but with this type of epoxy grout where the size of the existing steel filler is much larger than the diameter of the nano-particle is not a very suitable choice to determine the improvement of mechanical properties. Epoxy grout without existing steel filler should be tested with this methodology to make a direct comparison of the original epoxy grout without compromising the epoxy grout during the calendaring process of the three roll mill. In addition, more percentages variables of carbon nano filler added into epoxy grout can be done to get the optimum percentage of the filler to be added. The optimum percentage is important to optimize the amount of carbon nano filler used for the enhancement of the performance of the infill material.

## REFERENCES


Alexander, C.R. (2007). Development of a Composite Repair System for Reinforcing Offshore Risers. Doctor of Philosophy, Texas A&M University.

Alexander, C. R. and Francini, B. (2006). State of the Art Assessment of Composite Systems Used to Repair Transmission Pipelines. Proceedings of 6th International Pipeline Conference. 25-29 September 2006. Calgary, Alberta, Canada. Paper No. IPC2006-10484.

Chan, P.H., Tshai, K.Y., Johnson, M., and Li, S. (2015). The Flexural Properties of Composite Repaired Pipeline: Numerical Simulation and Experimental Validation. Composite Structures, vol 133, pp. 312-321.

Cunha, S. B. and Netto, T. A. (2012). Analytical solution for stress, strain and plastic instability of pressurized pipes with volumetric flaws. Int. J. Press Vess Piping, vol. 89, pp. 187-202.

Cercone, L. and Lockwood, J.D. (2005). Review of FRP Composite Materials for Pipeline Repair. Pipelines, pp1001-1013.

Duell, J.M., Wilson, J.M., and Kessler, M.R. (2008). Analysis of a Carbon Composite Overwrap Pipeline Repair System. International Journal of Pressure Vessels and Piping. 85, 782-788.

Gibson, A.G. (2003). The Cost Effective Use of Fibre Reinforced Composites Offshore. Norwich: University of Newcastle upon Tyne, HSE Books.

Kou, J. and Yang, W. (2011). Application Progress of Oil and Gas Pipeline Rehabilitation Technology. Proceeding of the International Conference on Pipelines and Trenchless Technology (ICPTT). 26–29 October 2011. Beijing, China. 1285–1292.

Leong, A.Y.L., Leong, K.H., Tan, Y.C., Liew, P.F.M., Wood, C.D., Tian, W. and Kozielski, K.A. (2011). Overwrap Composite Repairs of Offshore Risers at Topside and Splash Zone. Proceedings of 18th International Committee on Composite Materials (ICCM-18). 21st -26th August 2011. Jeju Island, Korea.

Lim, K. S., S. N. A. Azraai, N. M. Noor, and N. Yahaya. (2016). An Overview of Corroded Pipe Repair Techniques Using Composite Materials. World Academy of Science, Engineering and Technology, International Journal of Chemical, Molecular, Nuclear, Materials and Metallurgical Engineering, Vol. 10 (1), pp. 19-25.

Ma, W.F., Luo, J.H., and Cai, K. (2011). Discussion about Application of Composite Repair Technique in Pipeline Engineering. Advanced Materials Research. 311-313, 185-188.

Saeed, N. (2015). Composite Overwrap Repair System for Pipelines - Onshore and Offshore Application. Doctor of Philosophy, The University of Queensland, Australia.

Seica, V.M. and Packer, A.J. (2007). FRP Materials for the Rehabilitation of Tubular Steel Structures, for Underwater Applications. Comp. Struct., 80, 440-450.

Shamsuddoha, M., Islam, M.M., Aravinthan, T., Manalo, A., and Lau, K.T. (2012). Fibre Composites for High Pressure Pipeline Repairs, In-air and Subsea-An Overview. Proceedings of the Third Asia-Pacific Conference on FRP in Structures (APFIS 2012). 2nd – 4th February 2012, Hokkaido University, Japan.

Shamsuddoha, M., Islam, M.M., Aravinthan, T., Manalo, A., and Lau, K.T. (2013). Effectiveness of Using Fibre-Reinforced Polymer Composites for Underwater Steel Pipeline Repairs. Compos. Struct., 100,40-54.

United State Department of Transport. (2007). Corrosion Costs and Preventive Strategies in the United States. U.S.A: United State Department of Transport.

United State Department of Transport. (2013). Selection of Pipe Repair Methods. U.S.A: United State Department of Transport.